LOOP SPACES AND CHOREOGRAPHIES IN DYNAMICAL SYSTEMS

A thesis submitted to the University of Manchester
for the degree of Doctor of Philosophy
in the Faculty of Engineering and Physical Sciences

2011

Katrina Steckles

School of Mathematics

Contents

Word count 50132

List of Tables

List of Figures

The University of Manchester

Katrina Steckles
Doctor of Philosophy
Loop Spaces and Choreographies in Dynamical Systems
July 14, 2011

We consider a subset of the set of solutions to the n-body problem, termed choreographies, which involve a motion of particles where each follows the same path in space with a fixed time delay. Focusing on planar choreographies, we use the action of symmetry groups on the spatial and temporal motion of such systems to restrict a space of loops and study the topology of the resulting manifolds.

As well as providing a framework of notation and terminology for the study of such systems, we prove various useful properties which allow us to classify the possible groups of symmetries, and discuss which are likely to be realisable as that of a motion of bodies.

Declaration

No portion of the work referred to in this thesis has been submitted in support of an application for another degree or qualification of this or any other university or other institute of learning.

Copyright Statement

i. The author of this thesis (including any appendices and/or schedules to this thesis) owns any copyright in it (the "Copyright") and s/he has given The University of Manchester the right to use such Copyright for any administrative, promotional, educational and/or teaching purposes.

ii. Copies of this thesis, either in full or in extracts, may be made **only** in accordance with the regulations of the John Rylands University Library of Manchester. Details of these regulations may be obtained from the Librarian. This page must form part of any such copies made.

iii. The ownership of any patents, designs, trade marks and any and all other intellectual property rights except for the Copyright (the "Intellectual Property Rights") and any reproductions of copyright works, for example graphs and tables ("Reproductions"), which may be described in this thesis, may not be owned by the author and may be owned by third parties. Such Intellectual Property Rights and Reproductions cannot and must not be made available for use without the prior written permission of the owner(s) of the relevant Intellectual Property Rights and/or Reproductions.

iv. Further information on the conditions under which disclosure, publication and exploitation of this thesis, the Copyright and any Intellectual Property Rights and/or Reproductions described in it may take place is available from the Head of the School of Mathematics.

Acknowledgements

My thanks go to my supervisor, James Montaldi, for his support and guidance, and to John and Stephanie Forrest, of Forrest Recruitment, for kindly funding my research.

I am deeply grateful to my family, friends, colleagues and especially Paul for all their love, advice and support.

Finally, to Bill: I hope I have made you proud.

Chapter 1

Introduction

The n-body problem is that of determining, given the initial positions and velocities of n bodies moving in space, the path which they will take. The particles will interact by gravitational attraction. Solutions to the n-body problem will be curves which describe a valid motion of the particles, given a set of masses and a formula for gravitational potential.

The study of n-body problems has deep roots in the history of mathematics, and was originally motivated by the motion of the planets and stars. Such mathematics may also be applied to the study of molecular particles, and also to point vortices in fluid dynamics [6]. Many different approaches have been taken to try to understand such systems.

In particular, my study focuses on a subset of n-body solutions termed **choreographies**. These are motions where each of the particles follows the same path but with a fixed time delay. Leading figures in the study of choreographies include Chenciner and Montgomery, who discovered the figure eight choreography [12], which we will use extensively as an example in this thesis; and Gerver, whose 'super-eight' choreography is also useful in studying a particular class of examples which we find interesting. These three have worked together with Simó in [11], where they prove some fundamental results about the nature of choreographical solutions.

Conventionally, the existence of solutions has been proven using variational methods. The existence of planar n-body choreographies may be proved using computer-assistance. Simó's [29] numerical calculations have proven the existence of many choreographical motions, and he has also produced beautiful animations of many such examples. Kapela and Zgliczynski ([18], [16]) have done similar work employing interval arithmetic. Many of the examples in this thesis have been proven to exist in this way. There also exist computer assisted proofs [17] of the existence of non-symmetrical planar choreographies.

The work of Ferrario and Terracini [14] involves using the inherent spatial and temporal symmetries implied by the definiton of a choreography to restrict the space of loops being considered. This topological approach considers the effect of the action of the symmetry group on the spaces of loops in the configuration space of n particles. Ferrario and Terracini also provide conditions to ensure the success of variational methods, which guarantee the solutions will exist and be without collisions.

In this thesis, we attempt to apply techniques from algebraic topology and the study of loop spaces on manifolds to the behaviour of bodies in a dynamical system. In particular, we will be considering the action of symmetry groups on systems of particles, and using the symmetries to consider a restricted set of motions, following the methods proposed by Ferrario and Terracini.

In Chapter 2, we describe our aim to study spaces of loops possessing symmetries. We begin by considering relative loops. These are not closed loops, but paths which run from a point to its image under some automorphism of the space on which they are defined. We also define a system of notation, and a set of maps between such spaces of loops. We will also introduce some key motivating examples, namely those of n-body problems and k-centre problems.

The particular subset of paths we will be considering is that of choreographies. In Chapter 3, the concept of a choreography will be defined and explored in detail, determining what effect such a restriction has on the space of loops being considered.

We introduce a system of representations for the group of symmetries, which allows us to interpret the effect of each symmetry on the space and time in which the

particles move. In Chapter 4 we attempt to classify the different types of symmetry group possible, using these representations, and define certain special types of symmetry depending on how they act on the passage of time. We will also discuss how each symmetry group leads to multiple connected components of the loop space, each of which possesses the same group of symmetries but is in a different homotopy class of loops.

Many examples will be considered and studied in detail to build up a picture of how different groups of symmetries give different types of orbit, and how each system may be specified. We also prove several useful results regarding the different types of symmetries which exist, and how this affects the choreographies.

In Chapter 5, and in the Appendix, we discuss several classes of examples and explore their relationship with each other and the way they may be realised as subspaces of the space of relative loops.

It is also possible, using minimisation of the energy of the system, to determine when certain homotopy classes of paths will be realisable as a motion of particles. In Chapter 6 we will discuss some approaches which have been made in this area, and highlight in particular what this means for the choreographies we have been studying, in terms of whether they will be realisable.

Chapter 7 deals with other considerations which may lead on to further study, some of which have been touched on earlier in the thesis, and others which would possibly be interesting to investigate further.

Chapter 2

Preliminaries

This chapter is devoted to introducing some of the notation, structures, maps and definitions which will be relied on during this work. We will start by considering spaces of loops, and then introducing the concept of relative loops. We will define several different spaces of loops and relative loops on a given manifold, with respect to the action of a group, and a set of maps between the different spaces which behave in a sensible way. We also consider some key motivating examples, and how they fit into this framework.

2.1 Introductory concepts

In this work, we will be studying group actions on manifolds and their effect on the spaces of loops defined on those manifolds. Groups will usually be denoted G, group elements g, and manifolds, which we assume to be connected unless otherwise stated, will be denoted M. In general, groups will be discrete, and manifolds will normally be the configuration space of a physical system.

We will use the standard notation for the fundamental group $\pi_1(M, x)$, the based loop space $\Omega(M, x)$ and free loop space $\Lambda(M)$, given a topological space M and base point $x \in M$.

When discussing dihedral groups, we will use D_n to denote the group of symmetries of the regular n-gon, which will be a group of order $2n$.

We will also be considering the **relative loop spaces** - which are defined as follows, with the compact-open topology. Let G be a group acting on a manifold M.

Definition 2.1.1. We define the **based relative loop space** of a manifold M, with respect to an automorphism g of the manifold and a basepoint $x \in M$, to be the space of continuous maps of the interval $[0,1]$ into M such that 0 is mapped to x, and 1 is mapped to gx, the image of x under g. Alternatively, this can be thought of as the space of all paths which run from the point $x \in M$ to the point gx. We denote this space

$$\Omega^g(M,x) = \{\gamma : [0,1] \to M \mid \gamma(0) = x, \gamma(1) = gx\}.$$

Compare this with the space of ordinary closed based loops, which is usually given by

$$\Omega(M,x) = \{\gamma : [0,1] \to M \mid \gamma(0) = \gamma(1) = x\}.$$

Definition 2.1.2. We define the **free relative loop space** of M to be the space of all paths in M which run from any point to its image under g. This can be thought of as the union of all the based loop spaces over $x \in M$. We denote this space

$$\Lambda^g(M) = \{\gamma : [0,1] \to M \mid \gamma(1) = g\gamma(0)\}.$$

Again, compare with the free loop space

$$\Lambda(M) = \{\gamma : [0,1] \to M \mid \gamma(1) = \gamma(0)\}$$

or equivalently, $\Lambda(M) = C(\mathbb{S}^1, M)$, the space of continuous maps of $\mathbb{S}^1$ into M.

If we consider the quotient of the based loop space up to homotopy, in the case of ordinary closed loops, we obtain the fundamental group:

$$\Omega(M,x)/_\sim = \pi_1(M,x)$$

In the case of relative loops, taking the quotient with respect to homotopy does not result in a group, but a torsor which we call the **relative fundamental torsor** of M with respect to the basepoint x, denoted $\pi_1^g(M,x)$.

$$\Omega^g(M,x)/_\sim = \pi_1^g(M,x)$$

Remark 2.1.3. A **torsor**, sometimes also called a **principal homogeneous space** for a group G, is a set X on which the group G acts both freely and transitively, so that for any x, y in X there exists a unique $g \in G$ such that $g \cdot x = y$. A familiar example is the way in which an affine space is related to a vector space - here, the affine space corresponds to the torsor and the vector space to the group.

The fundamental group $\pi_1(M, x)$ acts on $\pi_1^g(M, x)$ by composition, with $\gamma \in \pi_1(M, x)$ taking a homotopy class of paths from x to gx to a different class of paths, given by passing along γ first, then the path to gx. This action is free, since the action is defined up to homotopy and two homotopic paths will be given by the action of homotopic loops. It is transitive, since π_1 is the set of all possible homotopy classes, and π_1^g all paths, and any path may be mapped to any other path by the action of composition with some loop.

The relative fundamental torsor consists of homotopy classes of paths running from x to gx. It does not have a group structure like the usual fundamental group, since paths do not return to the same point, so there is no natural way to compose two paths. It can be given a group structure by choosing a path τ_x which runs from x to gx. Then, by travelling along a path which is an element of π_1^g and returning via τ_x, we have an element of π_1. Hence, the choice of τ_x gives us an identification of the torsor with the underlying fundamental group, where τ_x corresponds to the identity element. This allows us to multiply two elements of π_1^g together, by mapping both to the fundamental group and composing the two elements under the multiplication there, before mapping back to the torsor. The result of this operation depends on the choice of τ_x. The structure of π_1^g and more concrete notation for these maps is outlined in Section 2.3.1.

These spaces consist of paths which are not closed loops but run between two distinct points. We will later find it useful to denote such a space in generality by $\mathcal{P}(Y, Y_1, Y_2)$ where Y_1 and Y_2 are subspaces of Y. This denotes the space of paths in Y which start at a point in Y_1 and end at a point in Y_2.

Next, we will set out some notation which will be of use.

2.2 Paths and loops

In general, the letters $\gamma, \delta, \sigma, \lambda$ will be used to denote loops and paths as necessary. Additionally, we have specific notation for certain useful paths, namely ω and τ_x, described below.

A path from x to an alternative basepoint $y \in M$ will be called ω, and we will use the notation $\omega : x \rightsquigarrow y$ to mean ω runs from x to y, or more strictly $\omega : ([0,1], 0, 1) \to (M, x, y)$. In order to reduce the number of elements which must be chosen, we must choose such a path $\omega : x \rightsquigarrow z$ for each z in M, and then we can select a path between any two points in M, by travelling via the point x. We will, when it is necessary to specify the start and endpoints, denote a path from y to z by ω_{yz}.

The reverse of any loop or path γ will be denoted $\overline{\gamma}$, and means the same path traversed in the opposite direction. The reverse of a path is the inverse of the path as an element of the fundamental group or relative fundamental torsor, in the sense that composition of the path with its inverse is homotopic to the trivial path.

The composition of two paths γ, δ will be denoted $\gamma * \delta$, which means travelling along γ then along δ.

$$\gamma * \delta(t) = \begin{cases} \gamma(2t) & t \in [0, \frac{1}{2}] \\ \delta(2t-1) & t \in [\frac{1}{2}, 1] \end{cases}$$

A path from x to its image gx will be denoted τ_x, so we may write $\tau_x : x \rightsquigarrow gx$. We may also make use of $\tau_y : y \rightsquigarrow gy$, which may be defined in terms of τ_x in order to simplify the maps. Given $\omega : x \rightsquigarrow y$, we set $\tau_y = \overline{\omega} * \tau_x * g\omega$, which runs from y to gy via x and gx. In this way, a single choice of τ_x gives a canonical choice of path from any point to its image, given our already chosen path ω from x to that point. This can be seen in Figure 2.1.

This method of choosing paths then allows us to find τ_y in terms of τ_z, by $\tau_y = \overline{\omega_{yz}} * \tau_z * g\omega_{yz}$ provided our path ω_{yz} from y to z is that which travels via x, as discussed previously.

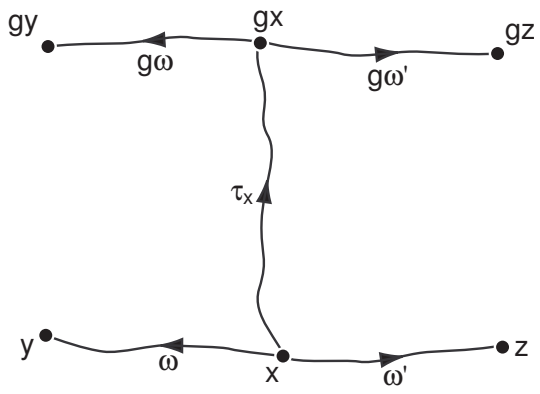

Figure 2.1: Finding τ_y and τ_z given τ_x

Indeed, let ω be a path from x to y, and ω' a path from x to z. Then $\tau_y = \overline{\omega} * \tau_x * g\omega$, then we can rearrange to obtain $\tau_x = \omega * \tau_y * \overline{g\omega}$. Substituting into $\tau_z = \overline{\omega'} * \tau_x * g\omega'$, we obtain $\tau_z = \overline{\omega'} * \omega * \tau_y * \overline{g\omega} * g\omega'$, which is equal to $\overline{(\overline{\omega} * \omega')} * \tau_y * g(\overline{\omega} * \omega')$. Here, $(\overline{\omega} * \omega')$ is a path from y to z, and hence is our ω_{yz} above. This is also easily seen in Figure 2.1.

2.3 Maps of the fundamental group

2.3.1 Some standard maps

All of the following maps may be defined on spaces of paths which run from one point to another - although they are described here as maps between relative fundamental torsors, since they induce maps which send homotopy classes of paths to other homotopy classes of paths.

Given a path $\omega : [0,1] \to M$ which runs from $x \in M$ to $y \in M$, and an appropriate loop or path $\gamma : [0,1] \to M$ for which $\gamma(1) = x$, we define $\omega_*(\gamma) = \gamma * \omega$ - that is, we travel along the path γ and then along ω. We may replace ω with its reverse, giving the map $\overline{\omega}_*(\gamma) = \gamma * \overline{\omega}$, for which we need $\gamma(1) = y$ in order for the path to be well-defined. We will also define $\widehat{\omega}_*(\gamma) = \omega * \gamma$, where the path ω is travelled along first, in which case we require $\gamma(0) = y$, and similarly $\widehat{\overline{\omega}}_*(\gamma) = \overline{\omega} * \gamma$ when $\gamma(0) = x$.

Remark 2.3.1. The maps $\overline{\omega}_*$ and $\widehat{\overline{\omega}}_*$ are the inverses of the maps ω_* and $\widehat{\omega_*}$. While

strictly $\overline{\omega}_* \circ \omega_* \neq id$, the loop resulting from applying these two maps will be homotopic to the original loop. The same holds for $\widehat{\overline{\omega}}_* \circ \widehat{\omega_*}$. The maps can be thought of as inverses when they induce maps on $\pi_1^g(M,x)$, since $\overline{\omega} * \omega$ is homotopic to the constant loop.

Under this notation, we may note that, given a path $\tau_x : x \rightsquigarrow gx$, τ_{x*} and its inverse $\overline{\tau_{x*}}$ induce maps between $\pi_1(M,x)$ and $\pi_1^g(M,x)$, and hence these are the maps which define the structure on $\pi_1^g(M,x)$ relative to the ordinary group structure on $\pi_1(M,x)$. Indeed, for γ, δ in $\pi_1^g(M,x)$, we can write their composition as:

$$\gamma \circledast \delta = \tau_{x*}(\overline{\tau_{x*}}(\gamma) * \overline{\tau_{x*}}(\delta))$$

Here $\overline{\tau_{x*}}(\gamma), \overline{\tau_{x*}}(\delta)$ are elements of $\pi_1(M,x)$ and can be composed as ordinary group elements, and then the whole thing is mapped back into $\pi_1^g(M,x)$ by applying τ_{x*}.

In order to clarify in the following the difference between composition of paths and composition of elements of the relative fundamental torsor, we will use the symbol $\circledast$ as above to denote this operation. This is the binary operation analagous to composition of group elements, and determines a group structure on π_1^g. Again, the definition of this group structure depends on a choice of τ_x.

We may verify the group structure on $\pi_1^g(M,x)$. For example, $\circledast$ is associative. For γ, δ and σ in $\pi_1^g(M,x)$, we have:

$$\begin{aligned}
(\gamma \circledast \delta) \circledast \sigma &= \tau_{x*}(\overline{\tau_{x*}}(\tau_{x*}(\overline{\tau_{x*}}(\gamma) * \overline{\tau_{x*}}(\delta))) * \overline{\tau_{x*}}(\sigma)) \\
&= \tau_{x*}(\overline{\tau_{x*}}(\gamma * \overline{\tau_x} * \delta * \overline{\tau_x}) * \tau_x) * (\sigma * \overline{\tau_x})) \\
&= \gamma * \overline{\tau_x} * \delta * \overline{\tau_x} * \not{\tau_x} * \not{\overline{\tau_x}} * \sigma * \not{\overline{\tau_x}} * \not{\tau_x} \\
&= \gamma * \overline{\tau_x} * \delta * \overline{\tau_x} * \tau_x * \overline{\tau_x} * \sigma
\end{aligned}$$

And also:

$$\begin{aligned}
\gamma \circledast (\delta \circledast \sigma) &= \tau_{x*}(\overline{\tau_{x*}}(\gamma) * \overline{\tau_{x*}}(\tau_{x*}(\overline{\tau_{x*}}(\delta) * \overline{\tau_{x*}}(\sigma)))) \\
&= \tau_{x*}((\gamma * \overline{\tau_x}) * \overline{\tau_{x*}}(\delta * \overline{\tau_x} * (\sigma * \overline{\tau_x}) * \tau_x)) \\
&= \gamma * \overline{\tau_x} * \delta * \overline{\tau_x} * \tau_x * \overline{\tau_x} * \sigma * \not{\overline{\tau_x}} * \not{\tau_x} * \not{\overline{\tau_x}} * \not{\tau_x} \\
&= \gamma * \overline{\tau_x} * \delta * \overline{\tau_x} * \tau_x * \overline{\tau_x} * \sigma
\end{aligned}$$

These are equal, since we may cancel τ_x with $\overline{\tau_x}$ up to homotopy, and hence we have associativity.

It is also worth noting that while these maps are defined here in the language of specific paths running from one point to another, they induce maps on the spaces of homotopy classes of such paths. When referring to 'an element γ of π_1', we will often denote by γ the homotopy class of paths containing γ. In cases where ambiguity arises, the homotopy class may be denoted $[\gamma]$ and the specific path γ.

Given a choice of ω (which specifies the two maps ω_* and $\widehat{\omega_*}$), we can define another map, denoted $\Phi_\omega : \pi_1(M,x) \to \pi_1(M,y)$, which acts by $\Phi_\omega(\gamma) = \overline{\omega} * \gamma * \omega$, and similarly $\Phi_{\overline{\omega}}(\gamma) = \omega * \gamma * \overline{\omega}$. This map gives a change of basepoint, for $\omega : x \rightsquigarrow y$, from $\pi_1(M,x)$ to $\pi_1(M,y)$. Note that $\Phi_\omega = \widehat{\overline{\omega}}_* \circ \omega_*$, and $\Phi_{\overline{\omega}} = \widehat{\omega}_* \circ \overline{\omega}_*$. Here $\circ$ denotes composition of maps.

All of the maps given above between the fundamental groups and relative fundamental torsors at different basepoints are isomorphisms. Given these maps, and two basepoints $x, y \in M$, with M path connected, we may construct the diagram seen in Figure 2.2.

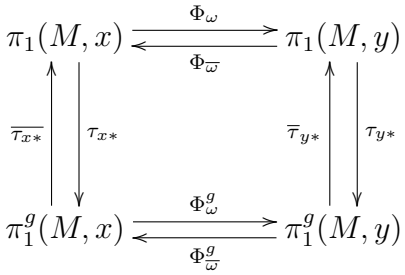

Figure 2.2: The maps between the fundamental groups and relative fundamental torsors based at x and y

Here, the map Φ^g_ω is a modification of Φ_ω where we map γ to $\overline{\omega} * \gamma * g\omega$, and this gives a map between the two relative fundamental torsors. It may be noted also that $\Phi^g_\omega = \widehat{\overline{\omega}}_* \circ \omega^g_*$, where ω^g_* is the map given by $\gamma \mapsto \gamma * g\omega$.

For different choices of ω, we obtain different isomorphisms Φ_ω between $\pi_1(M,x)$ and $\pi_1(M,y)$. We also have:

Proposition 2.3.2. *If $\pi_1(M)$ is an abelian group, for M path connected, then the*

map Φ_ω is independent of the choice of ω.

Proof. Let M be such that $\pi_1(M,x)$ is abelian, and let ω, ω' be paths from $x \in M$ to $y \in M$. Here $\sim$ denotes homotopy equivalence. Then, for an equivalence class γ in $\pi_1(M,x)$,

$$\begin{aligned}\Phi_\omega \circ \Phi_{\overline{\omega'}}(\gamma) &\sim \overline{\omega} * (\omega' * \gamma * \overline{\omega'}) * \omega \\ &\sim (\overline{\omega} * \omega') * \gamma * (\overline{\omega'} * \omega) \\ &\sim (\overline{\omega} * \omega') * (\overline{\omega'} * \omega) * \gamma\end{aligned}$$

(since $\pi_1(M,x)$ is abelian, and $(\overline{\omega} * \omega')$, $(\overline{\omega'} * \omega)$ are elements of $\pi_1(M,x)$)

$$\sim \gamma$$

Hence, Φ_ω and $\Phi_{\omega'}$ are equal. □

We may now prove the following:

Proposition 2.3.3. *The diagram given in Figure 2.2 above, using a choice of τ_y defined in terms of τ_x and ω as described earlier, commutes.*

Proof. Let us take an element γ of $\pi_1(M,x)$, a homotopy class of loops, and take its image under each of the maps around the diagram, until we return to $\pi_1(M,x)$.

$$\begin{aligned}\gamma &\in \pi_1(M,x) \\ \tau_{x*}(\gamma) &= \gamma * \tau_x \in \pi_1^g(M,x) \\ \Phi_\omega^g(\tau_{x*}(\gamma)) &= \Phi_\omega^g(\gamma * \tau_x) = \overline{\omega} * (\gamma * \tau_x) * g\omega \in \pi_1^g(M,y) \\ \overline{\tau}_{y*}(\Phi_\omega^g(\tau_{x*}(\gamma))) &= \overline{\omega} * (\gamma * \tau_x) * g\omega * \overline{\tau_y} \in \pi_1(M,y) \\ \Phi_{\overline{\omega}}(\overline{\tau}_{y*}(\Phi_\omega^g(\tau_{x*}(\gamma)))) &= \omega * \overline{\omega} * (\gamma * \tau_x) * g\omega * \overline{\tau_y} * \overline{\omega} \in \pi_1(M,x) \\ &= \gamma * \tau_x * g\omega * \overline{\tau_y} * \overline{\omega}\end{aligned}$$

Now, given that $\tau_y = \overline{\omega} * \tau_x * g\omega$, we have

$$\begin{aligned} &= \gamma * \tau_x * g\omega * (\overline{\overline{\omega} * \tau_x * g\omega}) * \overline{\omega} \\ &= \gamma * \tau_x * g\omega * (\overline{g\omega} * \overline{\tau_x} * \omega) * \overline{\omega} \\ &= \gamma * \tau_x * \not{g\omega} * \not{\overline{g\omega}} * \overline{\tau_x} * \not{\omega} * \not{\overline{\omega}} \\ &= \gamma * \tau_x * \overline{\tau_x} \\ &= \gamma \end{aligned}$$

And hence the diagram commutes. □

2.3.2 Loops based at gx

The map Φ_{τ_x} will act as a change of base point map from $\pi_1(M, x)$ to $\pi_1(M, gx)$. In this case, we have a similar diagram to that above, seen in Figure 2.3, and again we assume M is path connected.

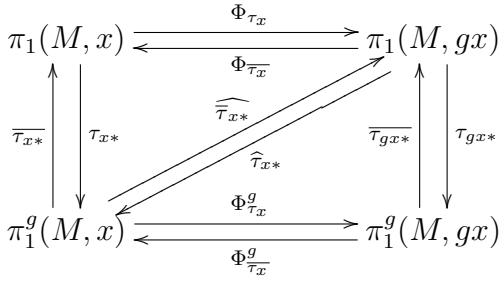

Figure 2.3: The maps between the fundamental groups and relative fundamental torsors based at x and gx

This diagram also now incorporates the map τ_{gx*} and its inverse, which are defined in terms of a path τ_{gx}, which runs from gx to its image g^2x. If g is a transformation of order greater than two, this will, in general, be distinct from x. The logical choice of τ_{gx}, in order to simplify calculations and ensure this diagram commutes, is $g(\tau_x)$, the image of the path τ_x we have already chosen under the map g. This ensures that the map $\Phi^g_{\tau_x}$ is equal to $\widehat{\overline{\tau}_{x*}} \circ \tau_{gx*}$, since $\widehat{\overline{\tau}_{x*}} \circ \tau_{gx*}(\gamma)$ is given by $\overline{\tau}_x * \gamma * \tau_{gx}$, which is the same as $\overline{\tau_x} * \gamma * g(\tau_x)$, which is how $\Phi^g_{\tau_x}$ is defined.

Proposition 2.3.4. *The diagram in Figure 2.3 also commutes, given a choice of* τ_x.

Proof. Since we have already proved that the outer ring of the diagram commutes for a change of basepoint from x to y, $y = gx$ is just a special case of this. Hence, it suffices to prove the maps running diagonally in this second diagram commute with those on the outer ring. Consider an element $\gamma \in \pi_1(M, x)$.

$$\begin{aligned}
\gamma &\in \pi_1(M, x) \\
\Phi_{\tau_x}(\gamma) &= \overline{\tau}_x * \gamma * \tau_x \in \pi_1(M, gx) \\
\widehat{\tau}_{x*}(\Phi_{\tau_x}(\gamma)) &= \widehat{\tau}_{x*}(\overline{\tau}_x * \gamma * \tau_x) = \tau_x * (\overline{\tau}_x * \gamma * \tau_x) \in \pi_1(M, gx) \\
&= \gamma * \tau_x \in \pi_1^g(M, x) \\
\overline{\tau_{x*}}(\gamma * \tau_x) &= \gamma * \tau_x * \overline{\tau}_x \in \pi_1(M, x) \\
&= \gamma
\end{aligned}$$

Hence we are back to our original element. Since all the maps are isomorphisms and the square outer ring commutes, the whole diagram commutes. □

The maps $\widehat{\tau}_{x*}$ and $\widehat{\overline{\tau}_{x*}}$ are maps between $\pi_1^g(M, x)$ and $\pi_1(M, gx)$, which work in an analogous way to the maps τ_{x*} and $\overline{\tau_{x*}}$, except instead of interpreting composition of paths from x to gx by considering loops based at x, we instead consider loops based at gx, the other end of the path. This allows us, in a similar way to that defined using loops at x, to impose another kind of group structure on $\pi_1^g(M, x)$ given the existing group structure on $\pi_1(M, gx)$.

Proposition 2.3.5. *The group structure induced on $\pi_1^g(M, x)$ from $\pi_1(M, x)$ via the maps τ_{x*} and $\overline{\tau_{x*}}$ is the same as that drawn from $\pi_1(M, gx)$ via the maps $\widehat{\tau}_{x*}$ and $\widehat{\overline{\tau}_{x*}}$.*

Proof. This follows from Proposition 2.3.4, and that Φ_{τ_x} is an isomorphism between $\pi_1(M, x)$ and $\pi_1(M, gx)$ - if the composition of two elements from $\pi_1^g(M, x)$ is mapped to a particular element in $\pi_1(M, x)$, then under the isomorphism it will be the same as that mapped to in $\pi_1(M, gx)$. Similarly, the identity of $\pi_1^g(M, x)$ will be τ_x under either structure. □

2.4 Equivariant fundamental group

Let M be a manifold, and let G be a finite group acting on M. Let us define

$$\pi_1^G(M,x) = \{([\gamma], g) \mid \gamma : [0,1] \to M \text{ s.t } \gamma(0) = x,\ \gamma(1) = gx,\ g \in G\}$$

Here $[\gamma]$ denotes a homotopy class of paths running from x to gx. This construction is called the **equivariant fundamental group** of M with respect to the group G.

It is indeed a group, with structure as follows:

- The identity element of $\pi_1^G(M,x)$ is a pair $([e], id)$ where e denotes the trivial loop based at x, and id the identity transformation.

- The operation in the equivariant fundamental group is given by, for paths γ, δ and $g, h \in G$:

$$([\gamma], g) \cdot ([\delta], h) = ([\gamma * g\delta], gh)$$

Here $\gamma : x \rightsquigarrow gx$, $\delta : x \rightsquigarrow hx$ and $\gamma * g\delta : x \rightsquigarrow ghx$, as seen in Figure 2.4.

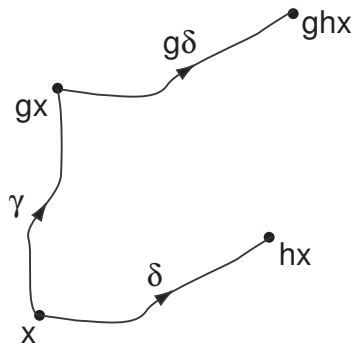

Figure 2.4: The operation in the equivariant fundamental group

- The inverse of an element is given by

$$([\gamma], g)^{-1} = ([g^{-1}\overline{\gamma}], g^{-1})$$

Then we have

$$([\gamma], g) \cdot ([g^{-1}\overline{\gamma}], g^{-1}) = ([\gamma * gg^{-1}\overline{\gamma}], gg^{-1}) = ([e], id)$$

We may note that there exists a homomorphism $\beta : \pi_1^G(M,x) \to G$ given by

$$\beta : ([\gamma], g) \mapsto g$$

In this case, $\ker \beta = \pi_1(M,x)$ since this is the subgroup of π_1^G corresponding to $g = id$. We then have that the following sequence is exact:

$$1 \longrightarrow \pi_1(M,x) \longrightarrow \pi_1^G(M,x) \xrightarrow{\beta} G \longrightarrow 1$$

Remark 2.4.1. The equivariant fundamental group can also be defined for G an infinite group. However, not all of the following results will still hold. Since all of the examples we will be considering use a finite G, assume G is always finite.

Remark 2.4.2. In the field of equivariant homotopy, there exists a construction called the equivariant fundamental group, which is the first homotopy group of the so-called Borel space for the action of G on M, usually denoted M_G. In fact, in the case where G is a discrete group, it is the same as our equivariant fundamental group, and hence we will use this name without confusion.

Depending on how G acts on M, we have the following results.

Proposition 2.4.3. *Let G be a finite group acting on a manifold M.*

1. *If G acts freely on M, then $\pi_1^G(M,x) \simeq \pi_1(M/G, \bar{x})$, where $\bar{x}$ is the orbit of x under the action of G*

2. *If G fixes some $x \in M$, that is, $gx = x$ for every $g \in G$, then*

$$\pi_1^G(M,x) \simeq \pi_1(M,x) \rtimes G$$

where the G-action is given by

$$\rho_g : \pi_1(M,x) \to \pi_1(M,x), \quad \rho_g : [\gamma] \mapsto g([\gamma])$$

3. *If $K \lhd G$ and K acts freely on M, then $\pi_1^G(M,x) \simeq \pi_1^{G/K}(M/K, \bar{x})$, where $\bar{x}$ is the orbit of x under the action of K.*

Proof. 1. Consider M as a covering space for M/G. The point $x \in M$, as well as the points gx for $g \in G$, will sit above $\bar{x}$ in the covering and be mapped to $\bar{x}$ under the projection map p.

Since we have a covering, the map p is a local homeomorphism, and so we have by the path lifting property (see [15], p.60) that loops based at $\bar{x}$ in M/G may be lifted to paths running between two of the gx for $g \in G$, and these lifts may always be found, since the action of G on M is free. That is, for a path in M/G based at $\bar{x}$, it may be lifted to a path in M, and this path will be continuous as the action has no fixed points.

The free action also ensures that under the assumption that we lift the start of the path to $x \in M$, this lift may be chosen uniquely, and the lifted paths will end at gx, for some $g \in G$. Since the action is free, g is uniquely determined by the path.

We also know that by the homotopy lifting property, there exist homomorphisms

$$\pi_1^G(M,x) \underset{\text{lifting } \ell}{\overset{\text{projection } p}{\rightleftarrows}} \pi_1(M/G,\bar{x})$$

which are well defined on homotopy classes of paths and loops.

The compositions $p \circ \ell$ and $\ell \circ p$ both exist and are equal to the identity map in their respective domains. A uniquely chosen lift will project down to the same original loop, and the image of a path may always be lifted to the original path. Hence, $\pi_1^G(M,x) \simeq \pi_1(M/G,\bar{x})$ since we have isomorphism.

2. First, note that elements of $\pi_1^G(M,x)$ will be a pair $([\gamma],g)$ where $[\gamma] \in \pi_1(M,x)$, since x is fixed by G, so $[\gamma] : x \rightsquigarrow gx$ is actually $[\gamma] : x \rightsquigarrow x$. So we have that $\pi_1^G(M,x)$ has the elements of $\pi_1(M,x) \times G$.

We may also note that G acts on $\pi_1(M,x)$ by automorphism, where, as stated earlier,

$$\rho_g : [\gamma] \mapsto g([\gamma]), \quad \rho_g : \pi_1(M,x) \to \pi_1(M,x)$$

It takes elements of $\pi_1(M,x)$ to elements of $\pi_1(M,x)$, since in this case x is a fixed point of the action and so $gx = x$ and $g^2x = gx = x$ for all g.

The product in $\pi_1^G(M,x)$ is given by

$$([\gamma], g) \cdot ([\delta], h) = ([\gamma * g\delta], gh)$$

Since $\rho_g(\delta) = g\delta$, this means the product is exactly $([\gamma * \rho_g(\delta)], gh)$, and hence we have a semidirect product.

3. The proof of this follows largely as the proof of part (1), but now our covering is given by $M \to M/K$, where K acts freely on M. Since $K \lhd G$, the action of G on M induces an action of G/K on M/K by sending Kx to $Kgx = gKx$. The point $x \in M$, as well as the points kx for $k \in K$, will sit above $\bar{x} = Kx$ in the covering and be mapped to Kx under the projection map p.

   Since the map p is a local homeomorphism, we have by the path lifting property that paths from $\bar{x} \rightsquigarrow h(\bar{x})$, for some $h \in G/K$, may be lifted to paths running from $x \rightsquigarrow g(x)$ for some $g \in G$ for which $g \in Kh$, and these lifts may always be found, since the action of K on M is free. The free action also ensures that under the assumption that we lift the start of the path to $x \in M$, this lift may be chosen uniquely, and the lifted paths will end at khx, for a unique $k \in K$. Since the action is free, k is uniquely determined by the path.

   We also know that by the homotopy lifting property, there exist homomorphisms

$$\pi_1^G(M,x) \underset{lifting\ \ell}{\overset{projection\ p}{\rightleftarrows}} \pi_1^{M/G}(M/K, \bar{x})$$

   which are well defined on homotopy classes of paths and loops.

   The compositions $p \circ \ell$ and $\ell \circ p$ both exist and are equal to the identity map in their respective domains. A uniquely chosen lift will project down to the same original path, and the image of a path may always be lifted to the original path. Hence, $\pi_1^G(M,x) \simeq \pi_1^{M/G}(M/K, \bar{x})$ since we have isomorphism.

□

The following examples illustrate the use of Proposition 2.4.3.

Example 2.4.4. 1. Let $M = \mathbb{R}^2 \setminus \{a, b\}$, the twice punctured plane (considered again in Section 2.6.2, Key examples).

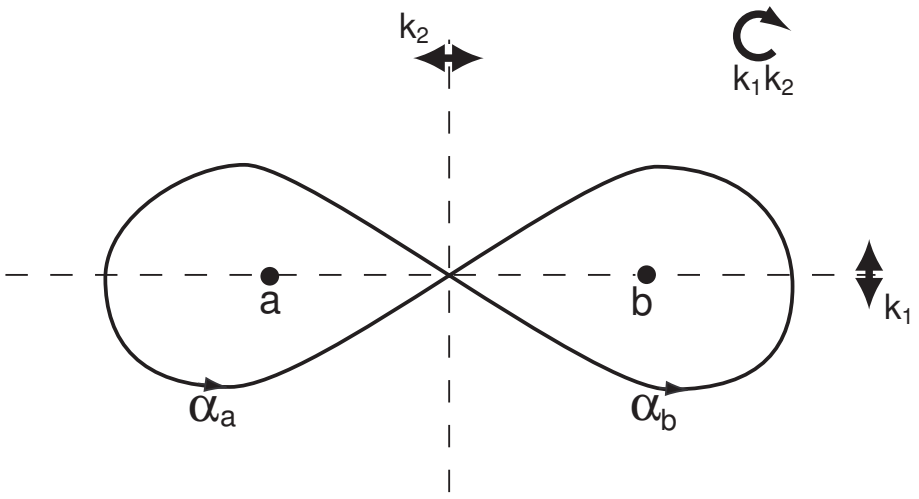

Figure 2.5: The twice punctured plane, with symmetries

Let $G = \mathbb{Z}_2 \times \mathbb{Z}_2$ be the group acting on the space, generated by the reflections κ_1 and κ_2, as shown in Figure 2.5. Without loss of generality, we may consider the two removed points to be arranged as shown. Then, κ_1 fixes a and b, and κ_2 and the rotation $\kappa_1\kappa_2$ both swap a and b over.

The centre of the plane, x_0 is a fixed point of the action of G, and so by Proposition 2.4.3(2), we have

$$\pi_1^G(M, x_0) \simeq \pi_1(M, x_0) \rtimes G$$

Here $\pi_1(M, x_0) = \mathbb{F}_2$, the free group on two generators, which is generated by the loops α_a and α_b, as shown in Figure 2.5. This means $\pi_1^G(M, x_0) \simeq \mathbb{F}_2 \rtimes (\mathbb{Z}_2 \times \mathbb{Z}_2)$.

The action of $\mathbb{Z}_2 \times \mathbb{Z}_2$ on $\mathbb{F}_2$ is given as follows: κ_1 sends α_a and α_b to their inverses, the rotation $\kappa_1\kappa_2$ swaps the two generators, and κ_2 sends α_a to the inverse of α_b and vice versa.

2. Now let $M = \mathbb{R}^2 \setminus \{a, b, c\}$, the thrice punctured plane, and let the three punctures be arranged so as to be collinear, as shown in Figure 2.6(a).

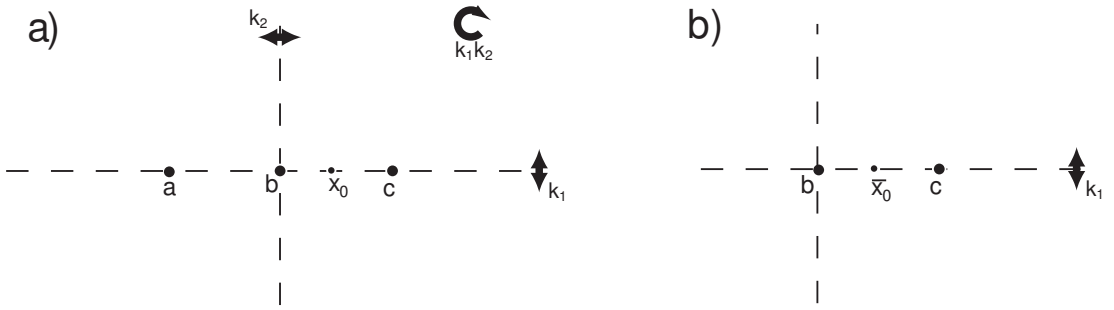

Figure 2.6: (a) The thrice punctured plane, with symmetries (b) The quotient space by $\mathbb{Z}_2$

Again we consider the action of $G =< \kappa_1, \kappa_2 > \simeq \mathbb{Z}_2 \times \mathbb{Z}_2$ on this space, but in this case the action has no fixed points, since the point b is removed.

Now consider the group $G = \langle \kappa_1, \kappa_2 \rangle = \{id, \kappa_1, \kappa_2, \kappa_1\kappa_2\}$ and in particular consider the subgroup $K = \langle \kappa_1\kappa_2 \rangle$. This is a normal subgroup of G, since G is abelian. The quotient space M/K, shown in Figure 2.6(b), is the quotient of $\mathbb{R}^2 \setminus \{a, b, c\}$ under the rotation by π given by $\kappa_1\kappa_2$. This means that points a and c are identified, and b remains in place. The base point x_0 is replaced by $\overline{x_0}$, also denoted Kx_0, which is a pair of points opposite each other either side of b. The action of K on this M/K is free, since its only fixed point is again b which is removed. The cosets $\kappa_1 K$ and $\kappa_2 K$ are equal, and the two reflections are equivalent in this quotient space.

Then, by Proposition 2.4.3(1), we have that

$$\pi_1^G(M, x_0) \simeq \pi_1^{G/K}(M/K, \overline{x_0})$$

That is,

$$\pi_1^{\mathbb{Z}_2\times\mathbb{Z}_2}(M, x_0) \simeq \pi_1^{\mathbb{Z}_2\times\mathbb{Z}_2/\mathbb{Z}_2}(M/\mathbb{Z}_2, \overline{x_0})$$

The quotient space M/K is the twice punctured plane. If we choose our base-point $\overline{x_0}$ to be a point on the horizontal axis between b and c, it is fixed under the action of $G/K \simeq \mathbb{Z}_2$ (acting by κ_1 reflection), and so we can then use Proposition 2.4.3(2) to find

$$\pi_1^{\mathbb{Z}_2\times\mathbb{Z}_2/\mathbb{Z}_2}(M/\mathbb{Z}_2, \overline{x_0}) \simeq \pi_1(M/\mathbb{Z}_2, x_0) \rtimes G/K$$

So we have

$$\pi_1^G(M, x_0) \simeq \pi_1(\mathbb{R}^2 \setminus \{b, c\}, x_0) \rtimes \mathbb{Z}_2 = \mathbb{F}_2 \rtimes \mathbb{Z}_2$$

where the action of $\mathbb{Z}_2$ on the free group is by κ_1 reflection, which sends each of the generators to its inverse.

This gives us the short exact sequence:

$$1 \longrightarrow \pi_1(M, x) \longrightarrow \pi_1^G(M, x) \xrightarrow{\beta} G \longrightarrow 1$$

$$1 \longrightarrow \mathbb{F}_3 \longrightarrow \mathbb{F}_2 \rtimes \mathbb{Z}_2 \xrightarrow{\beta} \mathbb{Z}_2 \times \mathbb{Z}_2 \longrightarrow 1$$

We can understand the maps involved in this sequence by considering the way in which the generators of each group are acted on.

Here $\mathbb{F}_2 \rtimes \mathbb{Z}_2$ is generated by a loop around b and a loop around c, each based at x_0. The $\mathbb{Z}_2$ part indicates whether the loop goes from x_0 to itself, or from x_0 to its image under κ_1, which is the same point.

The $\mathbb{F}_3$ is generated by three loops, based at x_0 and each passing around only one of the three punctures. This is mapped into $\mathbb{F}_2$ by the way the rotation $\kappa_1\kappa_2$ quotients the plane. We find the loop around c goes to itself, b goes to b^2 (since to go around b in the full plane, we go from x_0 to a point which is the image of x_0 under κ_1 and then back to x_0) and a goes to bcb^{-1}. These three elements of $\mathbb{F}_2$ generate a copy of $\mathbb{F}_3$ as a normal subgroup.

The map β takes an element $([\gamma], g)$ of $\pi_1^G(M, x)$ to the element g in $\mathbb{Z}_2 \times \mathbb{Z}_2$.

2.5 Reidemeister conjugacy

In the case of ordinary loop spaces, we have the following.

Lemma 2.5.1. *Conjugacy classes in the usual fundamental group $\pi_1(M, x)$ correspond to connected components of the free loop space $\Lambda(M)$.*

Proof. If we have a pair of homotopy classes of loops based at x, called $\alpha, \beta \in \pi_1(M, x)$, then the element $\alpha * \beta * \overline{\alpha}$ will be conjugate to β in π_1. This element can

be seen to be in the same connected component of $\Lambda(M)$ as a loop representing β, since we need simply move the basepoint x along the loop α, which we may do in the space of free loops, to obtain a path to β. □

In the case of relative loops, we may consider a 'twisted' conjugacy, which we call Reidemeister conjugacy.

Definition 2.5.2. For a group H, if we consider a map $\phi : H \to H$ which is an automorphism, then we can construct a 'twisted' conjugacy by, for $h, h' \in H$, $h \sim h' \Leftrightarrow$ there exists $j \in H$ such that $h = j * h' * \phi(j)^{-1}$. The equivalence classes under such a type of conjugacy are called **Reidemeister conjugacy classes** (with respect to the automorphism ϕ). In the case where ϕ is the identity map, this is just usual conjugacy.

We may find the Reidemeister conjugacy classes of the relative fundamental torsor $\pi_1^g(M, x)$, with a group structure donated from the fundamental group by choice of ω, with respect to the automorphism ϕ defined by the transformation $g \in G$ as it acts on paths in $\pi_1^g(M, x)$. That is, for γ a path in M,

$$\phi : \pi_1^g(M, x) \to \pi_1^g(M, x), \phi(\gamma(t)) = g\gamma(t)$$

Reidemeister conjugacy in this case is given by:

$$\delta \sim \sigma \Leftrightarrow \text{ there exists } \gamma \in \pi_1^g(M, x) \text{ such that } \delta = \gamma \circledast \sigma \circledast \overline{g\gamma},$$

where the operation $\circledast$ is as previously defined - by mapping the paths from $x \rightsquigarrow gx$ into the space of closed loops, then composing them, and mapping the result back. We find that this twisted form of conjugacy is very useful in the case of relative loops.

Theorem 2.5.3. *Two elements δ, σ of $\pi_1^g(M, x)$, the relative fundamental torsor of M based at x, are in the same Reidemeister conjugacy class of $\pi_1^g(M, x)$, with ϕ defined as above, (that is, there exists $\gamma \in \pi_1^g(M, x)$ such that $\delta = \gamma \circledast \sigma \circledast \overline{g\gamma}$), if and only if δ and σ are in the same connected component of the free relative loop space, $\Lambda^g(M)$ of paths in M whose endpoints are related by g.*

Proof. ($\Rightarrow$)

Let δ, σ, γ be such that $\sigma = \gamma \circledast \delta \circledast \overline{g\gamma}$. Let us calculate the result of composing these three elements of $\pi_1^g(M,x)$. That is,

$$\sigma = \tau_{x*}(\overline{\tau_{x*}}(\gamma) * \overline{\tau_{x*}}(\delta) * \overline{\tau_{x*}}(\overline{g\gamma})).$$

First we must note that while δ and γ are defined elements of $\pi_1^g(M,x)$, it is not clear what is meant by $\overline{g\gamma}$, or indeed $\overline{\tau_{x*}}(\overline{g\gamma})$, since it is not obviously an element of $\pi_1^g(M,x)$. First, given γ we apply g, which gives an element of $\pi_1^g(M,gx)$. We then need to find its inverse, so we map it into $\pi_1(M,gx)$ using $\overline{\tau_{gx*}}$, which gives $g\gamma * \overline{\tau}_{gx}$, a loop based at gx. Its inverse is $\overline{g\gamma * \overline{\tau}_{gx}}$, and this is then mapped into $\pi_1(M,x)$ by $\Phi_{\overline{\tau_x}}$, giving the element $\tau_x * \overline{(g\gamma * \overline{\tau}_{gx})} * \overline{\tau}_x$, which is our $\overline{\tau_{x*}}(\overline{g\gamma})$ as required.

We may now calculate σ as given above.

$$\begin{aligned}
\sigma &= \tau_{x*}(\overline{\tau_{x*}}(\gamma) * \overline{\tau_{x*}}(\delta) * \overline{\tau_{x*}}(\overline{g\gamma})) \\
&= \tau_{x*}((\gamma * \overline{\tau}_x) * (\delta * \overline{\tau}_x) * (\tau_x * \overline{(g\gamma * \overline{\tau_{gx}})} * \overline{\tau_x})) \\
&= \gamma * \overline{\tau}_x * \delta * \not{\tau}_x * \not{\tau}_x * \overline{(g\gamma * \overline{\tau_{gx}})} * \not{\tau_x} * \not{\tau}_x \\
&= (\gamma * \overline{\tau}_x) * \delta * \overline{(g\gamma * \overline{\tau_{gx}})}
\end{aligned}$$

The last part of this, to the right of δ, is a path from gx to itself, and it is easily seen that it is the image under g of the inverse of the path $\gamma * \overline{\tau}_x$, a loop at x. This means that this object consists of the path δ from x to gx, with a loop at each end, which are inverses up to the action of g. This is illustrated in Figure 2.7. We can use this to construct a homotopy between this object, which from the above is equal to σ, and δ, by taking the objects σ_s in which $s \in [0,1]$ and each σ_s is given by the path travelling along δ plus adding the sections of the loops at each end of δ given by travelling a distance of s along each. This gives a homotopy in Λ^g, as required, since both endpoints of such paths will always be related by g.

($\Leftarrow$)

Let σ_s be a homotopy between σ and δ. Then, the path $\sigma_s(0)$ may be used in place of γ to show that the two paths are Reidemeister conjugate in $\pi_1(M,x)$. $\square$

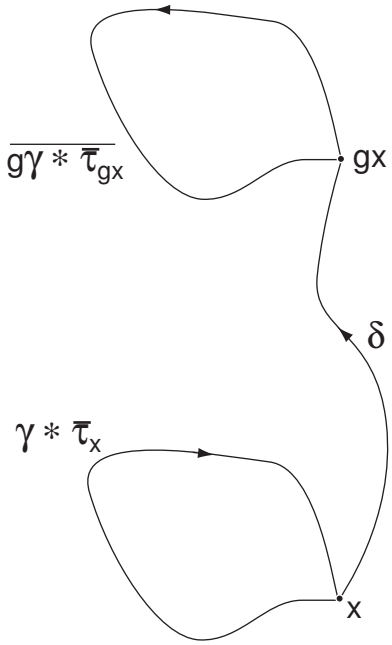

Figure 2.7: The resulting path $\sigma = \gamma \circledast \delta \circledast \overline{g\gamma}$, which is homotopy equivalent to δ

Remark 2.5.4. This result is the same as Theorem 2.1 from [24], where it is expressed in a different way, without defining Reidemeister conjugacy classes as such. For a more detailed analysis, see Section 6.4.

2.5.1 Reidemeister conjugacy and the equivariant fundamental group

The notion of Reidemeister conjugacy is also connected with π_1^G, the equivariant fundamental group. Consider the short exact sequence:

$$\pi_1(M,x) \to \pi_1^G(M,x) \xrightarrow{\beta} G$$

The map β maps $(\gamma, g) \in \pi_1^G(M,x)$ to $g \in G$. For a given $g \in G$, we may find $\beta^{-1}(g) \subset \pi_1^G(M,x)$. This is a subset of π_1^G consisting of $\{(\gamma,g)|\gamma(0) = x, \gamma(1) = gx\}$ up to homotopy.

In fact, it is a coset of $\pi_1(M,x)$ and can easily be seen to be equal to $\pi_1^g(M,x)$, where $\pi_1^g = \omega_*(\pi_1)$, for $\omega : x \rightsquigarrow gx, \omega \in \pi_1^g$.

Proposition 2.5.5. *Reidemeister conjugacy in the torsor $\pi_1^g(M,x) \simeq \beta^{-1}(g)$ is ordinary conjugacy in $\pi_1^G(M,x)$, the equivariant fundamental group.*

That is, if two elements in π_1^g are Reidemeister conjugate, then their images in π_1^G under the inclusion map will be conjugate.

Proof. Let δ, σ be two Reidemeister conjugate elements of $\pi_1^g(M,x)$, so that $[\delta] = [\gamma * \sigma * \overline{g\gamma}]$ in the relative fundamental torsor. Now consider the images of δ and σ in $\pi_1^G(M,x)$, denoted $([\delta], g)$ and $([\sigma], g)$. There exists an element in $\pi_1^G(M,x)$ which conjugates these elements to each other under usual conjugacy, namely $([\gamma], e)$, where e is the identity element of G. Then

$$\begin{aligned} ([\gamma], e)([\sigma], g)([\bar{\gamma}], e) &= ([\gamma * \sigma], g)([\bar{\gamma}], e) \\ &= ([\gamma * \sigma * \overline{g\gamma}], g) \end{aligned}$$

This is the element of $\pi_1^G(M,x)$ corresponding to $[\gamma * \sigma * \overline{g\gamma}]$ in $\pi_1^g(M,x)$, and since this is equal to $([\sigma], g)$ we have conjugacy in $\pi_1^G(M,x)$, as required. □

2.6 Key examples

2.6.1 n-body problems

An important motivating example in which we study the spaces of loops defined on a manifold is that of n-body problems. If we consider the problem of n particles moving in $\mathbb{R}^d$, and we wish to exclude any case where a collision of one or more particles occurs, we find of interest the space

$$M = (\mathbb{R}^d)^n \setminus \Delta = \{\underline{x} = (\underline{x}_1, \ldots, \underline{x}_n) \mid \underline{x}_i \in \mathbb{R}^d, \underline{x}_i \neq \underline{x}_j \text{ for all } i \neq j\}$$

This space then consists of all valid arrangements of n particles in $\mathbb{R}^d$, and paths in this space will describe motion of the particles. Closed loops here will be closed orbits in which all of the particles trace out individual paths, without colliding, and return to their original positions.

The space M is the complement of a subspace arrangement, so we remove from $(\mathbb{R}^d)^n$ all the linear subspaces corresponding to collisions between one or more particles.

Remark 2.6.1. In the case $d = 2$, in which we will mainly be working, we will use the notation

$$X^{(n)} = (\mathbb{R}^2)^n \setminus \Delta$$

That is, $X^{(n)}$ denotes M in the case where $d = 2$.

We may consider the space $X^{(n)}$ as a the complement of a complex hyperplane arrangement. The diagonal set of collisions Δ is made up of complex hyperplanes $H_{ij} \subset \mathbb{C}^n = (\mathbb{R}^2)^n$ defined by the equations $z_i = z_j$, such that $\Delta = \bigcup H_{ij}$. Such spaces may be easier to work with. In general, we do not have the complement of a hyperplane arrangement, since the codimension is not 1.

In this work, we will frequently be working in $X^{(n)}$, using planar configurations of particles, rather than the more general case. The space $X^{(n)}$ has fundamental group P_n, the **pure braid group** on n strands (proven below in Proposition 2.6.2). The pure braid group on n strands is sometimes called the **coloured braid group**. This is the normal subgroup of the braid group in which each strand returns to its original position. There exists an inclusion of P_n into B_n, the full braid group on n strands, since every element of P_n already exists there, and we can also define a projection map φ from B_n into S_n, the group of permutations on n objects. Each braid in B_n is mapped to the permutation corresponding to the final arrangement of the strands once the braid has been applied. The pure braid group will be equal to the kernel of this map, since $\varphi(p) = id$ for all $p \in P_n$, and if $\varphi(p) \neq id$ then $p \notin P_n$.

We have a short exact sequence:

$$1 \longrightarrow P_n \longrightarrow B_n \longrightarrow S_n \longrightarrow 1$$

2.6.1.1 Presentation of the pure braid group - the case $n = 3$

The pure braid group on three strands can be presented as:

$$P_3 = \left\langle a_{12}, a_{13}, a_{23} \mid a_{12}^{-1} a_{23} a_{12} = a_{13} a_{23} a_{13}^{-1} = a_{13} a_{23} a_{13} a_{23}^{-1} a_{13}^{-1} \right\rangle$$

Here, the three generators a_{ij} correspond to strands i and j being fully twisted around each other once and returning to their original positions. In usual braid notation,

where σ_i denotes a braid passing strand i over strand $(i+1)$, and where $*$ denotes composition in the braid group, such twists can be written

$$\begin{aligned} a_{12} &= \sigma_1 * \sigma_1 \\ a_{23} &= \sigma_2 * \sigma_2 \\ a_{13} &= \sigma_2^{-1} * \sigma_1 * \sigma_1 * \sigma_2 \end{aligned}$$

It is important to note that a_{13}, which is a twisting together of the first and third strands, requires the seconds strand to be moved off to one side in order to perform the twist. It is irrelevant whether this strand moves to the left or right, and the braid $\sigma_1 * \sigma_2 * \sigma_2 * \sigma_1^{-1}$ is equal to a_{13} as a braid. However, it is significant that the middle strand sits behind the other two - a braid which performs the same action but with the middle strand in front, such as $\sigma_2 * \sigma_1 * \sigma_1 * \sigma_2^{-1}$ or its equivalent $\sigma_1^{-1} * \sigma_2 * \sigma_2 * \sigma_1$ is not equal to the generator a_{13} (in fact such a braid is equal to $a_{23} * a_{13} * a_{23}^{-1}$).

In the notation given by these generators, the full twist, an element which commutes with every element in the braid group, is written $a_{12} * a_{13} * a_{23}$. This will also commute with every pure braid.

In the general case of n strands, the set of generators of the pure braid group is given by (from [22]):

$$a_{ij} = \sigma_{j-1}\sigma_{j-2}\ldots\sigma_{i+1}\sigma_i^2\sigma_{i+1}^{-1}\ldots\sigma_{j-2}^{-1}\sigma_{j-1}^{-1} \text{ for } 1 \leq i < j \leq n$$

that is, a_{ij} wraps the ith strand around the jth strand. The group relations are given by

$$a_{rs}^{-1} a_{ij}\, a_{rs} = \begin{cases} a_{ij} & \text{if } i < r < s < j \text{ or } r < s < i < j \\ a_{rj} a_{ij}\, a_{rj}^{-1} & \text{if } r < i = s < j \\ a_{rj} a_{sj} a_{ij}\, a_{sj}^{-1} a_{rj}^{-1} & \text{if } i = r < s < j \\ a_{rj} a_{sj} a_{rj}^{-1} a_{sj}^{-1} a_{ij}\, a_{sj} a_{rj} a_{sj}^{-1} a_{rj}^{-1} & \text{if } r < i < s < j \end{cases}$$

Proposition 2.6.2. *The space $X^{(n)}$ as defined above has fundamental group P_n, the pure braid group on n strands.*

Proof. We have $X^{(n)} = (\mathbb{R}^2)^n \setminus \Delta$. Loops in this space will consist of motions of the n particles in the plane which return to their original positions.

Consider the map which takes such motions to a corresponding braid, by plotting the evolution of the two-dimensional system in three dimensions, with time on a third axis as shown in Figure 2.8.

The starting points of the particles are regularly spaced along the x axis, and their paths run along in the direction of the z axis. Strands may cross over and under each other in the y dimension whenever the particles move around each other in the plane. If we take a cross sectional slice through parallel to the xy plane, we obtain a single position of the n points in the plane - this can be thought of as a snapshot of an instant of motion. Looking down in the y direction, we see usual braid diagrams, where strands pass over or under each other as they would in a braid diagram. This defines a map between such motions and the diagrams of braids, up to homotopy. We can map any existing braid to a motion of the particles in this way also.

Any closed motion of particles (one returning to its original configuration) will be homotopic to some braid in the pure braid group. Hence, this is the fundamental group of the space. □

Figure 2.8 does not show a closed loop - it illustrates the braid denoted $\sigma_1^2\sigma_2^{-1}$. Given a motion of particles, it is possible to express this as a braid in the notation

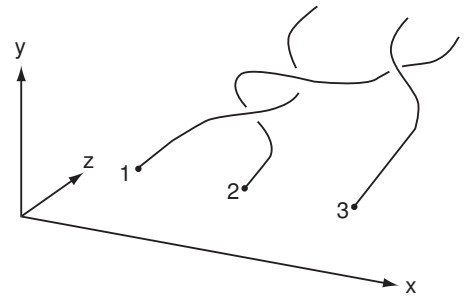

Figure 2.8: The braid denoted $\sigma_1^2\sigma_2^{-1}$.

$\sigma_i^{x_i}\sigma_j^{x_j}\ldots$ by choosing and fixing a line of reference, and then numbering the particles from left to right with respect to this baseline - by drawing perpendicular lines to this baseline. Then, at any point during the motion if any particle passes above another

with respect to the baseline, this counts as the relevant braid generator.

For example, if the left most particle passes above the second particle, this is σ_1. The particles are renumbered from left to right after each generator. Continue naming braid generators in this way until the end of the motion. This will give a braid which corresponds to the motion, with respect to that baseline.

If it happens that two pairs of particles pass above or below each other at the same time, then choose another baseline with respect to which the crossings occur at slightly different times.

The majority of our work here will be considering the case of n particles in $\mathbb{R}^d$, and in particular the case where $d = 2$ - where the particles move in a plane.

2.6.2 k-centre problems

Another case to which we may apply such considerations is that commonly called the k-centre problem. In this we consider the motion of a single particle, in a space where k particles are fixed. The configuration space is k-times punctured Euclidean space. We study the planar case; topologically, this means we are considering the motion of the particle in the k-times punctured plane:

$$M = (\mathbb{R}^2 \setminus \{a_1, a_2, \ldots, a_k\})$$

Here $a_1, a_2, \ldots, a_k \in \mathbb{R}^2$ are distinct points which are removed to form our k punctures.

The k-times punctured plane $\mathbb{R}^2 \setminus \{a_1, \ldots a_k\}$ is a topological space homotopic to the wedge of k circles, with fundamental group $\mathbb{Z} * \mathbb{Z} * \ldots * \mathbb{Z}$, the free group on k generators. If we consider the possible curves traced out by a single free particle in this space, then we are considering loops in the k-times punctured plane, and hence elements of this fundamental group.

We may apply our study of group actions to this system as for the n-body problem - the arrangement of the punctures will determine which symmetries of the plane need to be considered.

For example, if we consider the twice punctured plane ($k = 2$) with a single particle moving in the space $M = \mathbb{R}^2 \setminus \{a, b\}$, we may (without loss of generality) assume the points sit on the horizontal axis, an equal distance either side of the vertical axis, to make symmetries easier to define. Then the space has the symmetry group of a rectangle, that is, the dihedral group D_2, consisting of a rotation by π and two reflections, in the horizontal and vertical axes.

In the case $k = 3$, there are different arrangements of punctures to consider - different symmetries are present if the three points are collinear or if they sit at the points of a triangle. Example 2.4.4 from page 31 earlier in this section considers the 2- and 3-times punctured plane.

The different possible symmetry groups will lead to different relative loop spaces, although for a given value of k the spaces will have the same fundamental group.

2.7 Examples of Reidemeister conjugacy classes

Here we consider the example of three bodies in $\mathbb{R}^2$, with the transformation g being reflection in the horizontal axis, which we will denote κ_1. We will calculate the Reidemeister conjugacy classes in this case.

In this case, $M = \mathbb{R}^{2\times 3} \setminus \Delta$, and the fundamental group $\pi_1(M, x)$ here is the pure braid group on three strands, P_3. Generators of P_3 are $a_{12} = \sigma_1^2$, $a_{23} = \sigma_2^2$ and $a_{13} = \sigma_2^{-1}\sigma_1^2\sigma_2$. We must first determine how κ_1 acts on each of these generators.

When we interpret a motion of particles as a braid, we must choose an axis in the plane to interpret as the direction of the x-axis as seen in Figure 2.8. In this case, we choose the horizontal axis, which means any time the leftmost particle passes above the centre particle relative to this axis, we count it as being an instance of the braid generator σ_1. Hence, the braid σ_1^2, which corresponds to the leftmost two particles passing around each other anticlockwise in a circle, is mapped to σ_1^{-2}, its inverse, under the action of κ_1. Similarly, $\kappa_1(\sigma_2^2) = \sigma_2^{-2}$. The third braid generator, $\sigma_2^{-1}\sigma_1^2\sigma_2$, is mapped to $\sigma_2\sigma_1^{-2}\sigma_2^{-1}$. This is not equal to the inverse of a_{13}, since the reflection κ_1 turns each σ_i into its own inverse but does not change the ordering of the

generators, whereas inverting reverses the order. We in fact have that $\kappa_1(a_{12}) = a_{12}^{-1}$, $\kappa_1(a_{23}) = a_{23}^{-1}$, and $\kappa_1(a_{13}) = a_{23} \cdot a_{13}^{-1} \cdot a_{23}^{-1}$.

This then allows us to calculate the Reidemeister conjugacy classes of pure braids. For instance, a braid γ would be Reidemeister conjugate to a braid $a_{12} \cdot \gamma \cdot \overline{\kappa_1(a_{12})}$, which based on our calculation above would be $a_{12} \cdot \gamma \cdot a_{12}$. We in fact have

$$\begin{aligned} \gamma &\sim a_{12} \cdot \gamma \cdot a_{12} \\ \gamma &\sim a_{23} \cdot \gamma \cdot a_{23} \\ \gamma &\sim a_{13} \cdot \gamma \cdot a_{23}^{-1} \cdot a_{13} \cdot a_{23}^{-1} \end{aligned}$$

However, we must note that $\overline{\kappa_1(a_{12}a_{23})} = a_{23}a_{12}$, not $a_{12}a_{23}$. Indeed,

$$\gamma \sim a_{12} \cdot a_{23} \cdot \gamma \cdot a_{23} \cdot a_{12}$$

Also,

$$\begin{aligned} \gamma &\sim a_{23} \cdot a_{13} \cdot a_{12} \cdot \gamma \cdot a_{12} \cdot (a_{23} \cdot a_{13} \cdot a_{23}^{-1}) \cdot a_{23} \\ &\sim a_{23} \cdot a_{13} \cdot a_{12} \cdot \gamma \cdot a_{12} \cdot a_{23} \cdot a_{13} \end{aligned}$$

Hence, any braid is Reidemeister conjugate under the action of κ_1 to a braid which has the arrangements of generators as specified above, with a_{12} and a_{23} mirroring each other, and a_{13} as shown. Hence the Reidemeister classes will each contain distinct 'core' braids which do not have this property, and cannot have such generators 'cancelled' from either end.

By Proposition 2.5.5, we have that the Reidemeister conjugacy in this case is just ordinary conjugacy in $\pi_1^{\mathbb{Z}_2}(X^{(3)}, x)$, where the map ϕ defining the Reidemeister conjugacy classes is given by composition with τ_x, a path from $x \rightsquigarrow gx = \kappa_1 x$.

Chapter 3

Choreographies

When considering the motivating example of n-body problems and particle dynamics, we will mainly be considering a subset of n-body solutions which possesses a specific kind of symmetry. These solutions are called **choreographies**. In this chapter we will define a choreography, and give some examples, as well as constructing a framework of group representations which allow us to describe the properties of such an orbit in terms of its spatial, temporal and labeling symmetries.

3.1 Definition of a choreography

We define a choreography as follows:

Definition 3.1.1. A periodic solution of the n-body problem is said to be a **choreography** if each of the n particles trace the same curve in space, with a fixed time delay and without colliding.

Such orbits are visually quite attractive, and the term 'choreography' was coined by Simó (see [30]) on noting the way the particles seem to dance around each other in a fixed pattern.

If we denote the orbit of a system with n particles by γ , we may write

$$\gamma(t) = (x_1(t), x_2(t), \ldots, x_n(t))$$

In this notation, the condition for such a path to be a choreography can be written

$$\gamma(t) = (x(t), x(t + {}^{T}/_{n}), x\left(t + {}^{2T}/_{n}\right), \ldots, x\left(t + \frac{(n-1)T}{n}\right)$$

Here T denotes the time taken for each particle to complete one full orbit. Each particle x_k follows the same path as the particle x_{k+1}, and particle x_n follows x_1.

We proceed by giving some examples to solidify the notion of a choreography, as well as applying symmetry constraints to systems of particles, including that imposed by the condition of being a choreography. We also attempt a classification of all orbits satisfying the choreography constraint.

3.2 Basic examples

The **circular choreography** is one of the simplest examples of a choreography, and consists of n masses moving with constant velocity on a circle of fixed radius, centred at the centre of mass of the system. The example of three bodies as the three points of an equilateral triangle rotating with constant velocity on its circumscribing circle was found by Lagrange in 1772. In the case of more than three masses, this is replaced by a regular n-gon.

Another example of note is the **figure eight**, discovered by Chenciner and Montgomery (see [12]), consisting of three particles moving on a figure eight shape.

Example 3.2.1 (Three particles on a figure eight)**.** The figure eight choreography, shown in Figure 3.1, was discovered by Chenciner and Montgomery [12] and is one of the simplest examples of a choreographic motion. The particles visit all three'Euler' configurations, where the three particles are collinear, during the course of an orbit.

The figure eight curve has the symmetry group of a rectangle, which is generated by the vertical reflection κ_1 and the horizontal reflection κ_2, and includes the rotation by π, $\kappa_1\kappa_2$.

Much more complicated choreographical motions have been shown to exist, and many have been found numerically, including long chains of loops, flowers, foils, and

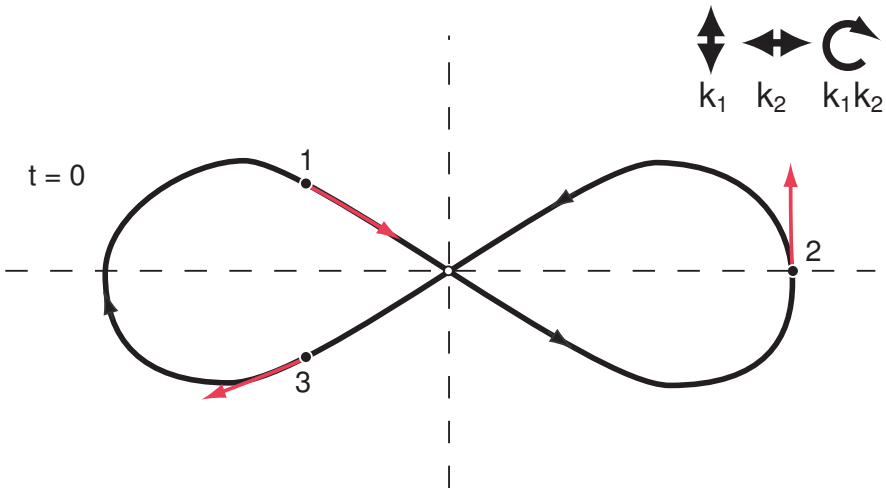

Figure 3.1: Three particles on a figure eight, at $t = 0$

even shapes which possess no rotational or reflectional symmetries as a curve. Many examples of such choreographies will also be studied later.

3.3 Types of choreography

The following definitions are due to Chenciner et al (see [11]).

Definition 3.3.1. A **simple choreography** is one as defined in Definition 3.1.1, in which all masses move on the same curve.

A **double, or multiple choreography** is a choreography in which the bodies separate into two or more groups, and the bodies of each group form a simple choreography. Two bodies in the same group move on the same curve, exchanging their position after a fixed period of time, which is the same for all groups.

Definition 3.3.2. We say two choreographies are **equivalent** if they move on similar curves, with the same number of particles, and if the motions described are the same but with a different value of $t = 0$ or length of period.

A **satellite choreography** is a non-equivalent choreography which is derived from an existing choreography. A **main choreography** is one which is not the satellite of any other choreography.

Satellite choreographies can be found from any main choreography in a number of ways:

- Subharmonics – travelling around the same curve a multiple of times
- Varying the angular momentum, resulting in a very long period choreography which looks like the other one being slowly rotated – as an example, see Figure 5.1 from [11] which has a figure eight shape which precesses and forms a closed curve after 37 passes along the figure eight.
- Combinations of the above

Transformations, such as reflections, rotations, rescaling or phase shift result in equivalent choreographies. In each of the examples we study, we will select an arrangement of particles corresponding to $t = 0$ and a spatial orientation of the curve which gives the simplest calculations - for instance, so that reflectional symmetries occur in coordinate axes where possible.

In most of our work we will be considering primarily simple choreographies which are of main type, unless otherwise stated.

3.4 Properties of choreographies

The definition of a choreography leads on to some interesting results.

Proposition 3.4.1. *In a choreography, for $n \leq 5$ and $d = 2$, all n particles must be of the same mass.*

Proof. See [9], Proposition 3. □

Additionally, in the same paper, Chenciner proves in Proposition 4 that for $n = 6$ the only way the bodies could be not of all equal mass is if they are in two groups which are each themselves choreographies with the same centre of mass. A double choreography of this type can be seen in Example 7.1.1 of six particles on a star of David, on page 145, although it is considered with all masses equal.

Chenciner also proves in Proposition 5 of [9] that the planar relative equilibrium solutions of Lagrange, featuring points at the corners of a regular n-gon, must also have equal masses for all $n > 3$.

3.5 Symmetries of the n-body problem

In order to study n-body orbits and in particular, choreographies, it has been useful to adopt the method given by Ferrario and Terracini in [14], which is described here using notation conventions which have been adapted to suit our existing notation.

We may consider the group of symmetries G acting on a given system of n particles moving in $\mathbb{R}^d$ by taking three representations, as detailed below. We also require that G be a finite group.

- A representation $\rho : G \to O(d)$, which provides information about what $g \in G$ does to the $\mathbb{R}^d$ in which the particles are moving. The transformation $\rho(g)$ can be a rotation or a reflection. For $d = 2$, the elements $\rho(g)$ for $g \in G$ will sit in some dihedral group, a subgroup of $O(2)$.

  As an example, if our choreography is on the regular figure eight curve in the plane ($d = 2$), it possesses the same spatial symmetries as a rectangle, and so the $\rho(g)$ will be from $D_2 = \langle a, b \mid a^2 = b^2 = 1, ab = ba \rangle$, consisting of a rotation by π, and two reflections, in the horizontal and vertical axes.

  When $d > 2$, the number of possible symmetry groups becomes very large. Even for $d = 3$, there are seven infinite families of 3-dimensional point groups, and seven others.

  While we do not extensively consider any examples with $d \geq 3$ in this thesis, there have been discovered choreography type motions in three dimensions, such as Hip-hop orbits (see [2]) in which the symmetry group of the curve is a subgroup of a cylindrical symmetry group, with a symmetry plane perpendicular to the axis of rotation.

  Remark 3.5.1. We have specified that G is a finite group. This specifically

excludes the example of n particles on a circle, described earlier, since the group of symmetries of a circle in the plane is $O(2)$ and not finite. All of the other examples of choreographies in the plane we will discuss have finite G.

The example of the circle is considered in more detail in Example A.2.4 on page 168.

- A representation $\tau : G \to O(2)$, the group of symmetries of the time circle $\mathbb{T}$. To distinguish between the two different copies of $O(2)$ involved we will write $\tau : G \to \hat{\mathbb{S}}^1$. This representation provides information about what $g \in G$ does to the time circle $\mathbb{T} \simeq \mathbb{S}^1$. Since choreographies are closed periodic orbits, we may consider time to run as $t \in [0, T]$, and if we identify 0 with T, we call this circle $\mathbb{T}$. We will use T to denote the time taken for one complete orbit, and in all of our examples we take $T = 2\pi$, to make the time circle easier to visualise. Again, $\tau(g)$ will in many of our examples sit in some dihedral subgroup of $O(2) = \hat{\mathbb{S}}^1$ for a given choreography; although which dihedral group will vary with n and with the degree of symmetry of the curve.

  We define the following types of symmetry based on the nature of $\tau(g)$. We say a symmetry is **time reversing** if $\tau(g)$ is a reflection, such as $\tau(g) : t \mapsto -t$, or $\tau(g) : t \mapsto -t + {}^{kT}/_{n}$. Otherwise, it is **non-time reversing**.

  We also define a symmetry to be **time preserving** if $\tau(g) : t \mapsto t$, that is, $\tau(g)$ is the trivial transformation of $\mathbb{T}$. These types of symmetry will become important tools in studying the curve $\gamma(t)$.

- A representation $\sigma : G \to S_n$, where n is the number of particles, giving information about how $g \in G$ acts to permute the n different copies of $\mathbb{R}^d$ when the symmetry is applied. In fact, since the order in which the particles move on the curve cannot change, for a simple choreography this permutation can only ever be an n-cycle or a product of disjoint transpositions which corresponds to fully reversing the order of the particles, as in a reflection. Hence, we can think of σ as $\sigma : G \to D_n \subset S_n$.

Remark 3.5.2. In the case of multiple choreographies, the restriction to a dihedral subgroup applies to the subset of the particles on each curve. So, for example, if there are two sets of five particles, each moving on a different curve, the permutations will be elements of $D_5 \times D_5$, as a subgroup of S_{10} with the natural inclusion (by one copy of D_5 acting on particles 1-5, and the other on 6-10).

Since the nature of the permutation $\sigma(g)$ will be related to the action of $\rho(g)$ on the space, the type of permutation (cyclic (rotation) or involution (reflection)) will be the same for each component of a multiple choreography, since the action of $\rho(g)$ affects them all in the same way.

The action of all three of these representations on a curve $\gamma(t) = (x_1(t), x_2(t), \ldots, x_n(t))$ may be written

$$(x_1(t), x_2(t), \ldots, x_n(t)) \mapsto$$

$$(\rho(g)x_{\sigma(g)(1)}(\tau(g)t), \rho(g)x_{\sigma(g)(2)}(\tau(g)t), \ldots, \rho(g)x_{\sigma(g)(n)}(\tau(g)t))$$

That is, the position of each particle is moved by the transformation $\rho(g)$ which acts on the space $\mathbb{R}^d$ in which the particles live; the n copies of $\mathbb{R}^d$ in which the particles live (and hence the particles) are permuted by the permutation $\sigma(g)$; and the time circle is acted on by $\tau(g)$.

If a group element g is to be a symmetry of the path $\gamma(t)$, we must have that the left and right hand sides of the above mapping are equal.

Proposition 3.5.3. *For all elements $g \in G$, the symmetry $\rho(g)$ is a symmetry of the curve in $\mathbb{R}^d$ on which the particles travel. That is, if $\gamma(t)$ is a curve in $\mathbb{R}^d$ then for every t we have*

$$\rho(g) \cdot \gamma(t) = \gamma(t')$$

for some t'.

Proof. Let $g \in G$. We have

$$\gamma(t) = (x_1(t), x_2(t), \ldots, x_n(t))$$

For g to be a symmetry of this system, we must have that $\rho(g)$ maps each particle to a position where itself or some other particle either is at time t, or will be after some time delay; that is, some other point $\gamma(t')$ also on the curve. In fact, since whenever g is a symmetry of the curve, we have

$$x_i(t) = \rho(g) \cdot x_{\sigma(g)(i)}(\tau(g) \cdot t)$$

The point $x_i(t)$ is mapped by $\rho(g)$ to $x_{\sigma(g)(i)}(\tau(g) \cdot t)$. So, this will be on the curve $\gamma(\tau(g) \cdot t)$, and so t' in the above is $\tau(g) \cdot t$. □

We now consider an example of a symmetry g and determine the values of $\rho(g), \tau(g)$ and $\sigma(g)$.

Example 3.5.4. Let us consider the example of three particles moving on a figure eight, as shown in Figure 3.1 on page 46. Take $g_0 \in G$ to be the element for which $\rho(g_0) = \kappa_1$. Then we may find $\tau(g_0)$ by noting that this reflection reverses the direction in which the particles are moving on the curve, but it also maps all the particles onto the positions previously held by themselves or by other particles. Hence, its effect on the time circle contains no time shift, but does contain a reversal in direction. So we have $\tau(g_0) : t \mapsto -t$. Finally, the corresponding permutation can be seen to swap particles 1 and 3, and leave 2 fixed. So $\sigma(g_0) = (13)$.

3.5.1 The choreography symmetry

Since we are considering choreographies, a symmetry which will always be present in such cases, by the definition of a choreography, is that which we refer to as the **choreography symmetry**. It is given by g for which:

$$\rho(g) = id \qquad \tau(g) : t \mapsto t + {}^{T}/_{n} \qquad \sigma(g) = (12 \dots n)$$

This means that no transformation is applied to the space, but the particles are all pushed forward in time by ${}^{T}/_{n}$ – and, since the time delay for the motion of the particles is equal for each particle, this means that they are each moved round to the position previously occupied by the preceding particle. The corresponding permutation is the given n-cycle.

In order for a choreography to exist, we must therefore have that the group of symmetries of the system must contain as a subgroup the cyclic group generated by this element, which will have order n.

Lemma 3.5.5. *If $\rho(g)$ acts trivially, for some $g \in G$, then g must be a choreography symmetry. That is, $\tau(g)$ must act by $\tau(g) : t \mapsto t + {}^{kT}/_{n}$, and $\sigma(g)$ must be some power of the cyclic permutation $(12\ldots n)$ moving all n indices.*

Proof. Let g be a symmetry for which $\rho(g) = id$. Then, we need to show that $\sigma(g)$ is cyclic and moves all n indices, and that $\tau(g) : t \mapsto t + {}^{kT}/_{n}$.

Particles must be mapped to particles, and since there is no action of $\rho(g)$ moving the particles, this must either be trivially or by the movement of time. The only non-trivial way for τ to map all the particles directly on to each other is $\tau(g) : t \mapsto \pm t + {}^{kT}/_{n}$. However, since the action of $\rho(g)$ is trivial, there cannot be time reversal, since this would require a reflection or rotation of the curve to take place and so we have $\tau(g) : t \mapsto t + {}^{kT}/_{n}$.

Given this $\tau(g)$, and the fact that no $\rho(g)$ action moves the position of the particles, the resulting $\sigma(g)$ action must move each of the particles to the position they are moved to by $\tau(g)$, which is that they all move along the curve by some multiple of ${}^{T}/_{n}$. This will result in $\sigma(g)$ being a permutation which moves all n particles as required. Hence, we have a choreography symmetry. □

Any closed loop $\hat{\gamma}$ in the space M describing a motion of particles which satisfies the definition of a choreography may be considered as the composition of a series of relative loops $\gamma, g\gamma, g^2\gamma \ldots$ for which g is the choreography symmetry. That is, each segment of the full loop runs from a point x to its image gx (where the particles have all moved on to the next position), and from there to g^2x, the image of gx, and so on up to $g^n x = x$ (since the choroeography symmetry has order n). We will denote the full loop by $\hat{\gamma}$, and the segments by $\gamma, g\gamma, \ldots, g^i\gamma$. In our notation of the composition of relative loops, we write

$$\hat{\gamma} = \gamma \circledast g\gamma \circledast \cdots \circledast g^{n-1}\gamma$$

We may also examine the effects of other symmetries on the full loop $\hat{\gamma}$, in order to study the properties of choreographies possessing those symmetries.

3.5.2 Symmetries of the time circle

The action of elements of G on the progress of time along the curve is represented by $\tau(g)$, and manifested on the time circle, denoted $\mathbb{T}$ and running from 0 to $T = 2\pi$. Then, symmetries g for which $\tau(g)$ reverses time will correspond to reflections of this circle, and if $\tau(g)$ pushes time forward by some amount, this will be a rotation of $\mathbb{T}$.

Since for a given finite symmetry group G, there will only be finitely many such rotations and reflections, the time circle can in fact be thought of as a 'time polygon', an ℓ-sided figure where the number of sides ℓ will be dependent on the number of particles, and the degree of symmetry of the curve.

Note that, if the time polygon has an odd number of sides, all reflections of this shape will be conjugate to each other - their axes of reflection all pass through a vertex and the centre of an edge. If the number of sides is even, there will be two conjugacy classes of reflections, since some will have axes of reflection which pass through two vertices, and some will pass through the centres of two edges. This can easily be seen in Figure 3.2 on page 55, which shows the cases $\ell = 6$ and $\ell = 5$.

Lemma 3.5.6. *The order of the group G is equal to the number of particles n times the order of the group of spatial symmetries of the curve.*

Proof. Consider the representation ρ, as defined previously. By the first isomorphism theorem, we have that $|G| = |\mathrm{im}(\rho)| \times |\ker \rho|$.

By Proposition 3.5.5, we have that $|\ker \rho| = n$, since it consists only of the choreography symmetry. Additionally, $|\mathrm{im}(\rho)|$ is by definition the order of the group of spatial symmetries of the curve. Hence, the result holds. □

If the symmetry group of the curve is the dihedral group D_k of order $2k$, and the number of particles is n, then $\ell = kn$, which by the above is $\frac{|G|}{2}$.

Exceptions to this include curves with no time-reversing symmetries, such as Example 5.3.1(2) of three particles on a distorted figure eight shape, on page 131

- in which case the time circle is not a regular polygon, as it has only rotational symmetries, and in this case ℓ is not equal to $\frac{|G|}{2}$, but instead $\ell = |G|$. This includes cases where the curve possesses no symmetries at all, such as Example A.2.1 of six particles on a non-symmetrical figure, on page 158. Another exception is multiple choreographies, which display other properties, discussed in Section 7.1.

The other important exception to this is the case in which the choreography possesses a time-preserving symmetry, such as in the case of four particles on a super-eight. In this case, ℓ is given by $\frac{|G|}{2}$ divided by the order of $\ker \tau$. The time preserving symmetry divides the group into $|\ker \tau|$ cosets G_i, each of which is subject to our condition $\ell = \frac{|G_i|}{2}$. This is illustrated in Example 4.5.3 of four particles on a super-eight, on page 93 in the next section.

Table 3.1 shows the values of n, $2k$, ℓ and $|G|$ for the examples considered in this thesis. Entries marked with a dagger have time-preserving symmetries and hence $\ell = n$.

Table 3.1: The relationship between $|G|$, n, k and ℓ

Example	n	2k	ℓ	$\lvert G\rvert$
3 on a figure 8 (3.2.1)	3	4	6	12
† 4 on a super 8 (4.5.1)	4	4	4	16
4 on a trefoil (5.1.7)	4	6	12	24
5 on a 4-flower (5.1.10)	5	8	20	40
5 on a figure 8 (5.2.1)	5	4	10	20
5 on a 4-chain (5.2.3)	5	4	10	20
5 on a super 8 (5.2.2)	5	4	10	20
† 6 on a 3-flower (A.2.2)	6	6	6	36
6 on a non-symmetrical figure (A.1)	6	1	6	6
† 8 on a 4-flower (A.2.3)	8	8	8	64
9 on a bifurcated 6-chain (A.2.5)	9	2	9	18

Remark 3.5.7. The entry for 6 particles on a non-symmetrical figure (Example A.1) lists $2k$ as equal to 1. This curve has no non-trivial rotational or reflectional symmetries, and so it does not have D_k as its symmetry group for any k. The order of the group of symmetries is 1, and this fits with the conclusion of Lemma 3.5.6 that $|G|$ is n times the order of the symmetry group.

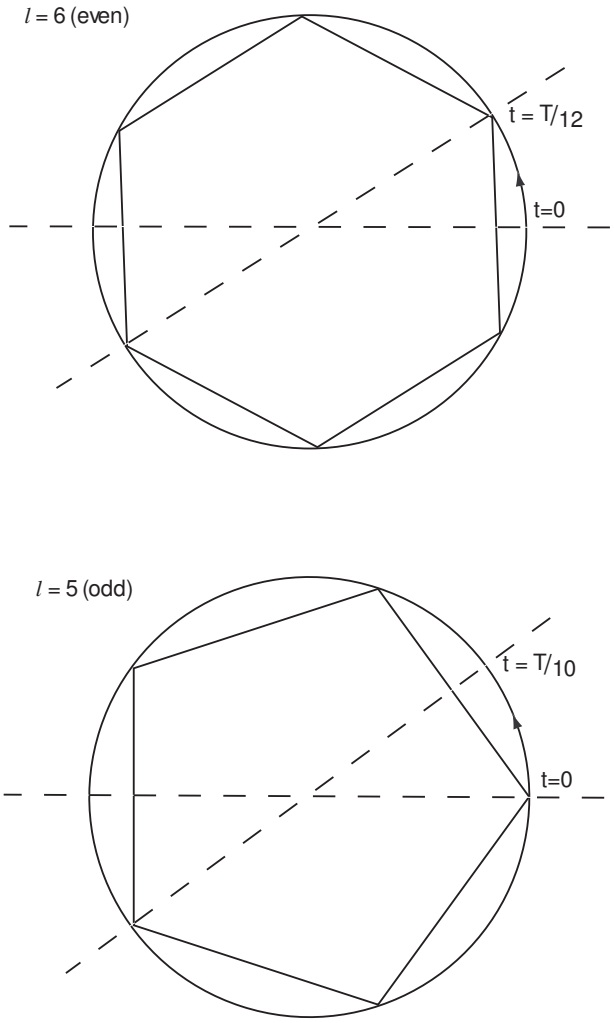

Figure 3.2: The time circle, shown as a 'time polygon' with five or six sides

Remark 3.5.8. In all of the examples listed in the table above, with one exception, the time polygon has an even number of sides, and hence there are two conjugacy classes of time reversing symmetries. The exception is Example A.2.5 on page 171 of nine particles on a bifurcated 6-chain, in which the symmetry is a single reflection (and hence $k = 1$), giving $\ell = kn = 9 \times 1 = 9$. Since ℓ is odd, this means that all reflections of the time circle (time reversing symmetries) are conjugate to each other. This can be seen in that all of the time reversing symmetries - the lower half of Table A.4 on page 175 - have the same cycle type in $\sigma(g)$, unlike most of our other examples, where there are two different cycle types present among the time reversals, such as in Table 4.2 on page 91 for four particles on a super-eight. An exception to this is when $n = 3$, for which D_n contains only one cycle type of involutions.

3.5.3 The full symmetry group

As proven in Lemma 3.5.6 in the section on the time circle, the order of G is given by the product of the number of particles n with the order of the group of symmetries of the curve.

For a given directed curve and number of particles, it is possible to determine the group of symmetries G, by writing a list of all the elements as a triple $[\rho(g), \tau(g), \sigma(g)]$ which exists as an element of $G \subset \Gamma = O(2) \times \hat{\mathbb{S}}^1 \times D_n$. We will use the following notation:

- For $\rho(g)$, write the element in terms of the generators - reflections κ_i, where by our convention κ_1 denotes a reflection in the horizontal axis, κ_2 denotes a reflection in the vertical axis, and κ_j for $j \geq 3$ are used to denote a reflection in an appropriate diagonal angled at a fraction of 2π (depending on the degree of rotational symmetry present). The identity element here will be denoted I.

- For $\tau(g)$, denote by A the map $\tau(g) : t \mapsto t+A$, and by $\overline{A}$ the map $\tau : t \mapsto -t+A$. Hence 0 is the identity, $\overline{0}$ is a time reflection about $t = 0$, $^T/_k$ is a pushing forward (rotation) of the time polygon by $^T/_k$, and $\overline{^T/_k}$ is a reflection on the time circle which fixes $^T/_{2k}$ and $^T/_2 + {}^T/_{2k}$, and so maps 0 to $^T/_k$.

- For $\sigma(g)$, which is an element of $D_n \subset S_n$, we use the disjoint cycle permutation notation (e.g. $(123), (12)(34)$) to describe how the particles are exchanged. We will use e to denote the identity element.

Here, we describe a method for creating a table of group elements for a given choreography, as seen in the examples given from now on.

The columns of the table are, from left to right: the symmetry of $\mathbb{R}^d$ given by $\rho(g)$; the symmetry of $\mathbb{T}$ given by $\tau(g)$; the permutation of the particles given by $\sigma(g)$; and in the fourth column, the order of the corresponding element g. Each row describes an element of the group G, and the tables have been obtained by the following method.

First, list the identity element $[I, 0, e]$, followed by the choreography symmetry $[id, {}^{T}/_{n}, (123...n)]$, and all powers of this element. This gives n group elements. Then the left column must be extended to contain all the symmetries of the curve (in the majority of cases, these will be the elements of some dihedral group) - for example, the group table for the figure eight lists all the elements of D_2, and that of the three-petal flower lists all elements of D_3. Each element in the left column will occur n times.

Next to each of these elements will be the action of $\tau(g)$ on the time circle, which in the case of a non-time reversing symmetry will be the value of t at which the spatial symmetry applies. If the symmetry is time reversing, the elements in the second column will be of the form $\overline{0}$ or $\overline{{}^{T}/_{k}}$. The value listed is that which gives both fixed points - if the fixed points are at ${}^{T}/_{2k}$ and ${}^{T}/_{2} + {}^{T}/_{2k}$, then this column will list $\overline{{}^{T}/_{k}}$.

The corresponding permutations will be written in the third column, where in the case of time reversing symmetries the permutation is that applicable at the fixed points (this will be the same at both fixed points).

Having completed the table, we are able to fully ascertain the structure of the group G, firstly by examining the total number of elements (this is the product of n with the order of the symmetry group of the curve) and then the order of the elements, which are written in a fourth column on the right. This allows us to determine the structure of the group.

The table is also useful in the process of determining the images and kernels of the maps ρ, τ and σ. Several illustrative examples will be given in the following sections, such as Example 3.2.1 of three particles on a figure eight, on page 45, and further examples may be found in the Appendix.

Example 3.5.9 (Three particles on a figure eight)**.** Table 3.2 shows the symmetry group for our previously considered example of three particles on a figure eight shape. The symmetries are those of a rectangle, giving four different entries in the $\rho(g)$ column. There are three particles, meaning three rows correspond to each entry. The

first three rows can be seen to correspond to the choreography symmetry.

This group has order 12, and a dihedral structure generated by the starred elements, and hence is the dihedral group D_6.

$\rho(g)$	$\tau(g)$	$\sigma(g)$	Order
I	0	e	1
I	$T/3$	(123)	3
I	$-T/3$	(132)	3
κ_1	$\overline{0}$	(13)	2
κ_1	$\overline{T/3}$	(12)	2
κ_1	$\overline{-T/3}$	(23)	2
$*\kappa_2$	$T/6$	(132)	6
κ_2	$T/2$	e	2
κ_2	$-T/6$	(123)	6
$\kappa_1\kappa_2$	$\overline{T/6}$	(23)	2
$*\kappa_1\kappa_2$	$\overline{T/2}$	(13)	2
$\kappa_1\kappa_2$	$\overline{-T/6}$	(12)	2

Table 3.2: Three particles on a figure eight - elements of the symmetry group

3.6 The maps ρ, σ and τ

For a group G which is the group of symmetries of some choreography, we may consider the interactions between the three representations ρ, σ and τ. We introduce a diagram of the form seen in Figure 3.3.

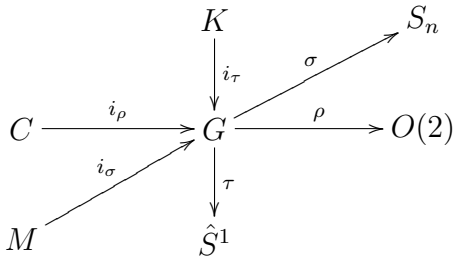

Figure 3.3: The maps ρ, σ and τ

Here, we see the representations and their images: $\rho : G \to O(2)$, $\sigma : G \to S_n$ and $\tau : G \to \hat{S}^1$. The diagram also shows the inclusion maps i_ρ, i_σ and i_τ from the kernels of the three maps, here denoted $C = \ker \rho$, $M = \ker \sigma$ and $K = \ker \tau$.

Information about these maps and their kernels may be determined by examining how the maps work and what they do to a given element of G. This allows us to examine the structure of G and the relationships between the maps. Recall that the action of G on a path $\gamma = (x_1(t), \ldots, x_n(t))$ may be written

$$g(x_1(t), \ldots, x_n(t)) = (\rho(g) \cdot x_{\sigma(g)\cdot(1)}(\tau(g) \cdot t), \ldots, \rho(g) \cdot x_{\sigma(g)\cdot(n)}(\tau(g) \cdot t)$$

- The image of σ will be either the dihedral group D_n or cyclic $\mathbb{Z}_n$, since it can only contain elements of S_n preserving the ordering of the particles. If there do not exist time reversing symmetries, then the image will be cyclic $\mathbb{Z}_n$. (This is proved in Proposition 4.1.2 on page 68).

- The image of ρ is either dihedral or cyclic, depending on the symmetries present.

- The image of τ will again be dihedral or cyclic, since it is a symmetry group of the polygon inherent in the time circle $\mathbb{T}$.

We may also analyse the kernels of the maps, leading to the following:

- $C = \ker \rho$ is always isomorphic to $\mathbb{Z}_n$, since by Proposition 3.5.5 we only have the choreography symmetry $t \mapsto t + {}^{T}/_{n}$, $(12 \ldots n)$, which generates $\mathbb{Z}_n$.

- $K = \ker \tau$ consists entirely of time preserving symmetries, meaning that if there are no time-preserving symmetries, we have $\mathrm{im}\tau \simeq G$. Examples of non-trivial K include Example 4.5.1 on page 88, of four particles on a super-eight, which has $K \simeq \mathbb{Z}_2$ since there exists a time-preserving symmetry.

  Time preserving symmetries will be discussed later in Section 4.5.

- The kernel of σ, denoted M, will contain any symmetry which does not exchange any of the particles. In G, there will be $\frac{|G|}{|\mathrm{im}\sigma|}$ copies of $\mathrm{im}\sigma$, and each will be either cyclic or dihedral. Hence there will be $\frac{|G|}{|\mathrm{im}\sigma|}$ elements of G for which $\sigma(g) = id$. So $|M| = \frac{|G|}{2n}$, when $\mathrm{im}\sigma = D_n$, and $|M| = \frac{|G|}{n}$ when $\mathrm{im}\sigma = \mathbb{Z}_n$.

  For example, if we examine Table 5.3 on page 120, which shows the group G for the motion of five particles on a four-flower, we see that in the $\sigma(g)$ column

there are four elements which map to the identity under σ. These four elements are shown in Table 3.3, and it can be seen that they form a cyclic group of order four. Comparing this to the full table allows us to see that there are four copies of D_5 present.

Table 3.3: Five particles on a four-flower - elements of $\ker\sigma$

$\rho(g)$	$\tau(g)$	$\sigma(g)$	Order
I	0	e	1
$\kappa_3\kappa_1$	$T/4$	e	4
$(\kappa_1\kappa_3)^2$	$T/2$	e	2
$\kappa_1\kappa_3$	$-T/4$	e	4

We can additionally determine the following facts about the intersections of the kernels of the maps.

- $K \cap C$, the intersection of the kernels of τ and ρ, will always be trivial. Indeed, by Lemma 3.5.5, the only g in $C = \ker\rho$, are choreography symmetries, and the only choreography symmetry for which $\tau(g)$ is trivial is the identity, since all the others involve a time shift of $^{kT}/_{n}$.

- $K \cap M$ will again always be trivial, since in the case where $K = \ker\tau$ is non-trivial, any elements in K will have $\rho(g)$ a rotation by Proposition 4.5.1, and $\tau(g) : t \mapsto t$. Then, any such element satisfying $\sigma(g) = e$ will only apply to all points colliding at the centre, and not to any collisionless motion.

We will use the kernel and images of these maps to classify the different possible types of symmetry group in Section 4.1.

We now return to our example of three particles on a figure eight shape, and consider the resulting diagram of maps.

Example 3.6.1 (ρ, σ and τ for three particles on a figure eight)**.** Let us consider the setup given in Example 3.2.1 on page 45, of three particles on a figure eight. In this case, $G \simeq D_3 \times \mathbb{Z}_2 \simeq D_6$, as given in Table 3.2 on page 58, and the diagram from Figure 3.3 can be completed as seen in Figure 3.4.

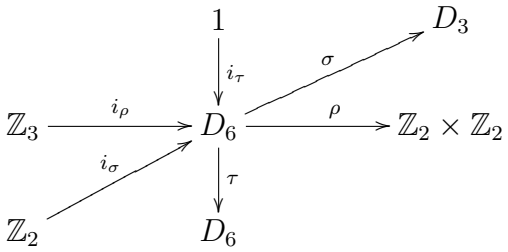

Figure 3.4: The maps ρ, σ and τ for three particles on a figure eight

Here, the kernel of τ is trivial, since there are no non-trivial symmetries which act trivially on the time circle $\mathbb{T}$, and so the image of τ is isomorphic to the full group G. The action of ρ will always have kernel $\mathbb{Z}_n$, since it contains only those elements which are powers of the choreography symmetry, so in this case it is $\mathbb{Z}_3$. The action of σ has $\mathbb{Z}_2$ as its kernel, since the non-time-reversing action of κ_2 has a power which leaves the elements unpermuted with a time shift of $T/2$.

Solutions of the n-body problem which fit our requirement of planar simple choreographies, with a given set of spatial symmetries, will exist as some subspace of the space of free loops in $X^{(n)} = (\mathbb{R}^2)^n \setminus \Delta$. The following constraints may initially be placed on the loops:

- The motion must obey the choreography symmetry - as described in the section defining choreographies, this means the loop $\hat{\gamma}$ must be composed of $\gamma \circledast g\gamma \circledast \ldots \circledast g^n\gamma$, where γ is a relative loop running from a point in M to its image under the choreography symmetry, and hence the particles will behave as in a choreography.

- The curve on which the particles are moving must obey the given spatial symmetries.

This restricts the subset of the loop space which we are considering to those whose motion is choreographical, and then further to those obeying the spatial symmetries.

Each spatial symmetry, when applied to the system, will correspond to some permutation of the particles, if the arrangement of the particles also possesses that

symmetry, and otherwise will correspond to some permutation of the particles combined with an alteration of the map to the time circle, such as a shift forward in time around the circle.

3.7 Time reversing symmetries

The map ρ assigns to each element of the symmetry group an element of $O(d)$, and in the planar case we are considering, an element of $O(2)$. For a given curve in the plane, the values $\rho(g)$ can take will depend on the degree of symmetry of the curve, and will belong to some dihedral group D_k (given our finite group constraint).

These will therefore either be a reflection or a rotation, and, depending on the curve, will result in a curve which traces out time in the same direction as the original curve, or the opposite direction. In the case that $\rho(g)$ reverses the direction of time on the curve, we refer to g as a **time reversing symmetry**.

Example 3.7.1 (Three Particles on a Figure Eight)**.** The figure eight example possesses symmetries which are time reversing.

The arrangements of particles possess spatial symmetry at $t = {}^{kT}/_{12}$, as seen in Figure 4.2 on page 86 in the next section, with κ_1 symmetry at even values of k and $\kappa_1\kappa_2$ symmetry when k is odd. The symmetry of κ_2 involves a time shift of ${}^{T}/_{2}$. The choreography symmetry is present, as are time-reversing symmetries such as g_0 and g_1, given by $\rho(g_0) = \kappa_1$ with $\sigma(g_0) = (12)$, and $\tau(g_0) : t \mapsto -t$, and $\rho(g_1) = \kappa_1\kappa_2$ with $\sigma(g_1) = (13)$, and where $\tau(g_1) : t \mapsto -t + {}^{T}/_{6}$.

If a symmetry is time reversing at $t = 0$ such as g_0 in the example above, this corresponds to a reflection on the time polygon through $t = 0$, fixing 0 and $T/2$, and the path $\gamma : x \rightsquigarrow gx$ must also obey this symmetry. Coupled with the choreography symmetry, one or two time reflections will allow us to reduce the description of γ to be given on an even smaller small portion of the time circle, and the symmetries will give the full curve $\hat{\gamma}$. This is discussed in more detail in the next chapter.

It may be noted that whether a given reflection or rotation is time reversing is

dependent on the shape of the curve - in particular, the degree of the symmetry is significant, as well as the number of crossings present in the curve.

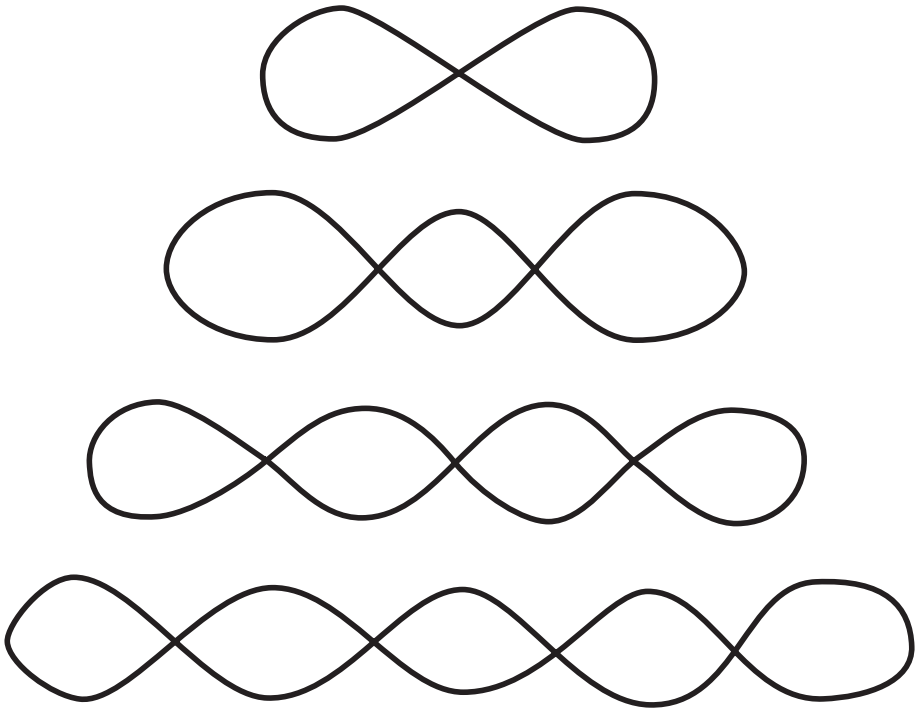

Figure 3.5: Linear chains, with one, two, three and four crossings

The shapes depicted in Figure 3.5 are called **linear chains**, and form an infinite family of curve shapes, for all of which $\rho(g)$ will be from D_2, due to the rectangular symmetry of such objects. It can be seen that the reflection in the horizontal axis, κ_1, is time reversing, while the reflection in the vertical axis, κ_2, is time reversing if and only if the curve contains an even number of crossings. The rotation by π, $\kappa_1\kappa_2$, is time reversing if and only if the curve has an odd number of crossings. Chains are considered in more detail in Chapter 5.

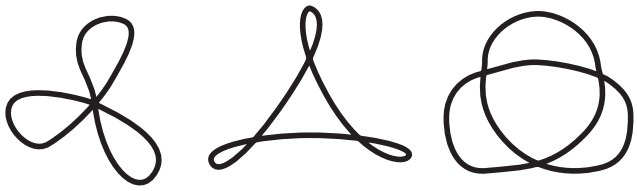

Figure 3.6: Curves with rotational symmetries of order three

For curves with k-fold rotational symmetry, such as the k-flowers, k-windmills and

k-foils defined in Chapter 5 and shown in Figure 3.6 for the case $k = 3$, any reflection will be time-reversing, but a rotation will not. This is because the motion proceeds around the central point in each case, and rotation merely moves the particles further along. Reflection, at any point, will reverse the direction of motion along the path.

In the general case, it is difficult to classify the many shapes of curves possible, but it is always simple to determine if a given symmetry is time-reversing, by examination. We have the following results:

Proposition 3.7.2. *For any simple choreography in $\mathbb{R}^2$, any symmetry g which is time-reversing for a given curve $\{x(t)|t \in [0, T]\}$ must have $\rho(g)$ with order two.*

Proof. Two cases:

- $\rho(g)$ is a reflection, in which case result follows.
- $\rho(g)$ is a rotation.

  Assume the rotation is of order ℓ, greater than two. The value of ℓ must be even, since the rotation reflects time with order 2.

  Since the curve has order ℓ symmetry, and this rotational symmetry is time-reversing, we require that the curve consists of ℓ petals, with alternating orientations, which all meet in the centre. This is because each petal must map onto each other, and with time running in the opposite direction. This cannot occur without creating an inconsistency in the orientation of the whole curve, unless all the petals meet at the centre of rotation.

  This means we must have an odd number of particles moving on our curve, since with an even number of petals, any particles which were $T/2$ apart would collide at the centre.

  As the symmetry g is time-reversing, then we may choose an arrangement at $t = 0$ such that $\tau(g) = \overline{0}$. This means the rotation of order ℓ must map all of the particles to the positions of other particles, since there cannot be any time shift.

Since we have an odd number of particles, this means one particle must sit at the centre of rotation at $t = 0$, since the rotation is of even order. Then $\sigma(g)$, the corresponding permutation, will leave this particle fixed and permute the remaining $n - 1$.

This permutation will be a product of cycles, and have order ℓ. However, such a permutation cannot be an element of D_n, where n is odd and ℓ even, and hence cannot permute the particles while preserving the ordering of particles on the curve. This cannot happen in a simple choreography. Hence we must have $\ell = 2$.

□

Corollary 3.7.3. *If a symmetry group possesses a rotational symmetry which is both time reversing and a rotation, then it cannot contain any other rotations.*

Proof. Let $g \in G$ be a time reversing rotation (of order two, by Proposition 3.7.2), and assume $g' \in G$ is a rotation of order $b > 2$ (since if g' were of order two, it would be the same as g since there is only one rotation of order two on any given object). Then the element gg' is a time reversing rotation of order $2b > 2$. Contradiction! Since, by Proposition 3.7.2, all time reversing rotations must be of order two. Hence, no other rotations can exist. □

Time reversing rotations and reflections of order two may be seen in Example 3.2.1 on page 45. Example 7.1.1 on page 145 shows a multiple choreography consisting of two groups of three particles on a star of David, which has time reversing rotations of order six due to the multiple components of the curve being differently oriented.

3.7.1 Table of time reversing symmetries

Table 3.4 gives a list of the time-reversing symmetries present in many of the examples considered here. From left to right, the columns indicate which example the symmetry occurs in, and which symmetry is being considered, the corresponding permutation, the homotopy type of the fixed point spaces F_i ($i \in \{0, 1\}$), defined in the next

Table 3.4: Time reversing symmetries

Choreography	Symmetry	$\sigma(g)$	Fixed pt space F_i	$\pi_0(F_i)$
3 on Fig 8	κ_1	(12)	2[pt]	2
Ex 3.2.1	$\kappa_1\kappa_2$	(13)	$\mathbb{S}^1$	1
4 on 3-foil	κ_2	(13)	4[pt]	4
Ex 5.1.7	κ_3	(24)	4[pt]	4
5 on 4-flwr	κ_1	(12)(35)	4[$\mathbb{S}^1$]	4
Ex 5.1.10	κ_3	(12)(35)	4[$\mathbb{S}^1$]	4
5 on 4-chn	κ_1	(25)(34)	4[$\mathbb{S}^1$]	4
Ex 5.2.3	$\kappa_1\kappa_2$	(25)(34)	$K(\mathbb{Z}\times\mathbb{F}_3,1)$	1
5 on fig8	κ_1	(25)(34)	4[$\mathbb{S}^1$]	4
Ex 5.2.1	$\kappa_1\kappa_2$	(25)(34)	$K(\mathbb{Z}\times\mathbb{F}_3,1)$	1
5 on sup8	κ_1	(25)(34)	4[$\mathbb{S}^1$]	4
Ex 5.2.2	κ_2	(25)(34)	4[$\mathbb{S}^1$]	4
4 on sup8	κ_1	(13)	4[pt]	4
Ex 4.5.1	κ_1	(12)(34)	4[pt]	4
6 on 3-flwr	κ_1	(13)(46)	6[pt]	6
Ex A.2.2	κ_1	(12)(36)(45)	6[pt]	6
8 on 4-flwr	κ_1	(28)(37)(46)	8[pt]	8
Ex A.2.3	κ_1	(18)(27)(36)(45)	8[pt]	8

chapter, and number of connected components possessed by these spaces. Here, for example, $4[\mathbb{S}^1]$ denotes a space consisting of the disjoint union of four copies of $\mathbb{S}^1$.

Note that for the bottom three entries, there additionally exists a time preserving symmetry and the fixed point spaces given have been restricted further by considering this time preserving symmetry. As we will discover in the next chapter, the fixed point spaces F_0 and F_1 may be further restricted to F_0' and F_1', which are the spaces given in this table.

Chapter 4

Loop Spaces

In this chapter, we discuss topological devices for studying the spaces of choreographical solutions, and how the symmetries of such motions, as expressed using the representations previously defined, may be used to reduce the space of loops being considered. These representations will allow us to first attempt a classification of the different possible symmetry groups. We will exploit the way in which $\tau(g)$ acts on the time circle, using reflections of the time circle and also the case in which $\tau(g)$ acts trivially, to place restrictions on the permitted arrangements of particles.

4.1 Classifying choreographies

4.1.1 Reversing and non-reversing symmetry groups

We define the following:

Definition 4.1.1. We say that a symmetry group is **reversing** if $\mathrm{im}\sigma \simeq D_n$, and **non-reversing** if $\mathrm{im}\sigma \simeq \mathbb{Z}_n$.

We may divide all symmetry groups into one of these two types. First, a preliminary result:

Proposition 4.1.2. *For a simple choreography, $\mathrm{im}\sigma$, the image of the map from G to S_n, must contain the cyclic subgroup generated by the n-cycle* $(12\ldots n)$.

Proof. Given that we have a choreography, we must have that G contains the subgroup corresponding to the choreography symmetry. For a simple choreography, where all n particles move on the same curve, the corresponding permutation of the symmetry will be the n-cycle $(12\dots n)$. All n powers of the choreography will also be present in the symmetry group, and so the corresponding permutations will be the powers of this n-cycle. These n elements will form a cyclic subgroup of imσ, as required. □

We now have:

Proposition 4.1.3. *For a simple choreography, we must have that either im$\sigma \simeq D_n$, in which case the symmetry group is reversing, or im$\sigma \simeq \mathbb{Z}_n$, in which case it is non-reversing.*

Proof. First we show that imσ must be $\mathbb{Z}_n$ or D_n.

We know that imσ must contain only elements of S_n which preserve the ordering of the particles, so it must be a subgroup of $D_n < S_n$. Non-trivial subgroups of D_n are exactly $\mathbb{Z}_m$ and D_m for $m \mid n$. We know that imσ must contain a cyclic subgroup of order n, corresponding to the powers of the n-cycle $(12\dots n)$ given by the choreography symmetry, by Proposition 4.1.2. The dihedral group D_m, for $m < n$, contains no cyclic subgroup of order n, and so we have that imσ must either be all of D_n, or the cyclic subgroup Z_n, as required.

Now, we must simple consider the fact that any symmetry of the choreography which reverses time must also reverse the order of the particles on the curve, in order for it to be a symmetry, and since all permutations in $\mathbb{Z}_n$ as a permutation group are cyclic, time reversing symmetries will be present if and only if im$\sigma \simeq D_n$. In the absence of time reversing symmetries, permutations of the particles (which must preserve the ordering of the particles around the curve) can only be cyclic, and so im$\sigma \simeq \mathbb{Z}_n$. □

Proposition 4.1.4. *The symmetry group of a choreography is reversing if and only if im$\rho \simeq D_k$, where D_k is the symmetry group of the curve.*

Proof. ($\Rightarrow$) Assume the curve has symmetry group D_k and $\text{im}\rho = D_k$; We will show that the symmetry group must contain reversing symmetries.

Indeed, assume there are not time reversing symmetries in G. This means $\text{im}\tau$ is cyclic $\mathbb{Z}_b$ for some b, since it consists only of symmetries which push time along and none that reverse it.

We may also note that since we have the short exact sequence

$$\mathbb{Z}_n \to G \xrightarrow{\rho} D_k$$

where $\mathbb{Z}_n$ is $\ker\rho$ and $D_k = \text{im}\rho$, we know that G is not a cyclic group since D_k has multiple generators, and hence so must G. This means that in the sequence

$$\ker\tau \to G \xrightarrow{\tau} \mathbb{Z}_b$$

we must have that $\ker\tau$ is non-trivial, since otherwise G would have to be equal to a cyclic group. This means there exist time-preserving symmetries of this choreography.

So, let $\ker\tau = \mathbb{Z}_\ell$, and note the following facts:

- ℓ must divide n, by Corollary 4.5.2 from page 92 in our section on time preserving symmetries. So, write $n = m\ell$, for some m.
- ℓ must also divide k, since there is an inclusion of $\ker\tau$ into $\text{im}\rho$, because any time preserving symmetry (one which is in $\ker\tau$) must move all of the particles, and therefore cannot map to the identity under ρ. So, write $k = r\ell$, for some r.

Then, we have the following diagram:

$$\begin{array}{ccccc} & & \mathbb{Z}_\ell & & \\ & & \downarrow{\scriptstyle i_\tau} & & \\ \mathbb{Z}_{m\ell} & \xrightarrow{i_\rho} & G & \xrightarrow{\rho} & D_{r\ell} \\ & & \downarrow{\scriptstyle \tau} & & \\ & & \mathbb{Z}_{2rml} & & \end{array}$$

Here we note that the order of G must be the product of $m\ell$ with $2r\ell = |D_{r\ell}|$, and hence $|G| = 2rm\ell^2$. Then, if $\ker\tau = \mathbb{Z}_\ell$, we have that $b = 2mr\ell$; that is, $\text{im}\tau = \mathbb{Z}_b = \mathbb{Z}_{2mr\ell}$.

However, by Proposition 4.1.5(1), since our symmetry group is non-reversing, we have that G is isomorphic to the direct product $\mathbb{Z}_{m\ell} \times D_{r\ell}$.

This group cannot contain an element of order $2mr\ell$, since the maximal order of an element of $D_{r\ell}$ is $r\ell$, and the maximal order of an element of $\mathbb{Z}_{m\ell}$ is $m\ell$, so their product will contain elements of order at most $mr\ell$.

Therefore, G cannot map into the cyclic group $\mathbb{Z}_{2rm\ell}$ under τ as we have here. This is a contradiction, and so we cannot have that there do not exist time reversing symmetries - the group G must be reversing, as required.

($\Leftarrow$) Assume the symmetry group is reversing, and we will show that if D_k is the symmetry group of the curve, it is also equal to imρ. We consider three cases, by different values of k.

- $k = 1$ Here the symmetry group of the curve is $D_1 \simeq \mathbb{Z}_2$, and hence possesses only one non-trivial symmetry, a rotation or reflection. If this rotation or reflection is time-reversing, which it must be if G is a reversing symmetry group, then im$\rho \simeq D_1$ as required.

- $k = 2$ Consider the map $Or : G \to \mathbb{Z}_2$, where

$$Or(g) = \begin{cases} +1 & \text{if } g \text{ acts trivially on the orientation of } \mathbb{T} \\ -1 & \text{otherwise.} \end{cases}$$

  Then if $k = 2$, we have $|G| = 2nk = 4n$, and $2n$ of these elements will map to -1 under Or and will hence be time reversing. In this case, D_2 consists of the identity, a rotation and two reflections. The n elements which are powers of the choreography symmetry will not be time reversing. This means at least one of the two reflections must be time reversing, and hence imρ contains a reflection. This means it must be the whole of D_2.

- $k > 2$ Here D_k must contain at least two rotations, and hence by Corollary 3.7.3, any time reversing symmetries present must be reflections since there cannot be more than one rotation if one of them is time reversing. So, imρ must again contain a reflection and hence must be all of D_k, as required.

□

This leads us to the following classification of G as reversing or non-reversing symmetry groups:

Proposition 4.1.5. *1. If G is non-reversing, and $S = im\sigma$ is isomorphic to the cyclic group $\mathbb{Z}_n$, then G is a direct product of $C = \ker\rho$ and $R = im\rho$; that is, $G \simeq C \times R$.*

2. If G is reversing, then we may classify it by $\mathbb{Z}_2$-extensions.

Proof. 1. $\text{im}\sigma = \mathbb{Z}_n$

Consider the sequence of maps

$$1 \longrightarrow C \xrightarrow{i_\rho} G \xrightarrow{\rho} R \longrightarrow 1$$

This sequence is exact.

We may define a map from G to C by σ, since $C = \ker\rho \simeq \mathbb{Z}_n$ always, and if $\text{im}\sigma = \mathbb{Z}_n$ then σ defines a map from G to $\mathbb{Z}_n$.

We need to show that $\sigma \circ i_\rho = id_C$. Indeed, take an element g of $C \subset G$. Then $i_\rho(g)$ will map under σ to the element of $\mathbb{Z}_n$ it originally represented, since C consists only of the choreography symmetries (by Proposition 3.5.5), each of which corresponds to a unique element of $\mathbb{Z}_n$. Hence, $\sigma \circ i_\rho = id_C$. Then this short exact sequence is left split, and hence by the splitting lemma (see [20] pp. 16-17), $G \simeq C \times R$ as required.

2. $\text{im}\sigma = D_n$

Consider the group G. The map σ will map half of the group G to $\mathbb{Z}_n$, namely the half consisting only of the rotations. Let this part be denoted $G' = \sigma^{-1}(\mathbb{Z}_n)$. Then, by part 1), G' is isomorphic to a direct product of C and R.

We know $C \simeq \mathbb{Z}_n$, and since G is reversing, we have $\text{im}\rho \simeq D_k$ by Proposition 4.1.4. So, $G' \simeq \mathbb{Z}_n \times D_k$.

We also have that G' is a normal subgroup of G, since it is of index two in G. We may now construct the following short exact sequence:

$$1 \longrightarrow (G' \simeq \mathbb{Z}_n \times D_k) \xrightarrow{i} G \xrightarrow{Or} \mathbb{Z}_2 \longrightarrow 1$$

Here, the map Or is that defined in Proposition 4.1.4, given by

$$Or(g) = \begin{cases} +1 & \text{if } g \text{ acts trivially on the orientation of } \mathbb{T} \\ -1 & \text{otherwise.} \end{cases}$$

□

We may use this exact sequence to determine G, for different values of n and k.

$$1 \longrightarrow (\mathbb{Z}_n \times D_k) \xrightarrow{i} G \xrightarrow{Or} \mathbb{Z}_2 \longrightarrow 1$$

Note that the sequence splits on the right, since we may define a map from $\mathbb{Z}_2$ into G which takes the non-identity element to a time reversing symmetry in G. The map Or composed with this map is the identity on $\mathbb{Z}_2$, and so we have that $G \simeq (\mathbb{Z}_n \times D_k) \rtimes \mathbb{Z}_2$.

4.1.2 Types of orbits

In [34], Terracini considers the representation τ, and makes use of the way the group $\overline{G} = G/\ker\tau$ acts on $\mathbb{T}$ to classify symmetries into one of three types. As previously discussed, the kernel of τ may be trivial, so $G/\ker\tau \neq G$ only in the case where there exist time preserving symmetries.

- If the group $\overline{G}$ acts trivially on the orientation of $\mathbb{T}$ - that is, there do not exist any time reversing symmetries, then $\overline{G}$ is a cyclic group and we say that the action of G on the space of loops is of **cyclic type**. Examples include the second part of Example 5.3.1 (which starts on page 131) of three particles on a distorted figure eight (possessing no κ_1 symmetry), and Example A.2.5 of nine particles on a bifurcated six-chain, on page 171 (possessing no κ_2 symmetry).

- Otherwise, we say that the action of G on the space of loops is of **dihedral type**. Most of the examples we have seen fall into this category.

These correspond to our definitions given above of reversing and non-reversing symmetry groups.

Remark 4.1.6. Terracini also defines an orbit of **brake type**, where $\overline{G}$ consists of a single reflection on $\mathbb{T}$. This corresponds to motions where a particle moves back and forth with a change of direction. None of our simple choreography examples fall into this category, since we consider choreographies with $n \geq 3$ particles, and if all particles must follow the same path, such behaviour would lead to a collision.

4.1.3 Map kernels and images

Given the maps ρ, σ and τ and their kernels and images, it is possible to attempt a classification of all the different groups G which could be the symmetry group of some choreography.

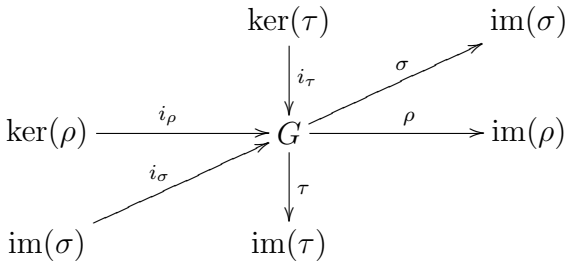

We begin by noting the following facts:

- $\ker \rho = \mathbb{Z}_n$, for n particles, since it contains only the choreography symmetry.
- $\ker \tau$ is trivial unless there exists a time preserving symmetry (see Section 4.5).
- $\mathrm{im}\sigma$ must be a dihedral or cyclic group, since it must permute the particles without altering their order on the curve (only rotations and reflections are permitted).
- $\mathrm{im}\rho$ must be the symmetry group of some object in $\mathbb{R}^d$, and for the case $d = 2$ which we are considering, of some object in the plane. This means it must be D_k or $\mathbb{Z}_k$ for some k, since we assume G is finite.

We now find there are two obvious approaches:

1. To classify G by $\mathrm{im}(\rho)$ - since it only has two broad possibilities, we may use the First Isomorphism Theorem

$$\mathrm{im}(\rho) = G/\ker(\rho)$$

and the fact that $\ker(\rho)$ is known, to list possibilities for G.

2. To classify G by $\ker(\tau)$ and $\mathrm{im}(\tau)$. Since $\ker(\tau)$ may be trivial, in this case $G = \mathrm{im}(\tau)$, for which there is a limited number of possibilities. If $\ker(\tau)$ is not trivial, we may classify G using both $\ker(\tau)$ and $\mathrm{im}(\tau)$.

4.1.3.1 Classification by im(ρ)

1. $\mathrm{im}(\rho) = D_k$

   The majority of examples fit here, and the value of k depends on the degree of symmetry of the curve. We have by Proposition 4.1.4 that G will contain time reversing symmetries. In this case, G will either be dihedral or a product of cyclic and dihedral groups.

2. $\mathrm{im}(\rho) = \mathbb{Z}_k$

   This occurs when the object possesses only a discrete rotational symmetry. In this case G will either be cyclic or dihedral, or a product of cyclic and dihedral groups. Dicyclic groups can be ruled out as a possibility for G, since they have no two disjoint non-trivial normal subgroups.

   The sub-case $k = 1$ here corresponds to the curve having no non-trivial symmetries, in which case $G = \mathbb{Z}_n$, since the system possesses only the choreography symmetry.

The case which fits in both of the above categories is when $\mathrm{im}(\rho) = \mathbb{Z}_2 \simeq D_1$. In this case, the curve possesses a single symmetry. This may either be time reversing or not, and the difference between these two cases can be seen in Section 5.3 where we discuss different subgroups of the symmetry group of three particles on a figure eight.

4.1.3.2 Classification by $\ker(\tau)$ and im(τ)

It would also be possible to attempt a classification by the kernel and image of the map τ, since we know the kernel of τ will be trivial except in the case where there exist time preserving symmetries.

Proposition 4.1.7. *If* $\ker(\tau)$ *is trivial,* G *will either be cyclic* $\mathbb{Z}_\ell$ *or dihedral* D_ℓ*.*

Proof. If $\ker(\tau) = 1$, then $G \simeq \text{im}(\tau)$. The image of τ consists of symmetries of the time polygon. If the time polygon has ℓ sides, then symmetries must be from D_ℓ or $\mathbb{Z}_\ell$. □

4.2 Classification of symmetry groups for $n = 3$

Using our now extensive set of results and discoveries about symmetry groups of choreographical motions, we may give a list of possible symmetry groups for the case $n = 3$.

In [5], Barutello, Ferrario and Terracini claim to list all possible symmetry groups of the planar three-body problem - however, see Remark 4.2.1 below. They include non-choreographical motions, including what they term the '2-1-choreography', which is a multiple choreography in which one particle moves on a different path to the other two. They consider the choreographies up to a rotating frame, and so they list the symmetry group for the Lagrange circular choreography as being of order six. They discuss which orbits are of cyclic, dihedral and brake type (as discussed earlier in Section 4.1.2), and since they do not require simple choreographies, several brake-type orbits are included.

We will consider only simple choreographies, in the case $n = 3$, and list all possible symmetry groups.

First, we must note that for a choreographical motion, the group G must contain as a subgroup the cyclic group of order three, corresponding to the choreography symmetry.

The other part of the group will be determined by the order of the planar symmetry group of the curve. By Proposition 3.5.6, the order of G will be n times the order of this symmetry group. The examples in this thesis treat many of the smaller cases. Starting with the trivial planar symmetry group and increasing its size, we find the possible G are as follows:

- $G \simeq \mathbb{Z}_3$. This corresponds to the trivial planar symmetry group of the curve, where the particles move with choreography symmetry. The space of loops $\pi_1^G(X^{(3)}, x)$, where G is the cyclic group of order three, will be the normal subgroup of the braid group B_3 of index two, corresponding to even permutations of the endpoints. By Proposition 2.5.3, the space of such loops will have connected components corresponding to the Reidemeister conjugacy classes in $\pi_1^g(X^{(3)}, x)$, where g is the choreography symmetry. It is not possible to construct fixed point spaces for this example, since there are no time reversing symmetries.

- $G \simeq \mathbb{Z}_6 = \mathbb{Z}_3 \times \mathbb{Z}_2$. Here the symmetry group of the planar curve possesses only a single non-time-reversing symmetry, and so the group is like that shown in Table 5.7 in Chapter 5, where it is cyclic of order six. It is again not possible to construct fixed point spaces, since there are no time reversing symmetries.

- $G \simeq D_3 = \mathbb{Z}_3 \rtimes \mathbb{Z}_2$. Here the symmetry group of the planar curve possesses only a single time reversing symmetry, and so the group is like that shown in Table 5.6 or Table 5.8 in Chapter 5, where the time reversing symmetry is either a rotation or a reflection. We may determine the connected components by constructing fixed point spaces of the time reversals, as in our other examples.

- $G \simeq D_6 = \mathbb{Z}_3 \rtimes D_2$. This is the symmetry group corresponding to our example of three particles on a figure eight, seen in Example 3.2.1.

Remark 4.2.1. The classification given by Barutello, Ferrario and Terracini stops at the symmetry group of the figure eight (in their notation, D_{12} but in ours D_6. However, we have discovered that larger planar symmetry groups than D_2 are permissible

- in fact, in Example A.12 on page 176 in the Appendix, we give an example of three particles moving on a curve with square symmetry, which has symmetry group D_{12} (of order 24). Curves with this symmetry have been found as minima of the action functional for both strong force and Newtonian potentials (see Section 6 for more about minimisation). This would suggest that their classification is incomplete.

Increasing the size of the symmetry group in the plane to larger dihedral groups would result in $G \simeq \mathbb{Z}_3 \rtimes D_k \simeq D_{3k}$, for $k > 2$, where $\mathbb{Z}_3$ is a normal subgroup being acted on by the dihedral group. However, by Proposition 3.7.2, we may only have time reversing rotations of order two, and Proposition 3.7.3 means that in such groups with rotations of higher order, there can be no time reversing rotations. This means the fixed point spaces will be of the type observed as F_0 for three particles in a figure eight, where two particles are related by reflection in an axis, and never of the type seen in F_1 where one particle is fixed at the origin. This is connected to why we only get semidirect products with $\mathbb{Z}_3$ for such groups.

It is conjectured that for $n = 3$, all finite symmetry groups are either $\mathbb{Z}_{3k}$ or D_{3k}, for some k. It is not known if there exist solutions for which the symmetry group is precisely $\mathbb{Z}_{3k}$ - although curves with this symmetry do exist. This is the subject of ongoing work.

Increasing the symmetry group to its maximum size, the infinite group $O(2)$, gives the Lagrange circular choreography. It has been seen that, for symmetry groups larger than D_6, many curves possessing such symmetry groups will correspond to solutions which in fact possess the larger symmetry group of the circle. In Chapter 6 we will discuss how real solutions may be found by minimising the action functional, and minima in such spaces will in many cases be the circular solution.

Remark 4.2.2. We will define and discuss time preserving symmetries in Section 4.5. We note that in the case where $n = 3$, there are no time preserving symmetries except in the case where we have the Lagrange circular solution. This is because, by Proposition 4.5.2, for a time preserving symmetry to exist, $|\ker \tau|$ must divide n, and hence $\ker \tau$ must be trivial or of order three. If it contains a rotation of order

three, such a rotation must move all three particles to each others' positions, as in the circular choreography - it cannot fix one, otherwise our choreography would not be simple.

4.3 Calculating the equivariant fundamental group for a choreography

Now that we have properly defined choreographies and know how to determine the full group of symmetries, we may apply this knowledge to these results from the previous section to find the equivariant fundamental group.

As seen in Proposition 2.4.3(1), if the action of G is free, the equivariant fundamental group of M is given by the ordinary fundamental group of the quotient space of M by G. While a free action is not often present, since many symmetry groups are reversing and hence have fixed points on the time circle, we can find examples where the symmetries present are a subgroup of the whole symmetry group containing no time reversing symmetries.

We consider the example of five particles on a super-eight, but with the curve distorted so that the symmetry of the curve is no longer from D_2 but instead consists of a single non-time-reversing rotation.

Example 4.3.1 (Five particles on a distorted super-eight)**.** We consider the case where five particles move on a 'super-eight' shape, like that seen in Example 5.2.2 on page 125 in Chapter 5. The super-eight curve will be seen again in Example 4.5.1 on page 88, and consists of an extended figure eight shape in which there are now two crossings, and a third region in the centre.

We also choose to distort the super-eight shape so that it has only a rotational symmetry by π, and no reflectional symmetries. This rotation is not time-reversing, and so the group of symmetries does not fix any points on the time circle.

In this case, the group of symmetries G can be shown to be $\mathbb{Z}_{10}$. Our space M is the plane with five particles, $X^{(5)} = (\mathbb{R}^2)^5 \setminus \Delta$.

The action of G on the space is free, since no points are fixed by the symmetries, and hence we have, by Proposition 2.4.3(1):

$$\pi_1^G(M, x) \simeq \pi_1(M/G, \bar{x})$$

That is,

$$\pi_1^{\mathbb{Z}_{10}}(X^{(5)}, x) \simeq \pi_1(X^{(5)}/G, \bar{x})$$

Here $\bar{x}$ is the orbit of x under the action of G.

4.4 Restriction of the loop space using time reversals

Given a time reversing symmetry g, we know that g will fix two points on the time circle $\mathbb{T}$. We can use this symmetry to restrict the set of loops we are considering.

The time circle, shown in Figure 3.2 on page 55, is already under the restriction of the choreography symmetry, as discussed in the previous section. This means that every T/n section of the path must be identical to the first.

If we additionally have a time reversing symmetry, for instance one which fixes $t = 0$, then we must have that the section of the path proceeding forward in time from $t = 0$ must be identical to that moving backwards in time, towards the point $t = T - T/n$. By the choreography symmetry, this must also be identical to the section running backwards from $t = T/n$ towards $t = 0$.

This symmetry can be seen in Figure 3.2, and it means that the section of path γ from $t = 0$ to $t = T/n$ must be repeated all the way round the circle, by the choreography symmetry, and must have reflectional symmetry within itself, around its midpoint.

Now, let t_0, t_1 be two points on the time circle which are

1. fixed by time-reversing symmetries,

2. consecutive among such points

Then, let the symmetries fixing t_0, t_1 be denoted g_0, g_1 respectively – that is, we have $\tau(g_0) \cdot t_0 = t_0$, and $\tau(g_1) \cdot t_1 = t_1$. We denote the subspaces of $X = (\mathbb{R}^2)^n \setminus \Delta$ fixed by g_0, g_1 respectively by F_0, F_1.

$$F_i = \{(x_1, \ldots, x_n) \in X \mid (\rho(g_i) \cdot x_{\sigma(1)}, \ldots, \rho(g_i) \cdot x_{\sigma(n)}) = (x_1, \ldots, x_n)\}$$

These fixed point spaces will be very useful in describing the motion of the whole curve, and in each of our examples we will examine the topology of F_0, $F_1 \subset X$.

Now consider the case $t_0 = 0$, $t_1 = t \neq 0$.

This means that if we consider the arrangement of particles at $t_0 = 0$, which will be some point in F_0, then the path γ must run from here to some point in F_1. This means $\gamma \in \mathcal{P}(X, F_0, F_1)$ - the space of paths in X running from a point in F_0 to a point in F_1. This is made more precise in Theorem 4.4.6 below.

We now return to the major example of three particles on a figure eight, which will provide a useful context to discuss some further properties of choreographies, including how the fixed point spaces F_0 and F_1 may be found, and how this allows us to restrict the space of loops.

Remark 4.4.1. In our calculation of fixed point spaces F_0, F_1 we will use notation as though $X = \mathbb{C}^n \setminus \Delta$, and points in X will be denoted $(z_1, \ldots, z_n)$ $z_i \neq z_j$ for $i \neq j$. This gives us an easier way to represent a spatial transformation – for instance, $\kappa_1 : z \mapsto \bar{z}$.

Example 4.4.2 (Three particles on a figure eight)**.** The time-reversing symmetries we will use to calculate our fixed point spaces are g_0 and g_1, given by $\rho(g_0) = \kappa_1$ with $\sigma(g_0) = (12)$, and $\rho(g_1) = \kappa_1\kappa_2$ with $\sigma(g_1) = (13)$, and where $\tau(g_0) : t \mapsto -t$ and $\tau(g_1) : t \mapsto -t + {}^{T}/_{6}$.

Fixed point space F_0:

$$\gamma(0) = g_0\gamma(0) = \kappa_1(12)\gamma(0)$$

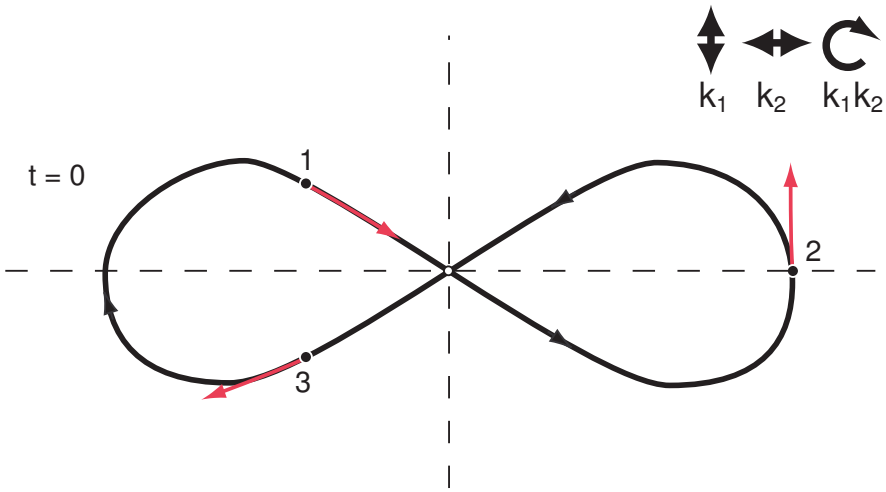

Figure 4.1: Three particles on a figure eight, at $t = 0$

Therefore,

$$\begin{aligned}(z_1, z_2, z_3) &= \kappa_1(12)(z_1, z_2, z_3) \\ &= (\bar{z}_2, \bar{z}_1, \bar{z}_3)\end{aligned}$$

The fact that $z_3 = \bar{z}_3$ means that z_3 must be real. Then z_1 and z_2 form a conjugate pair either side of the real axis, since $z_1 \neq z_2$. Hence the fixed point space $F_0 = \mathrm{Fix}(g_0)$ is given by a copy of $\mathbb{R}$, determining the position of z_3, crossed with a pair of half-planes which determines the position of z_1 (either $Im(z_1) > 0$ or $Im(z_1) < 0$), and the position of z_2 then follows.

This space has two contractible connected components. So F_0 is homotopic to $pt \sqcup pt$.

Fixed point space F_1:

$$\gamma({}^{T}/_{12}) = g_1\gamma({}^{T}/_{12}) = \kappa_1\kappa_2(13)\gamma({}^{T}/_{12})$$

Therefore at $t = {}^{T}/_{12}$,

$$\begin{aligned}(z_1, z_2, z_3) &= \kappa_1\kappa_2(13)(z_1, z_2, z_3) \\ &= (-z_3, -z_2, -z_1)\end{aligned}$$

The fact that $z_2 = -z_2$ means that z_2 must be at the origin. Then z_1 and z_3 form a pair either side of this point and each other's image under rotation by π. Hence

the fixed point space $F_1 = \mathrm{Fix}(g_1)$ is given by $\mathbb{C} \setminus \{0\}$ (homotopic to the circle $\mathbb{S}^1$), determining the position of z_1, and the position of z_3 follows. So $F_1 \simeq \mathbb{S}^1$.

Having found the space F_0 and F_1 of fixed points under time preserving symmetries fixing $t = 0$ and $t = {}^{T}/_{2n}$ respectively, we now have that paths $\hat{\gamma}$ obeying the symmetries of G must have $\hat{\gamma}(0) \in F_0$ and $\hat{\gamma}({}^{T}/_{2n}) \in F_1$.

Let $\tilde{\gamma}$ be a path running from a point in F_0 to a point in F_1 – so $\tilde{\gamma}(0) \in F_0, \tilde{\gamma}(1) \in F_1$. As defined in Chapter 2, the space of such paths is denoted $\mathcal{P}(X, F_0, F_1)$.

Since g_0 reverses time while fixing $t = 0$, any path satisfying g_0 must behave the same as t increases away from 0 in the positive direction as it does when t decreases away from 0 in the other direction around the time circle $\mathbb{T}$. Similarly, we have another reflection in the time circle about $t = {}^{T}/_{2n}$.

Given that the choreography symmetry dictated that the behaviour of the particles from $t = 0$ to $t = {}^{T}/_{n}$ must be repeated around the time circle $\mathbb{T}$ up to some cyclic renumbering, we find that the behaviour of particles on all of $\mathbb{T}$ can be extrapolated from that in the fundamental domain $D = [0, {}^{T}/_{2n}] \subset \mathbb{T}$.

Given any $t \in \mathbb{T}$, there will exist some element g of the dihedral group $< g_0, g_1 >$ generated by the two time reversing symmetries, whose action on the time circle maps t to a point in D - that is, $\tau(g) \cdot t \in D$. Then $\hat{\gamma}(t) = g \cdot \tilde{\gamma}(\tau(g) \cdot t)$, where $\tilde{\gamma}$ is the section of path as defined above, namely $\tilde{\gamma} = \hat{\gamma}(D)$.

The complete closed loop $\hat{\gamma}$ which results from this process of extending the section of path around the whole time circle is a choreography and possesses the symmetries defined by the action of the group G on the space X and on the time circle. We denote the space of such closed loops $\Lambda_G(X)$, and we call it the **space of G-loops**.

Given a group G, the number of sections of path which need to be joined together in this way to make a closed loop will be $m = \frac{|G|}{|\ker \tau|}$. This is because we simply need a group element which maps D to each section of the time circle. An element g, when multiplied by an element $h \in \ker \tau$, will map D to the same section of the time circle since h acts trivially on $\mathbb{T}$. Hence there will be $|\ker \tau|$ elements of G for each section of the time circle, and $\frac{|G|}{|\ker \tau|}$ cosets of $\ker \tau$ in G. We may choose one element from

each coset to make up the whole path.

The example given below has trivial $\ker\tau$, but later we will explore the cases where $\ker\tau$ is non-trivial, and Example 4.5.3 of four particles on a super-eight on page 93 demonstrates this division into cosets.

Remark 4.4.3. Note that the space $\Lambda_G(X)$ is given by

$$\Lambda_G(X) = \{\gamma \in \Lambda(X) \mid g \cdot \gamma \ = \ \gamma \ \forall g \in G\}$$

Here $\Lambda(X)$ denotes the free loop space of maps of $\mathbb{S}^1$ into X. The composition $g \cdot \gamma$ is more precisely defined as the map

$$g : \gamma_i(t) \mapsto \rho(g) \cdot \gamma_{\sigma(g)(i)}(\tau(g) \cdot t)$$

where γ_i is the component of the path γ travelled along by the i^{th} particle.

This is a stabiliser of the action of G on the space of free loops. While a stabiliser would usually be denoted by an upper index, it is important to note that other spaces of loops have been defined in which an upper index of g denotes a relative loop running from x to gx. In particular, the equivariant fundamental group π_1^G can be thought of as the union over $g \in G$ of the relative fundamental torsors π_1^g. This means that denoting the space of G-loops by Λ^G could lead to the inference it is related to Λ^g, the space of free relative loops, in a similar way, which it is not.

Definition 4.4.4. Let F_0, F_1 be subspaces of X which are fixed by the symmetries g_0, g_1 respectively. Precisely,

- We use g_0 to denote the symmetry for which $\tau(g_0) = \overline{0}$. This symmetry is time reversing about $t = 0$, and fixes $t = 0$ and $t = {}^{T}\!/_{2}$.
- We use g_1 to denote the symmetry for which $\tau(g_1) = \overline{{}^{T}\!/_{n}}$. This is time reversing and fixes $t = {}^{T}\!/_{2n}$ and $t = {}^{T}\!/_{2} + {}^{T}\!/_{2n}$.
- We denote by g_2 the symmetry for which $\tau(g_2) = \overline{{}^{2T}\!/_{n}}$, fixing $t = {}^{T}\!/_{n}$ and $t = {}^{T}\!/_{2} + {}^{T}\!/_{n}$.

These symmetries may be chosen such that $(g_2g_1)^2$ is the choreography symmetry. In fact, in the absence of time reversing symmetries, the choices of such symmetries are unique. We have that g_1 fixes F_1, and g_2 in fact fixes the points in F_0, since at $t = {}^T/_n$ the particles are in the same arrangement as they are at $t = 0$ but with different numbering, due to the choreography symmetry.

We define a map Θ: $\mathcal{P}(X, F_0, F_1) \to \Lambda_G(X)$ which takes a section of path γ running from a point in F_0 to a point in F_1, and extends it onto a loop $\hat{\gamma}$ in $\Lambda_G(X)$ by taking the image of γ under each element of G and concatenating them into a closed loop. $(g_2g_1)^2$ is the choreography symmetry. Then

$$\Theta : \mathcal{P}(X, F_0, F_1) \to \Lambda_G(X)$$

$$\Theta : \gamma \mapsto ((\gamma * \overline{g_1\gamma}) \ * \ g_2g_1(\gamma * \overline{g_1\gamma}) \ * \ (g_2g_1)^2(\gamma * \overline{g_1\gamma}) \ * \ \ldots \ * \ (g_2g_1)^{2n-1}(\gamma * \overline{g_1\gamma}))$$

Here we see that we repeatedly travel from points in F_0 to points in F_1 and back again, and we apply increasing powers of (g_2g_1), where $(g_2g_1)^2$ is the choreography symmetry. Such an ordering of the elements can be seen in Example 4.4.8 below, where the elements g_1 and g_2 are as given.

Remark 4.4.5. The group G can be generated by g_0 and g_1, or by g_1 and g_2. In the definition of the map θ given above, g_0 is actually the element $(g_2g_1)^{2n-1}\overline{g_1\gamma}$ which is the last one in the sequence. This is more clearly seen in the example, given shortly.

Theorem 4.4.6. *The map Θ: $\mathcal{P}(X, F_0, F_1) \to \Lambda_G(X)$, as defined above, is a homeomorphism.*

Proof. Let $\gamma \in \mathcal{P}(X, F_0, F_1)$.

The map given above is bijective, since each path γ gives a unique $\hat{\gamma}$, and a given $\hat{\gamma}$ can be truncated to the first ${}^T/_{2n}$ of its motion, so the inverse map exists and both are well defined. The maps are also continuous, since the action of the elements of G preserves open sets - the action is by permuting the n copies of $\mathbb{R}^d$, or applying an affine transformation to the $\mathbb{R}^d$. Also, concatenation of paths is continuous. Truncation of the path, the inverse map, is also continuous as it is a projection. Hence our map is a homeomorphism. □

The fact that these two spaces are homeomorphic gives us immediately the following corollary:

Corollary 4.4.7. *If two paths γ_1, γ_2 in $\mathcal{P}(X, F_0, F_1)$ are homotopic, then their associated G-loops $\Theta(\gamma_1), \Theta(\gamma_2)$ will be homotopic in $\Lambda_G(X)$.*

Example 4.4.8 (Three particles on a Figure Eight)**.** Let G be the group of symmetries of the figure eight choreography with three particles. As seen in Example 3.2.1, this group is the dihedral group D_6 with twelve elements.

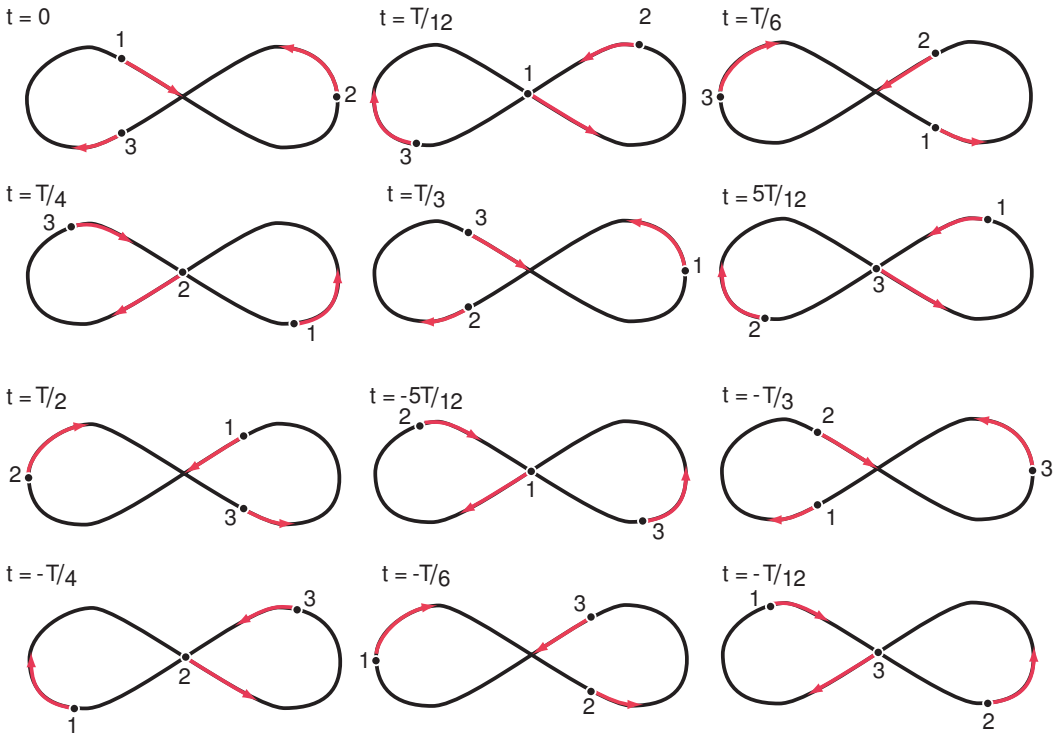

Figure 4.2: Three particles on a figure eight, at $t = {}^{kT}/_{12}$

The top left picture in Figure 4.2 shows the movement of the particles from $t = 0$ to $t = {}^{T}/_{12}$, and this is the path γ, which we will combine using the group elements to produce the full loop $\hat{\gamma}$. For instance, the next section of motion corresponds to the element g_1 for which $\rho(g_1) = \kappa_1\kappa_2$, $\tau(g_1) : t \mapsto -t + {}^{T}/_{6}$ and $\sigma(g_1) = (23)$. If we apply this to the section of path γ shown, we find that each particle starts this new section of path from the correct place, and we get the image in the second diagram.

The full motion of particles around the whole choreography is given by the group

elements in the order as given in Table 4.1. This helps to understand how the sections of path all fit together. Applying each of the group elements will give a different section of path, and the union of all these sections makes the path $\hat{\gamma}$.

The map Θ defined earlier uses the elements g_1 and g_2, and here g_1 is given by $\kappa_1\kappa_2$, $\overline{T/6}$ and (23), while g_2 is κ_1, $\overline{T/3}$ and (12). The choreography symmetry is given by $(g_2g_1)^2$.

Table 4.1: Three particles on a figure eight - the map from γ to $\hat{\gamma}$

Time from	Time to	$\rho(g)$	$\tau(g)$	$\sigma(g)$	g
0	$T/12$	I	0	e	id
$T/12$	$T/6$	$\kappa_1\kappa_2$	$\overline{T/6}$	(23)	g_1
$T/6$	$T/4$	κ_2	$T/6$	(132)	g_2g_1
$T/4$	$T/3$	κ_1	$\overline{T/3}$	(12)	$(g_2g_1)\cdot g_1$
$T/3$	$5T/12$	I	$T/3$	(123)	$(g_2g_1)^2$
$5T/12$	$T/2$	$\kappa_1\kappa_2$	$\overline{T/2}$	(13)	$(g_2g_1)^2\cdot g_1$
$T/2$	$-5T/12$	κ_2	$T/2$	e	$(g_2g_1)^3$
$-5T/12$	$-T/3$	κ_1	$\overline{-T/3}$	(23)	$(g_2g_1)^3\cdot g_1$
$-T/3$	$-T/4$	I	$-T/3$	(132)	$(g_2g_1)^4$
$-T/4$	$-T/6$	$\kappa_1\kappa_2$	$\overline{-T/6}$	(12)	$(g_2g_1)^4\cdot g_1$
$-T/6$	$-T/12$	κ_2	$-T/6$	(123)	$(g_2g_1)^5$
$-T/12$	0	κ_1	$\overline{0}$	(13)	$(g_2g_1)^5\cdot g_1$

4.5 Time preserving symmetries

In certain cases, there exist symmetries which act trivially on the time circle $\mathbb{T}$. Examples include the rotation by π of the Gerver super-eight (seen below), and the rotation by $\pi/2$ of the four-flower with eight particles (see Example A.2.3 on page 162). We call such symmetries **time preserving symmetries**, and they require us to restrict further our space of loops.

If there exists a symmetry for which $\tau(g) : t \mapsto t$, this means that for all values of t, the symmetries $\rho(g)$ and $\sigma(g)$ are possessed by the arrangement of particles. This means that we can restrict the manifold $X^{(n)} = (\mathbb{R}^2)^n \setminus \Delta$ in such cases to a manifold X' of n particles in $\mathbb{R}^2$ possessing the given symmetry.

The following example has a time preserving symmetry, and again is a simple and

convenient example to use in explaining how various properties of choreographies express themselves in the presence of a time-preserving symmetry.

4.5.1 Example - four particles on a Gerver super-eight

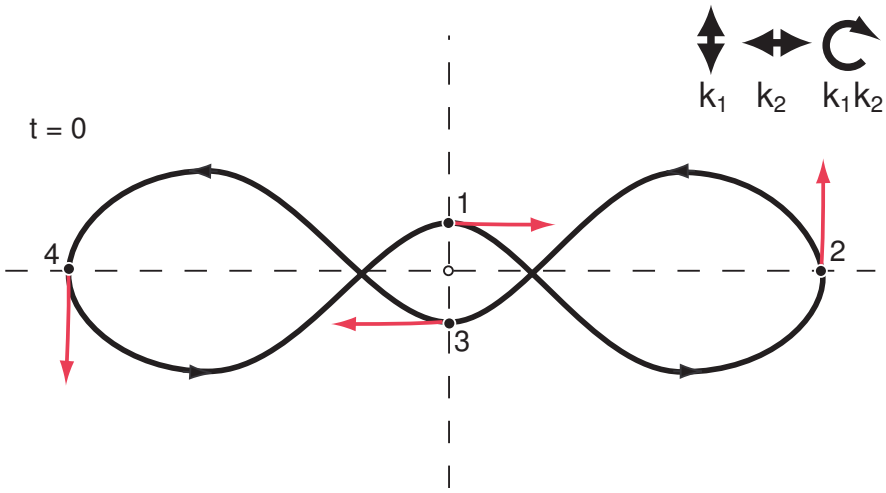

Figure 4.3: Four particles on a super-eight, at $t = 0$

The 'super-eight' choreography, shown in Figure 4.3 was discovered by Gerver ([11] p289, also Figure 4.1(b)). Its existence has not been proven analytically, although there is a computer assisted proof using interval arithmetic ([1] Item 3).

The super-eight curve has the symmetry group of a rectangle, which is generated by the vertical reflection κ_1 and the horizontal reflection κ_2, and includes the rotation by π, $\kappa_1\kappa_2$.

The arrangements of particles possess reflectional symmetry at $t = kT/8$, as seen in Figure 4.7 on page 94 in the next section. At even values of k, the points lie at the midpoints of the sides of a rectangle symmetrical with respect to the same axes (or equivalently, at the corners of such a rhombus), and the points lie at the corners of such a rectangle when k is odd. A rotational symmetry is present at all values of t.

The choreography symmetry is present, as are two time-reversing symmetries g_0, g_1, given by $\rho(g_0) = \kappa_1$ with $\sigma(g_0) = (13)$, and $\rho(g_1) = \kappa_1$ with $\sigma(g_1) = (12)(34)$ with a time shift of $T/4$. There exist equivalent symmetries under κ_2, with the same $\tau(g)$ but with $\sigma(g) = (24)$ and $(14)(23)$ respectively.

This choreography additionally possesses a time preserving symmetry, denoted g_t – that is to say, at all values of t, $\rho(g_t) = \kappa_1\kappa_2$ and $\sigma(g_t) = (13)(24)$ with $\tau(g_t) : t \mapsto t$ is a symmetry of the choreography. This is the reason why the above time reversing symmetries are equivalent, since combining either of the κ_1 symmetries with this time preserving symmetry g_t will result in the equivalent κ_2 symmetry. Figure 4.4 shows the four particles in a generic position, for some value of t between $-T/8$ and 0, and it can be seen that the rotational symmetry $\kappa_1\kappa_2$ still applies.

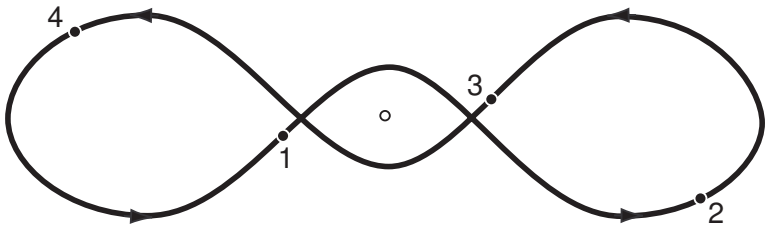

Figure 4.4: Four particles on a super-eight, at some $t \in (-T/8, 0)$

Fixed point space $F_0 = Fix(g_0, X)$:

$$\gamma(0) = g_0\gamma(0) = \kappa_1(13)\gamma(0)$$

Therefore,

$$\begin{aligned}(z_1, z_2, z_3, z_4) &= \kappa_1(13)(z_1, z_2, z_3, z_4) \\ &= (\bar{z}_3, \bar{z}_2, \bar{z}_1, \bar{z}_4)\end{aligned}$$

The fact that $z_2 = \bar{z}_2$ and $z_4 = \bar{z}_4$ means that z_2 and z_4 must be real. Then z_1 and z_3 form a conjugate pair either side of the real axis. Hence the fixed point space $F_0 = \mathrm{Fix}(g_0)$ is given by a copy of $\mathbb{R}^2 \setminus \Delta$, determining the positions of z_2 and z_4, crossed with a copy of $\mathbb{C} \setminus \mathbb{R}$ which determines the position of z_1, and the position of z_3 then follows. So $F_0 = (\mathbb{C} \setminus \mathbb{R}) \times (\mathbb{R}^2 \setminus \Delta)$. This space has four contractible connected components. So $F_0 \simeq pt \sqcup pt \sqcup pt \sqcup pt$.

Fixed point space $F_1 = \mathrm{Fix}(g_1, X)$:

$$\hat{\gamma}(T/8) = g_1\hat{\gamma}(T/8) = \kappa_1(12)(34)\hat{\gamma}(T/8)$$

Therefore,

$$\begin{aligned}(z_1, z_2, z_3, z_4) &= \kappa_1(12)(34)(z_1, z_2, z_3, z_4) \\ &= (\bar{z}_2, \bar{z}_1, \bar{z}_4, \bar{z}_3)\end{aligned}$$

These four points form two conjugate pairs either side of the real axis, where z_1 is conjugate to z_2, and z_3 is conjugate to z_4. Hence the fixed point space $F_1 = \mathrm{Fix}(g_1)$ is given by the positions of z_1 and z_3, which will be distinct points in the upper or lower half-plane. We must also have that as well as $z_1 \neq z_3$, we have $z_1 \neq \bar{z}_3$. This means we take the space $(\mathbb{C} \setminus \mathbb{R})^2$, and subtract two diagonal sets. The resulting space has four connected components, each of which is homotopic to $\mathbb{R}^4 \setminus \mathbb{R}^2 \simeq \mathbb{S}^1$. So $F_1 \simeq \mathbb{S}^1 \sqcup \mathbb{S}^1 \sqcup \mathbb{S}^1 \sqcup \mathbb{S}^1$.

The existence of g_t as a symmetry of this choreography means that when considering spaces of possible arrangements of particles which will result in this choreography, we may restrict the manifold X to a subspace X', which consists of the set of points which obey this symmetry. We find that

$$X' = \{(z_1, z_2, z_3, z_4) \in \mathbb{C}^4 \setminus \Delta \mid z_1 = -z_3, z_2 = -z_4, z_i \neq 0, z_i \neq z_j\}$$

Since the positions of z_3 and z_4 are dependent on z_1 and z_2, we can write this as

$$X' \simeq \{(z_1, z_2) \in \mathbb{C}^2 \mid z_1 \neq 0, z_2 \neq 0, z_1 \neq \pm z_2\}$$

This is the space $\mathbb{C}^2$ minus four complex planes. By Lemma A.1.1 on page 157 in the Appendix, this is $K(\mathbb{Z} \times \mathbb{F}_3, 1)$ where $\mathbb{F}_3$ is the free group on three generators. Given this restriction on the arrangement of points at all values of t, once we find our fixed point spaces they can be restricted to their intersection with this space.

$F_0' = \mathrm{Fix}(g_0, X') = F_0 \cap X'$ is then given by:

$$F_0 \cap X' = \{(z_1, z_2, z_3, z_4) | z_i \neq 0, z_1 \neq z_2, z_1 = -z_3 = \bar{z}_3, z_2 = -z_4, z_2 \text{ and } z_4 \in \mathbb{R}\}$$

So we have that $z_2 = -z_4$ are both real, and $z_1 = \bar{z}_3 = -z_3$, which must both lie in the imaginary axis and all are non-zero. Since the positions of z_3 and z_4 are determined by z_1 and z_2, the space F_0' is given by the positions of two points in $\mathbb{R} \setminus \{0\}$, so $F_0' \simeq (\mathbb{R} \setminus \{0\})^2$. This space has four contractible connected components.

$$\begin{aligned} F_1' &= \mathrm{Fix}(g_1, X') = F_1 \cap X' \\ &= \{(z_1, z_2, z_3, z_4) | z_1 = \bar{z}_2, z_3 = \bar{z}_4 \text{ and } z_1 = -z_3, z_2 = -z_4\} \\ &= \{z_1 = -\bar{z}_4 = \bar{z}_2 = -z_3\} \end{aligned}$$

So we find that the positions of the four points are all dependent on each other, and so the space F_1' is given by the position of the point z_1, which lies in $\mathbb{C} \setminus \{\mathbb{R} \cup i\mathbb{R}\}$ - it cannot be on either axis as this would lead to a collision of two or more points, so $F_1' \simeq \mathbb{C} \setminus \{\mathbb{R} \cup i\mathbb{R}\}$. This space has four contractible connected components.

The full group of symmetries is given in Table 4.2. It has order 16, but contains no elements of order 8, therefore it cannot be the dihedral group D_8. It is in fact $D_4 \times \mathbb{Z}_2$. The dihedral structure is generated by the starred elements, and the $\mathbb{Z}_2$-structure is given by the element marked †. The maps ρ, σ and τ for this group can

Table 4.2: Four particles on a Gerver super-eight

$\rho(g)$	$\tau(g)$	$\sigma(g)$	Order
I	0	e	1
I	$T/4$	(1234)	4
I	$T/2$	(13)(24)	2
I	$-T/4$	(1432)	4
* κ_1	$\overline{0}$	(13)	2
κ_1	$\overline{T/4}$	(14)(23)	2
κ_1	$\overline{T/2}$	(24)	2
κ_1	$\overline{-T/4}$	(12)(34)	2
κ_2	$\overline{0}$	(24)	2
κ_2	$\overline{T/4}$	(14)(23)	2
κ_2	$\overline{T/2}$	(13)	2
κ_2	$\overline{-T/4}$	(12)(34)	2
†$\kappa_1\kappa_2$	0	(13)(24)	2
$\kappa_1\kappa_2$	$T/4$	(1432)	4
$\kappa_1\kappa_2$	$T/2$	e	2
* $\kappa_1\kappa_2$	$-T/4$	(1234)	4

be seen in Figure 4.5.

As seen in the above example, the time preserving symmetry is a very powerful tool in restricting our space of loops to a given subset of the manifold, and allows us to choose initial starting positions quite specifically.

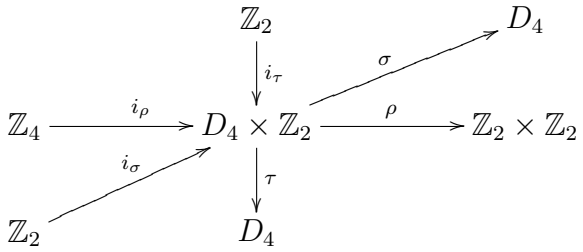

Figure 4.5: The maps ρ, σ and τ for four particles on a super-eight

Proposition 4.5.1. *All time preserving symmetries g_t of simple planar collision-free choreographies must have that $\rho(g_t)$ is a rotation, not a reflection.*

Proof. Let g be a time preserving symmetry. Then $\tau(g)$ is the identity map. This means that $\rho(g)$ must act trivially on the orientation of the curve. It also means that $\rho(g)$ must exactly map the positions of the particles to themselves or positions occupied by other particles, since we cannot shift time forward, and hence that the arrangement of particles must also possess the symmetry $\rho(g)$, at all values of t.

Assume $\rho(g)$ is a reflection. Then, if the curve crosses the axis of reflection, it must do so either perpendicular to the axis, or must form a crossing of $2a$ curve arcs, for some a, where the crossing lies on the axis. If it never crosses the axes of reflection, the choreography must have multiple components and hence is not simple.

If it crosses the axis at right angles, we may note that in this case it cannot preserve orientation. If it crosses the axis at a crossing, then the orientation of at least one pair of the arcs meeting at this crossing must be, without loss of generality, as given in Figure 4.6. If we then consider a particle which is moving along this part of the curve, which it must at some point do, it must have a partner which is moving on the opposite arc - then, these two particles will be bound to collide. Hence, if we require our choreographies to be collision-free, we have a contradiction. Hence, for a symmetry to be time-preserving, it cannot be a reflection. □

Corollary 4.5.2. *For a simple planar choreography of n particles to possess a time-preserving symmetry, n must be divisible by $|\ker \tau|$.*

Proof. If a choreography possesses a time-preserving symmetry g_t, then $\rho(g_t)$ must be

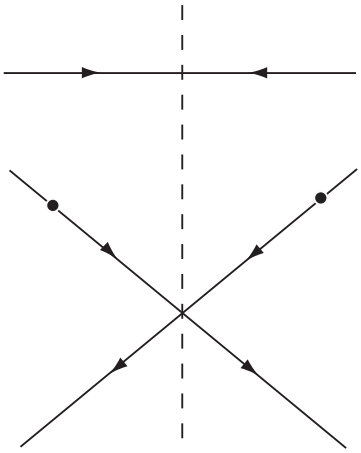

Figure 4.6: Meeting the axis at right angles, or at a crossing

a rotation, by Proposition 4.5.1, and it will be of order $|\ker\tau|$. Then, if this number does not divide the number of particles, one of the particles must be fixed by this rotation, and hence must be at the centre of rotation for all values of t, since the rotation applies for all t. This does not occur in a choreography, since all particles must perform the same motion and therefore we must have $|\ker\tau| \mid n$. □

Not many choreographies possess time-preserving symmetries, since as seen in Proposition 4.5.1, they must be a rotation, and must specifically also map the particles on to the positions of other particles - meaning that we need the choreography's arrangement of particles to possess the same rotational symmetry of the curve at all values of t.

In the presence of a time-preserving symmetry, the way in which the full loop $\hat{\gamma}$ is made up from copies of γ differs from that shown in Example 4.4.8. We now consider the same process but for our example of four particles on a Gerver super-eight.

Example 4.5.3 (Four particles on a super-eight)**.** Let G be the group of symmetries of the super-eight choreography with four particles. As seen in Example 4.5.1, this group is $D_4 \times \mathbb{Z}_2$, which has sixteen elements.

The top left picture in Figure 4.7 shows the movement of the particles from $t = 0$ to $t = T/8$, and this is the path γ, which we will combine using the group elements to produce the full loop $\hat{\gamma}$. Unlike in the case of three particles on a figure eight, in

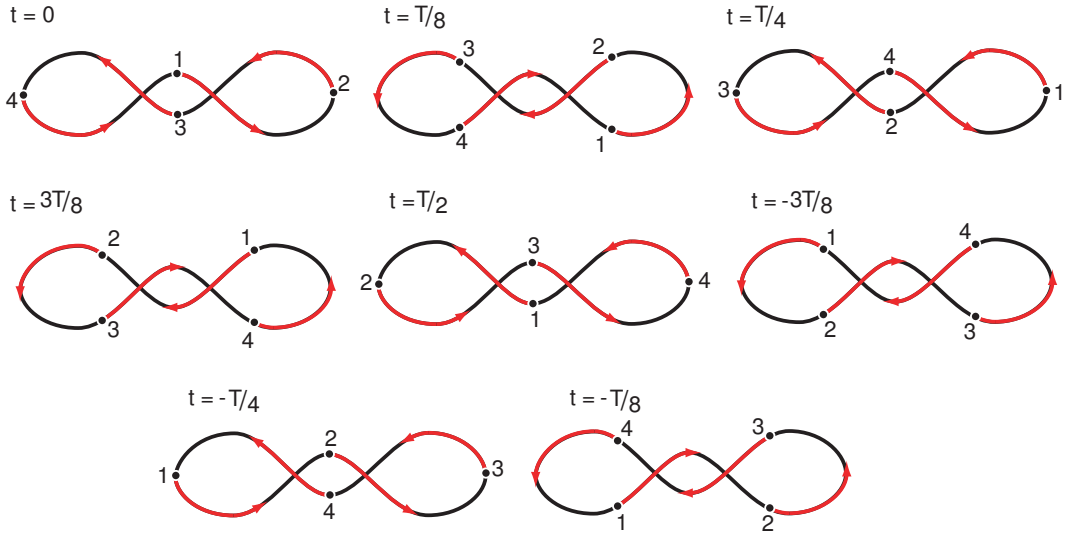

Figure 4.7: Four particles on a super-eight, at $t = {}^{kT}/_{8}$

which no time-preserving symmetries were present, in this case there are two group elements which could map γ onto the required section of $\hat{\gamma}$ - which are equivalent, up to multiplication by the element g_t, our time preserving symmetry. In Table 4.3, we see two columns of elements, where each element in the right hand side is the product of the corresponding element on the left with g_t, which is given by $\rho(g_t) = \kappa_1\kappa_2$, $\sigma(g_t) = (13)(24)$ and $\tau(g_t) = id$.

Elements from either side of the table could be used to map γ onto $\hat{\gamma}$, as long as one is taken from each row in order. The sides of the table represent the two cosets corresponding to the two elements of $\ker \tau$.

Table 4.3: Four particles on a super-eight - the map from γ to $\hat{\gamma}$

Time from	Time to	$\rho(g)$	$\tau(g)$	$\sigma(g)$	$\rho(g)$	$\tau(g)$	$\sigma(g)$
0	${}^{T}/_{8}$	I	0	e	$\kappa_1\kappa_2$	0	(13)(24)
${}^{T}/_{8}$	${}^{T}/_{4}$	κ_1	$\overline{{}^{T}/_{4}}$	(12)(34)	κ_2	$\overline{{}^{T}/_{4}}$	(14)(23)
${}^{T}/_{4}$	${}^{3T}/_{8}$	I	${}^{T}/_{4}$	(1234)	$\kappa_1\kappa_2$	${}^{T}/_{4}$	(1432)
${}^{3T}/_{8}$	${}^{T}/_{2}$	κ_1	$\overline{{}^{T}/_{2}}$	(24)	κ_2	$\overline{{}^{T}/_{2}}$	(13)
${}^{T}/_{2}$	${}^{-3T}/_{8}$	I	${}^{T}/_{2}$	(13)(24)	κ_2	${}^{T}/_{2}$	e
${}^{-3T}/_{8}$	${}^{-T}/_{4}$	κ_1	$\overline{{}^{-T}/_{4}}$	(14)(23)	$\kappa_1\kappa_2$	$\overline{{}^{-T}/_{4}}$	(12)(34)
${}^{-T}/_{4}$	${}^{-T}/_{8}$	I	${}^{-T}/_{4}$	(1432)	κ_2	${}^{-T}/_{4}$	(1234)
${}^{-T}/_{8}$	0	κ_1	$\overline{0}$	(13)	$\kappa_1\kappa_2$	$\overline{0}$	(24)

4.6 Topology of the Path Space $\mathcal{P}(X, F_0, F_1)$

Having determined the nature of the spaces F_0, F_1 and having gained a good idea of their relationship with X and choreographies, we may examine the resulting space of paths $\mathcal{P}(X, F_0, F_1)$ by considering the following. Assume, as always, that X is path connected.

First note that, given a choice of points $f_0 \in F_0$, $f_1 \in F_1$ we may choose a path $\omega : f_0 \rightsquigarrow f_1$ using which we have $\mathcal{P}(X, f_0, f_1) \simeq \mathcal{P}(X, f_0, f_0) \simeq \Omega(X, f_0)$, the space of closed loops based at f_0. Using a path $\omega' : f_0 \rightsquigarrow x$, we have that this space is $\Omega(X, x)$ for some arbitrary $x \in X$. This is useful, since we know $\pi_i(\Omega(X, x)) = \pi_{i+1}(X, x)$.

Theorem 4.6.1. *Let F_0, F_1 be such that $F_0 \times F_1$ is a manifold. Then*

$$\begin{array}{ccc} \mathcal{P}(X, F_0, F_1) & \xleftarrow{\quad i \quad} & \mathcal{P}(X, f_0, f_1) \\ \Big\downarrow{\scriptstyle \pi} & & \\ F_0 \times F_1 & & \end{array}$$

where f_0, f_1 are points in F_0 and F_1 respectively, is a fibration.

Proof. The fibration is given by a choice of f_0 and f_1 determining a subspace of $\mathcal{P}(X, F_0, F_1)$ of paths running exactly from f_0 to f_1, mapped by inclusion into $\mathcal{P}(X, F_0, F_1)$. An element in $\mathcal{P}(X, F_0, F_1)$ projects down to its endpoints in $F_0 \times F_1$.

We will show that this is a fibre bundle, and then (from [33]) since $F_0 \times F_1$ is paracompact (it is a manifold), we have a fibration.

Indeed, the fibre at every point is homeomorphic to $\Omega(X, x)$ as described above. We also have that given an open neighbourhood $(U(f_0), U(f_1)) \subset F_0 \times F_1$ we have that the preimage $\pi^{-1}(U(f_0), U(f_1))$ is homeomorphic to $U(f_0) \times U(f_1) \times \Omega(X, x)$, since F_0 and F_1 are locally path connected. Hence this is a fibre bundle and therefore a fibration, as required. □

Remark 4.6.2. We require here that $F_0 \times F_1$ is a manifold. Since F_0 and F_1 are fixed point spaces defined by affine symmetries of the particles, we have that in all our examples this is the case.

From this fibration, we may construct the following long exact sequence in homotopy:

$$\cdots \longrightarrow \pi_2(\Omega(X,x)) \longrightarrow \pi_2(\mathcal{P}(X,F_0,F_1)) \longrightarrow \pi_2(F_0 \times F_1) \xrightarrow{\delta}$$
$$\pi_1(\Omega(X,x)) \longrightarrow \pi_1(\mathcal{P}(X,F_0,F_1)) \longrightarrow \pi_1(F_0 \times F_1) \xrightarrow{\delta}$$
$$\pi_0(\Omega(X,x)) \longrightarrow \pi_0(\mathcal{P}(X,F_0,F_1)) \longrightarrow \pi_0(F_0 \times F_1) \xrightarrow{\delta}$$
$$0$$

Given our knowledge of many of these spaces, we can use this sequence to determine information about the others, as seen in the following examples.

4.6.1 Examples

- Three particles with the symmetry group of the Figure Eight (Example 3.2.1):

$$\cdots \longrightarrow 0 \longrightarrow \pi_1(\mathcal{P}(X,F_0,F_1)) \longrightarrow \mathbb{Z} \xrightarrow{\delta}$$
$$P_3 \longrightarrow \pi_0(\mathcal{P}(X,F_0,F_1)) \longrightarrow 0$$

  Here, we may note that since $\pi_i(\Omega(X,x)) = \pi_{i+1}(X,x)$, and that our space X is the $K(\pi,1)$ space $(\mathbb{R}^2)^3 \setminus \Delta$ for which $\pi_1(X,x) = P_3$, we have that $\pi_0(\Omega(X,x))$ is P_3, and all other $\pi_i(\Omega(X,x))$ are zero. Since $F_0 \times F_1$ is homotopic to $\mathbb{S}^1$, given that F_0 is has a single contractible connected component and $F_1 \simeq \mathbb{S}^1$, we have that $F_0 \times F_1$ is a $K(\pi,1)$ with $\pi = \mathbb{Z}$.

  The fundamental group of $F_1 \simeq \mathbb{S}^1$ as a subgroup of $\pi_1(X) = P_3$ is $\mathbb{Z}$ generated by the full twist, which corresponds to the two particles on the circle moving round the third particle and returning to their initial positions. The fundamental group of each connected component of F_0 is trivial. This means the map δ above maps $\mathbb{Z}$ into P_3 as the subgroup generated by the full twist.

  Since this map is injective, we have that $\pi_1(\mathcal{P}(X,F_0,F_1))$ is trivial. We also have that $\pi_0(\mathcal{P}(X,F_0,F_1))$ is $P_3/ < \Delta^2 >$, where Δ^2 is the full twist. This

means $\mathcal{P}(X, F_0, F_1)$ has infinitely many connected components, and all of its homotopy groups π_i are trivial for $i \geq 1$.

The figure eight solution given in Example 3.2.1 on page 45 lies in one of these connected components.

- Four Particles with the symmetry group of the super-eight (Example 4.5.1):

$$\cdots \longrightarrow 0 \longrightarrow \pi_1(\mathcal{P}(X, F_0', F_1')) \longrightarrow 0 \xrightarrow{\delta} P_4 \longrightarrow \pi_0(\mathcal{P}(X, F_0', F_1')) \longrightarrow 16 \xrightarrow{\delta} 0$$

In this case, F_0' and F_1' both have four contractible connected components, and hence $F_0' \times F_1'$ has 16 contractible components, and so $\pi_0(F_0' \times F_1')$ is 16 and all other homotopy groups are trivial. We also have that $X = K(P_4, 1)$, and so $\pi_0(\Omega(X, x))$ is P_4, and all other $\pi_i(\Omega(X, x))$ are zero.

Exactness forces that $\pi_1(\mathcal{P}(X, F_0', F_1')) = 0$. We also have a short exact sequence

$$0 \longrightarrow P_4 \longrightarrow \pi_0(\mathcal{P}(X, F_0', F_1')) \longrightarrow 16 \longrightarrow 0$$

There are 16 connected components of $F_0' \times F_1'$, corresponding to a renumbering of the four particles within the restrictions defining the spaces F_0', F_1'.

This means $\pi_0(\mathcal{P}(X, F_0', F_1'))$ consists of sixteen copies of P_4, and hence $\mathcal{P}(X, F_0', F_1')$ has infinitely many connected components. It also has all homotopy groups π_i trivial for $i \geq 1$.

This method can be applied to all of the examples in this thesis, to determine the topology of the path space $\mathcal{P}(X, F_0, F_1)$.

Example 4.6.3 (Different connected components for the symmetry group of 4 on a super-eight)**.** The sixteen components of $F_0 \times F_1$ in the example above correspond to a renumbering of the particles. A generic arrangement of particles for each choice of F_0, F_1 is shown in Figure 4.8.

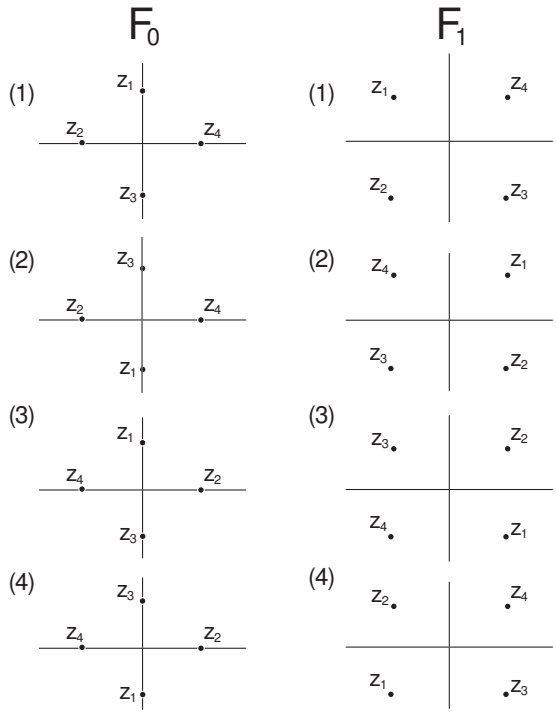

Figure 4.8: Different labellings for the particles giving different connected components

We can choose a diagram from each column and this will give us a connected component of choreographies for this n and symmetry group. There may be multiple paths joining the two points, and our choice of path is our γ which we use to construct the full loop.

The example of four particles on a super-eight, given in Example 4.5.1 on page 88 is in the connected component corresponding to $F_0(3)$ and $F_1(3)$.

In Figure 4.9 we see a path between the two configurations, and the corresponding image from our previous diagram of the motion. In this case our time preserving symmetry g_t dictates we must have $\kappa_1\kappa_2$ symmetry for all values of t, which is seen in our motion.

Choosing a different pair of fixed point space components can give a different curve. For example, $F_0(1)$ to $F_1(4)$ with the appropriate choice of path gives an equivalent choreography to the super-eight one shown above, but with different $t = 0$ and numbering of particles. Choosing $F_0(3)$ to $F_1(2)$ with a certain path gives a connected component containing the Lagrange circular solution, as does $F_0(1)$ to $F_1(1)$.

Figure 4.9 shows an example of a path γ, from $F_0(3)$ to $F_1(3)$, which can be seen to be equivalent to the section of motion described in the adjacent diagram, which shows the motion from $t = 0$ to $t = {}^{T}/_{8}$ in Example 4.5.1 of four particles on a super-eight.

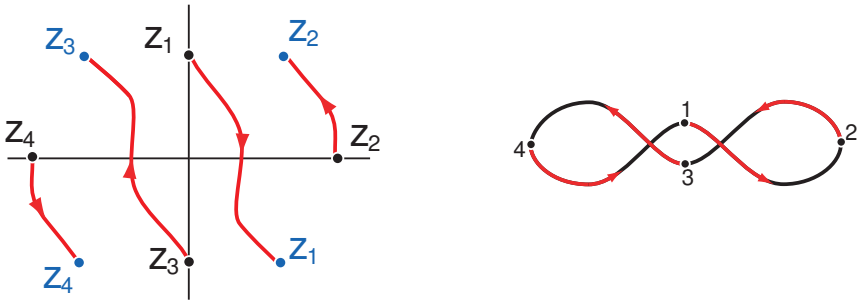

Figure 4.9: The path γ, from $F_0(3)$ to $F_1(3)$

Example 4.6.4 (Different connected components for the symmetry group of 3 on a figure eight)**.** While the fixed point spaces for four particles on a super-eight in the example above are very restricted, due to the application of the time preserving symmetry, we may similarly examine different ways to connect F_0 to F_1 for other examples. Below we present an alternative relative loop for the example of three particles on a figure eight, and see that we obtain a new solution which is in a different connected component.

The fixed point spaces for three particles with figure eight symmetry are given by:

$$F_0 = \{(z_1, z_2, z_3) \in \mathbb{C}^3 \setminus \Delta \mid z_1 = \bar{z}_2, z_3 = \bar{z}_3\}$$

$$F_1 = \{(z_1, z_2, z_3) \in \mathbb{C}^3 \setminus \Delta \mid z_2 = -z_2, z_1 = -z_3\}$$

Two different ways to connect these sets of points, for a given choice of numbering of particles, can be seen in Figure 4.10.

Extending path a) from Figure 4.10 results in the figure eight choreography, whereas path b) gives the choreography shown in Figure 4.11.

This curve is a local minimum for the action functional under the strong force, on the connected component given by path b) in Figure 4.10. The given path was

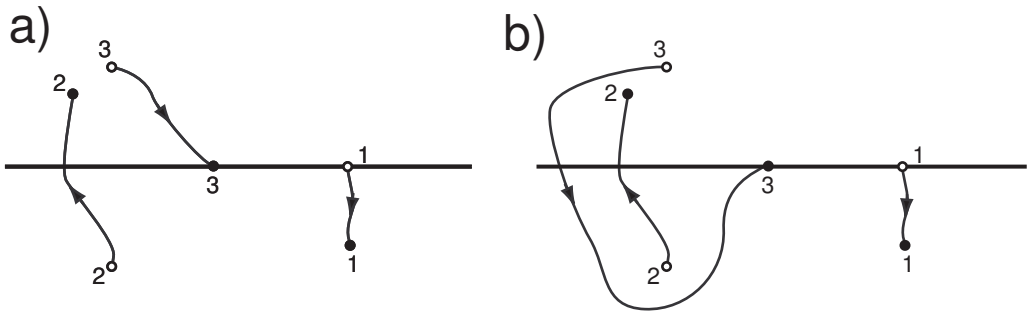

Figure 4.10: Two non-homotopic paths connecting F_0 (hollow dots) to F_1 (solid dots)

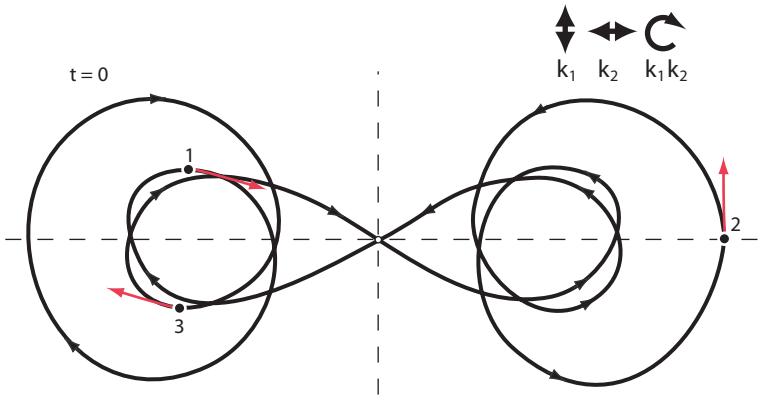

Figure 4.11: Three particles on a curve with figure eight symmetry which is in a different connected component to the figure eight

approximated by a Fourier series of order 23, subject to the constraint of the figure eight symmetry group, and this was iterated in the direction of negative slope of the action functional with strong force potential action until a local minimum was attained. This means the curve shown will be a choreographical solution of the n-body problem. For an explanation of the action functional and n-body solutions, see Chapter 6.

Proposition 4.6.5. *The two choreographies obtained from extending the sections of*

path shown in Figure 4.10 lie in different connected components of Λ_G.

Proof. The set of connected components of Λ_G, for the symmetry group G corresponding to the figure eight curve, is given by $\pi_0(\Omega(X, F_0, F_1)) = P_3/\langle\Delta^2\rangle$, as shown in Example 4.6.1. For two elements to be equal in this space, they must differ by a multiple of Δ^2.

If we consider the motion given by travelling along path a) and returning by travelling backwards along path b), this will give us the difference between these two paths. This curve is shown in Figure 4.12, and can be seen to be equivalent to the braid σ_1^2, which is not a multiple of Δ^2. Hence, the two choreographies lie in different connected components.

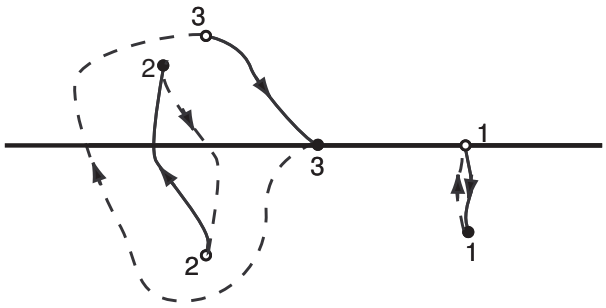

Figure 4.12: Travelling along path a) and returning along path b)

□

This method may be used to find solutions in different connected components for any given symmetry group - by starting with an existing choreography, reducing it to a path connecting the fixed point spaces, and choosing a different (non-homotopic) way of connecting the points. The method has been employed in Example A.12 on page 176 in the Appendix, to discover a choreography in which three particles move on a curve with square symmetry in the plane.

Chapter 5

Examples of n-body choreographies

In the previous chapters, we saw some examples demonstrating interesting properties, namely the example of three particles on a figure eight, and four particles on a super-eight. In this chapter we consider some more examples and families of examples which exist as solutions to n-body problems with certain sets of symmetries. We discuss some methods of classifying such examples up to homotopy, as well as the different connected components of the loop space of collisionless motions which are present.

5.1 Rotationally symmetrical examples

There are a large number of closed curves which possess the symmetry group D_k of the regular k-gon, consisting of k rotations by multiples of $^{2\pi}/_{k}$ and k reflections, in axes which differ by multiples of $^{\pi}/_{k}$. Here we attempt to classify some such curves and introduce notation.

5.1.1 Foil type curves

There exist familiar foil-type curves, such as the trefoil, seen in Figure 5.1, which is well known as the prime knot 3_1 from knot theory. (Here we consider the projection of a trefoil onto the plane; the orientation of crossings is irrelevant). In an attempt to generalise this concept, we note the following.

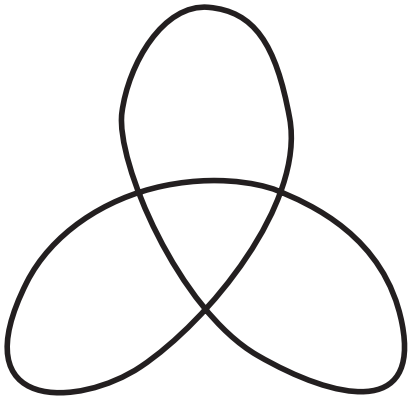

Figure 5.1: A trefoil

- The centre of the trefoil is a 'triangle' - made up of three curved arcs, which meet at three points
- The vertices of this central shape are joined to each other around the outside of the curve by arcs, and in the case of the trefoil, each is joined to an adjacent vertex

Two variables may be identified here, and will be defined as follows:

- Let p denoted the 'petal number' of a foil. This is the number of petals the curve will possess, and corresponds to the number of sides (equivalently, the number of vertices) possessed by the central 'polygon' made of arcs. It also corresponds to the degree of rotational symmetry of the curve. In the case of the trefoil, $p = 3$.
- Let j denote the 'joining number'. This will denote the way in which the arcs connect the vertices around the outside of the central shape. It counts, inclusive, the number of vertices between where each arc leaves and rejoins the shape. In the case of the trefoil, where arcs join adjacent vertices, $j = 2$. Were the arc to join a vertex to the next-but-one vertex, j would equal 3.

Note here that the definition of j relies on a choice of direction around the polygon in which to progress, but as long as all arcs are drawn in the same way, the resulting curve will be equivalent regardless of which direction that is.

Remark 5.1.1. The curve resulting from drawing the central polygon first and adding arcs does not always initially look smooth as a curve - however, this is merely a guideline to assist in constructing the curve, which may be refined to produce a smooth continuous and symmetrical path.

Further, the rotational symmetry constraint requires that each arc joins the polygon in a natural way, such that the side of the polygon it joins then receives an orientation which means particles travel in the same direction around the polygon. This is necessary to ensure each side of the polygon is traveled along exactly once.

Remark 5.1.2. It is possible to construct similar curves which do not have the orientation of the arcs around the central polygon all the same. If we alternate the direction of the arcs on successive sides of a p-gon (for even values of p), the (p, j)-foils as defined below may only be constructed for even values of j, since in other cases we find the arc would need to enter a corner toward which both arrows are pointing.

Curves constructed from contrarily oriented polygons will, as we will see, for the consistently oriented case with even p and j, be made up of multiple components, but these components will have opposite orientations. This is shown in Figure 5.2, which shows the two different $(6, 2)$-foils which can be obtained by differing orientations on the hexagon, each of which is made of two $(3, 1)$-foils, or triangles. The example with contrary orientations on successive arcs is explored in more detail in Example 7.1.1 on page 145.

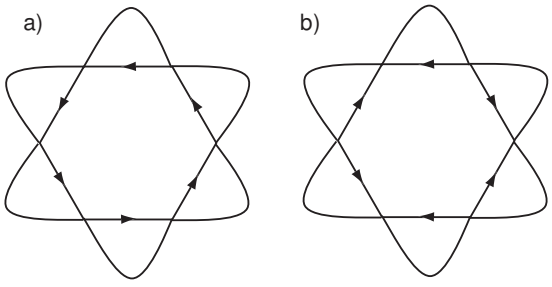

Figure 5.2: $(6, 2)$-foils, with a) complementary orientation, b) contrary orientation

5.1.2 The notation (p, j)

By defining a $(\mathbf{p}, \mathbf{j})$**-foil** as the curve with p-fold rotational symmetry made by drawing a p-gon made of arcs and connecting them all with joining number j, we may then describe a whole family of foil-type curves, which can generalise in two directions. The trefoil, for instance, would be a $(3, 2)$-foil, and Table 5.1 gives the number of connected components of curves made using several different values of p and j. The

Table 5.1: Table of (p, j)-foils - number of components

No. of petals p	Joining number j 2	3	4	5
3	1 (trefoil)	3 (circles)	1	1
4	2 (lozenges)	1	4 (circles)	1
5	1	1	1	5 (circles)
6	2 (triangles)	3 (lozenges)	2 (trefoils)	1

following facts may be noted:

- If p and j have highest common factor q, then the resulting curve will have q components, each of which is a curve of type $(p/q, j/q)$.
- In particular, if $p = j$ we obtain a curve made up of $p = j$ disjoint circles.
- If p and j are coprime, the curve has a single connected component.

Remark 5.1.3. Note that the smallest value of j which may be sensibly considered is $j = 2$, and we define $j = 1$ to mean there are no arcs drawn at the corners of the shape. Hence, foils of type $(p, 1)$ are not strictly foils - $(1, 1)$ is a circle, $(2, 1)$ is a lozenge with two straight sides joined with curves at each end, and $(3, 1)$ is a triangle with rounded corners.

These are not strictly foils, but these are the shapes which result when $j/q = 1$. One might expect that we could define a $(p, 1)$-foil as a shape in which we join back to the same corner, by means of a loop – but this is what we call a flower-type curve, and will be defined on page 107.

So, as seen in Table 5.1, a $(4, 2)$-foil consists of two overlapping lozenge shapes. A $(6, 4)$-foil is two trefoils which differ by a reflection.

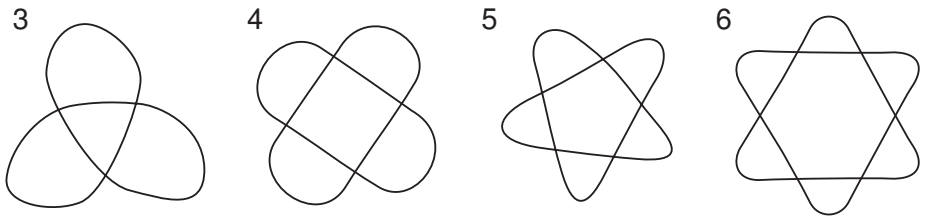

Figure 5.3: $(p, 2)$-foils, for $p = 3, 4, 5, 6$

Figure 5.3 shows a $(3, 2), (4, 2), (5, 2)$ and $(6, 2)$-foil shape. Note that for $j = 2$, even values of p give shapes made up of multiple curves, whereas odd values of p give a single curve.

5.1.3 The case of $(p, p-1)$-foils

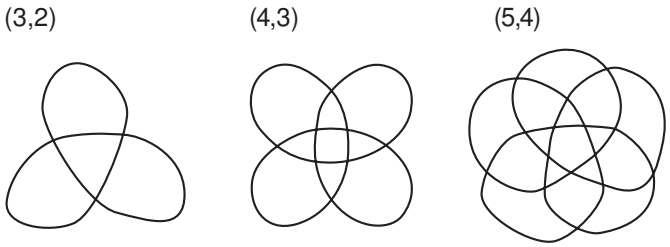

Figure 5.4: $(p, p-1)$-foils, for $p = 3, 4, 5$

Of particular interest in the study of simple choreographies are those curves possessing a single connected component. In particular we note that the foils making up the diagonal of Table 5.1, consisting of exactly those foils for which $p = j + 1$, all have a single component. These curves are of particular interest, because they may be considered as part of a family of homotopic curves which differ in appearance depending on a parameter in the equation of the curve. This may be considered geometrically to correspond to the size of the central curved polygon, as described below.

5.1.3.1 Windmills

If we reduce the size of the central polygon in such curves, deforming the whole curve homotopically, we will eventually obtain a shape where the arcs cross in the centre at

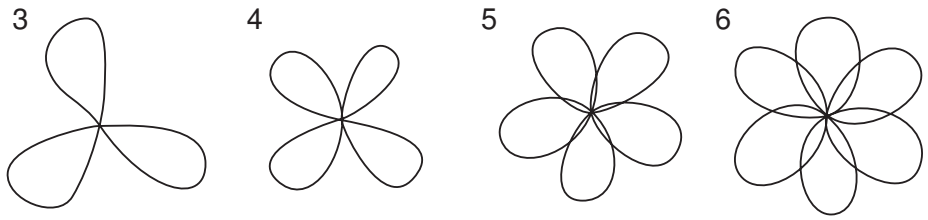

Figure 5.5: p-windmills, for $p = 3, 4, 5, 6$

a single point. This we call a **windmill** with p petals, and choreographies have been found numerically possessing this shape - one is given in the animations of n-body choreographies in [29], for which $p = 6$ and $n = 7$.

5.1.3.2 Flowers

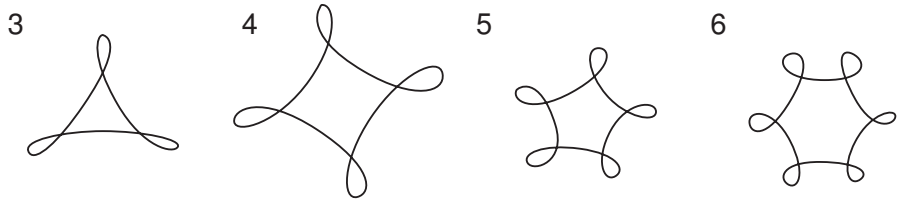

Figure 5.6: p-flowers, for $p = 3, 4, 5, 6$

If we continue to push the curves in the same direction, past the point where they meet in the middle, we find another p-sided shape forms in the centre, with a loop at each corner. This we call a **flower** with p petals, and again examples have been found with this shape - see Example 5.1.10 on page 116 and Example A.2.2 on page 158, among others.

Remark 5.1.4. The case of the flower differs notably from the foil in that on a foil-type curve, the particles will always be moving around the central point of the configuration in the same direction. On a flower, the direction of travel relative to the centre alternates between clockwise and anticlockwise each time a particle travels along one of the outer loops.

Remark 5.1.5. Not all curves of this type will permit a choreography solution for every number of particles n. The motion of a single particle on an m-flower can be broken down into m sections which consist of the same curve in space, up to a

rotation by $^{2\pi}/_{m}$. As shown in Figure 5.7, we can WLOG take $t = 0$ to be when the particle is at the base of the loop, and as t increases it proceeds around the loop.

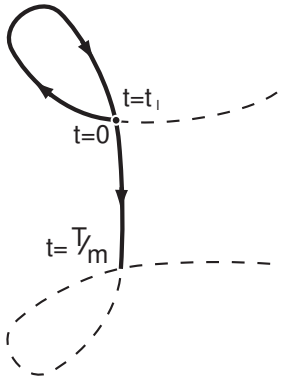

Figure 5.7: One section of the flower motion, for m petals

At some value of t, denoted t_ℓ, $0 < t_\ell < {}^{2\pi}/_{m}$ (the value of t_ℓ will depend on the relative sizes of the loop and central region) it will pass through the point where it started, then at $t = {}^{T}/_{m}$ it will arrive at the base of the next loop. This motion is then repeated on the next section.

This means that for $n < m$, we will never have a collision, since no two particles will ever be in the same section at the same time. Hence the only opportunity for collisions will occur when $n \geq m$, and in particular in the case where ${}^{kT}/_{n} = t_\ell$, which may occur for any value of n depending on the value of t_ℓ.

As we will see below, different values of t_ℓ will sometimes lead to different connected components in the space of loops, either side of a value of t_ℓ which results in a collision, for some values of m and n.

We may consider, as in the example given in Example 5.1.8 of the $(4, 3)$-foil on page 115, the curves to be defined using some coefficient in their equation, which corresponds to the position along a continuum from foil to flower, in terms of the relative size of the central polygon, with windmills at zero size and negative sizes in the case of flowers.

5.1.4 Different connected components

It may be noted that, depending on the number of particles n present on such a curve, there may be several different connected components of the loop space represented in the continuum from foil to flower. We now consider two useful examples demonstrating the transition from foil, through windmill, to flower, with different numbers of particles, and consider the points on the continuum at which connected components of the space of collision-free loops begin and end.

5.1.4.1 The trefoil, or $(3, 2)$-foil

- $n = 3$
  - It may be noted that in the case of three particles on a trefoil, the motion of the particles is homotopic to the Lagrangian motion of particles on a circle which sit at the points of an equilateral triangle rotating about its centre with constant speed. On a trefoil, three particles will be at the points of an equilateral triangle at all times, except that the size of the triangle varies from that at the ends of each loop to that at the middle of each side of the central curved triangle, and the speed will also fluctuate in a repeating way. The particles pass around the centre point twice for each complete orbit.
  - It is not permissible for three particles to move on a windmill shape with three petals, since the motion will inevitably lead to a collision of all three particles at the centre.
  - Three particles on a three-flower will again always sit at the points of a triangle, which will fluctuate in size during the course of an orbit. The motion will also alternate between clockwise and anticlockwise (although this does not mean they are ever stationary - at times when the direction changes, the triangle is still increasing or decreasing in size). This motion only passes around the centre once per complete orbit, unlike the foil case, and hence is in a different connected component.

Remark 5.1.6. This raises the question of whether there might exist motions where the particles pass around the centre k times per complete orbit. In fact, this corresponds to foils of type $(p, j + kp)$. Flowers will only ever pass around once.

- $n = 4$

  The example of four particles on a trefoil, which is treated in more detail as Example 5.1.7 later in this section, provides a very interesting range of connected components of the loop space. Let us first consider a trefoil in which the centre of the curve is a very large triangle, and gradually reduce its size, eventually obtaining windmills and flowers.

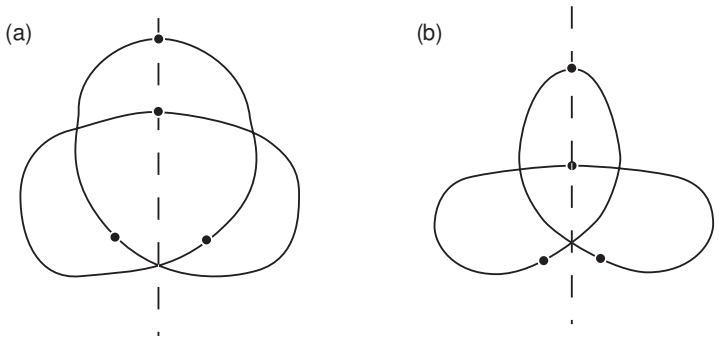

Figure 5.8: Four particles on a trefoil - (a) large triangle, (b) small triangle

  – Large triangle: Refer to Figure 5.8(a). If we let $t = 0$ when two of the particles lie on the vertical axis of reflection, the remaining two will lie on the central triangle (above the crossing).

    Smaller triangle: Refer to Figure 5.8(b). By reducing the size of the triangle, we find the same situation results in the two lower particles sitting **below** the crossing, outside of the central triangle.

    This means that at some intermediate triangle size, the two lower particles will be bound to collide at this crossing. So, these two states give two distinct connected components in the loop space.

  – Four particles may exist on a three-petal windmill, without colliding.

– If we continue to a flower shape, we again find that as we increase the size of the triangle, there will come a point at which the time taken to pass along one of the outer loops, from the crossing back to the crossing, is $T/4$. This will cause a collision. So, the flower-type curves with loop sizes either side of this value will represent two different connected components.

Example 5.1.7 (Four particles on a trefoil)**.** The trefoil is an example of a foil type curve, with three petals, and here we consider it with four particles. In this example, our diagram of a trefoil is as in Figure 5.8(b) where the triangle is small and the two points lie outside the central triangle, but we are actually considering all curves with this group of symmetries, and hence all connected components of such loops.

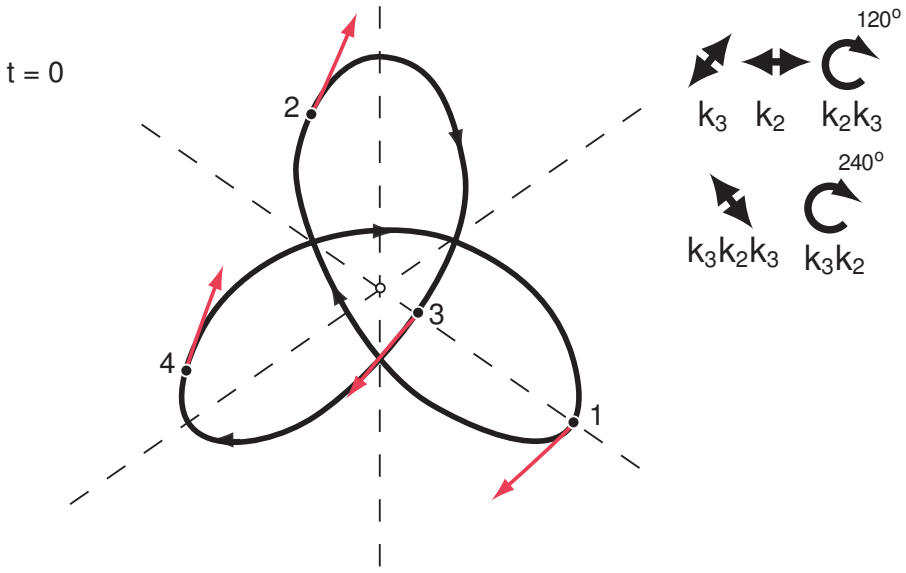

Figure 5.9: Four particles on a trefoil, at $t = 0$

The trefoil curve has the symmetry group of a triangle, which is generated by the horizontal reflection κ_2 and a diagonal reflection κ_3, which reflects in the axis with negative slope at an angle of $\pi/3$ below the horizontal. The other reflection is $\kappa_3\kappa_2\kappa_3$ and the possible rotations are by $2\pi/3$ clockwise, $\kappa_2\kappa_3$, and by $4\pi/3$ clockwise, $\kappa_3\kappa_2$.

The arrangements of particles possess symmetry at $t = kT/12$, with κ_3 reflection symmetry when $k = 0 \bmod 3$, κ_2 reflection symmetry when $k = 1 \bmod 3$, and $\kappa_3\kappa_2\kappa_3$ symmetry when $k = 2 \bmod 3$. The rotational symmetries $\kappa_3\kappa_2$ and $\kappa_2\kappa_3$ involves a time shift of some multiple of $T/12$.

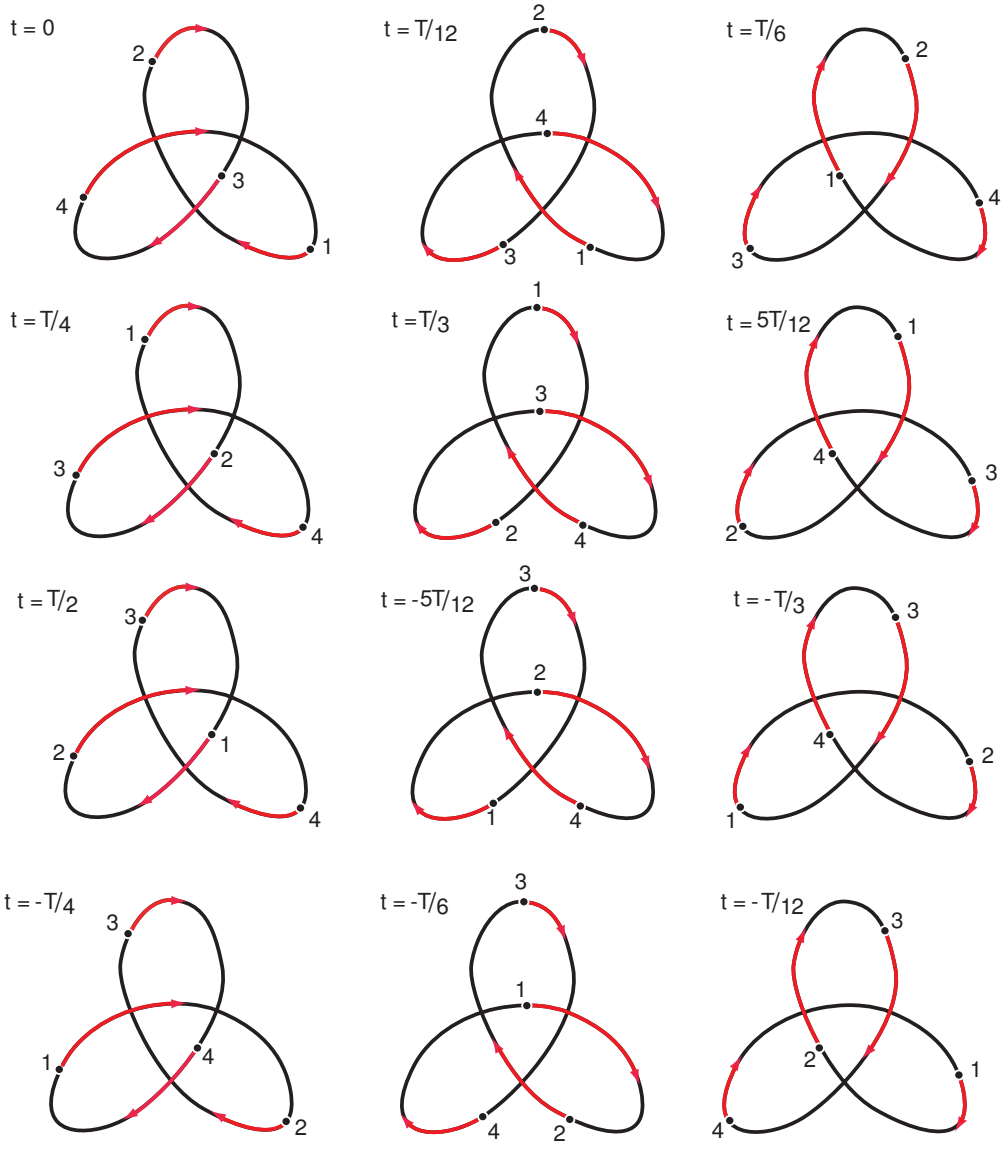

Figure 5.10: Four particles on a trefoil, at $t = {}^{kT}/_{12}$

The choreography symmetry is present, as are two time-reversing symmetries, given by $\rho(g_0) = \kappa_3$ with $\sigma(g_0) = (24)$, and $\rho(g_1) = \kappa_2$ with $\sigma(g_1) = (13)$, with a time shift of $T/6$.

Fixed point space F_0:

$$\gamma(0) = g_0\gamma(0) = \kappa_3(24)\gamma(0)$$

Therefore,

$$(z_1, z_2, z_3, z_4) = \kappa_3(24)(z_1, z_2, z_3, z_4)$$

This means that z_1 and z_3 must both lie on the axis of reflection of κ_3, and z_2 and z_4 form a pair where each is the image of the other under κ_3. This is equivalent to two distinct points lying on the real axis plus one conjugate pair. Hence the fixed point space $F_0 = \mathrm{Fix}(g_0)$ is given by two distinct points in $\mathbb{R}$, determining the positions of z_1 and z_3, crossed with a copy of $\mathbb{C} \setminus \mathbb{R}$ which determines the position of z_2, and the position of z_4 then follows.

This is therefore $(\mathbb{R}^2 \setminus \Delta) \times (\mathbb{C} \setminus \mathbb{R})$. This space has four contractible connected components. So $F_0 \simeq pt \sqcup pt \sqcup pt \sqcup pt$.

Fixed point space F_1:

$$\hat{\gamma}(T/12) = g_1\hat{\gamma}(T/12) = \kappa_2(13)\hat{\gamma}(T/12)$$

Therefore,

$$\begin{aligned}(z_1, z_2, z_3, z_4) &= \kappa_2(13)(z_1, z_2, z_3, z_4) \\ &= (-\bar{z}_3, -\bar{z}_2, -\bar{z}_1, -\bar{z}_4)\end{aligned}$$

The fact that $z_2 = -\bar{z}_2$ and $z_4 = -\bar{z}_4$ means that z_2 and z_4 must be on the imaginary axis. Then z_1 and z_3 form a pair either side of this axis, each other's image under the reflection κ_2. This is again equivalent to two real points and a conjugate pair. Hence the fixed point space $F_1 = \mathrm{Fix}(g_1)$ is also given by $\mathbb{R}^2 \setminus \Delta \times (\mathbb{C} \setminus \mathbb{R})$, and has four contractible connected components. So $F_1 \simeq pt \sqcup pt \sqcup pt \sqcup pt$.

This choreography has no symmetries which act trivially on the time circle - those symmetries which are not time-reversing require a time shift.

Table 5.2: Four particles on a trefoil

$\rho(g)$	$\tau(g)$	$\sigma(g)$	Order
I	0	e	1
I	$T/4$	(1234)	4
I	$T/2$	(13)(24)	2
I	$-T/4$	(1432)	4
κ_2	$\overline{T/6}$	(13)	2
κ_2	$\overline{5T/12}$	(12)(34)	2
κ_2	$\overline{-T/3}$	(24)	2
κ_2	$\overline{-T/12}$	(14)(23)	2
$*\kappa_3$	$\overline{0}$	(24)	2
κ_3	$\overline{T/4}$	(14)(23)	2
κ_3	$\overline{T/2}$	(13)	2
κ_3	$\overline{-T/4}$	(13)(34)	2
$*\kappa_3\kappa_2$	$T/12$	(1234)	12
$\kappa_3\kappa_2$	$T/3$	e	3
$\kappa_3\kappa_2$	$-5T/12$	(1432)	12
$\kappa_3\kappa_2$	$-T/6$	(13)(24)	6
$\kappa_2\kappa_3$	$T/6$	(13)(24)	6
$\kappa_2\kappa_3$	$5T/12$	(1234)	12
$\kappa_2\kappa_3$	$-T/3$	e	3
$\kappa_2\kappa_3$	$-T/12$	(1432)	12
$\kappa_3\kappa_2\kappa_3$	$\overline{T/12}$	(12)(34)	2
$\kappa_3\kappa_2\kappa_3$	$\overline{T/3}$	(24)	2
$\kappa_3\kappa_2\kappa_3$	$\overline{-5T/12}$	(14)(23)	2
$\kappa_3\kappa_2\kappa_3$	$\overline{-T/6}$	(13)	2

The full group of symmetries is given in Table 5.2. It has order 24, includes 12 reflections, and has a dihedral structure generated by the starred elements. It is the dihedral group D_{12}. The maps ρ, σ and τ for this group can be seen in Figure 5.11.

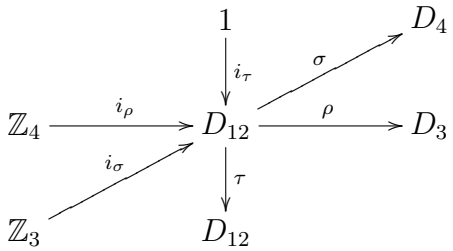

Figure 5.11: The maps ρ, σ and τ for four particles on a trefoil

- $n = 5$ The case for five particles follows similarly to that for four, in that there

are two kinds of flower and two kinds of foil, except that the top half of the trefoil contains three particles instead of two, as shown in Figure 5.12.

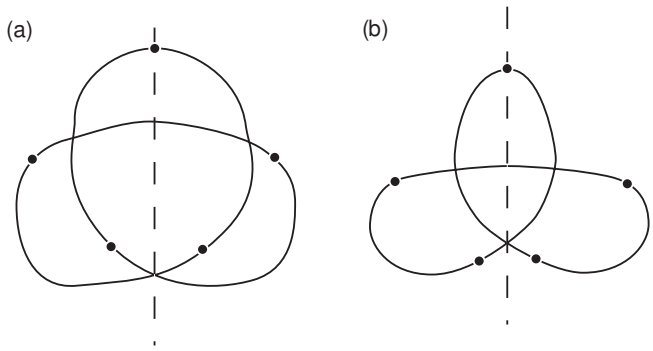

Figure 5.12: Five particles on a trefoil - (a) large triangle, (b) small triangle

Example 5.1.8 (The $(4,3)$-foil, or 4-superfoil)**.** It has been previously noted that the examples of (p,j)-foils which generalise to windmills and flowers are precisely the $(p,p-1)$-foils. Here, we present the $(4,3)$-foil which admits five particles. Figure 5.13 shows a curve given by $\gamma(t) = e^{3it} + ae^{-it}$, for six different values of a.

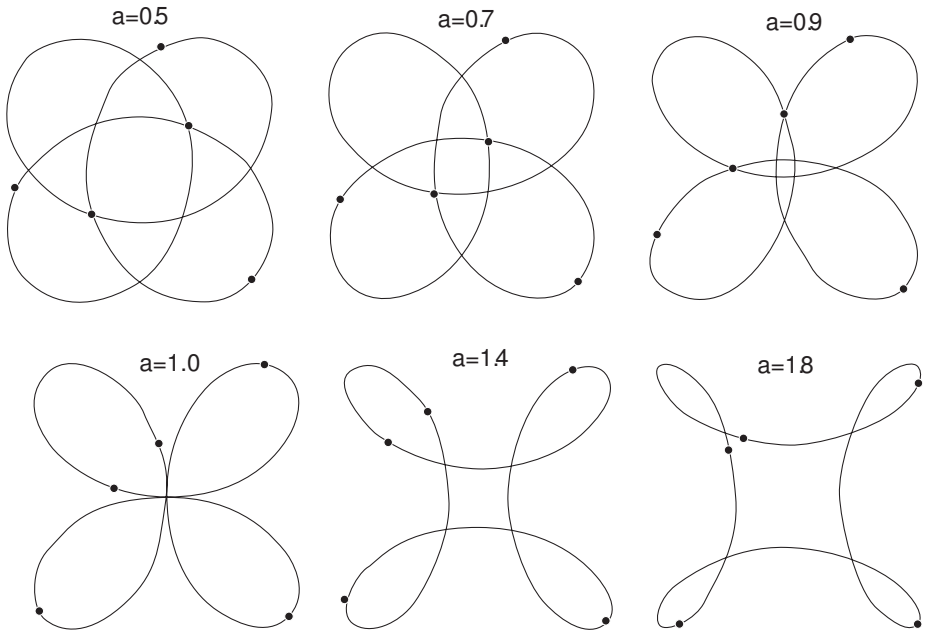

Figure 5.13: The curve $\gamma(t)$, with five particles

Proposition 5.1.9. *For all values of a, the curve given by $\gamma(t) = e^{3it}+ae^{-it}$ possesses the symmetry group D_4, symmetries of a square.*

Proof. The symmetry group of a square can be generated by a rotation by $\pi/2$ and any reflection. We will show that for each of these two symmetries, for all values of $t \in (0, 2\pi]$, there exists $u \in (0, 2\pi]$ such that $\gamma(u)$ is the image under the symmetry of $\gamma(t)$.

- Rotation by $\pi/2$

  Need that $\forall t\ \exists u$ such that $\gamma(u) = i\gamma(t)$. In fact, $u = t - \pi/2$.

  $$\gamma(t - \pi/2) = -ie^{3it} + ae^{-it} = i\gamma(t)$$

- Reflection in the real axis

  Need that $\forall t\ \exists u$ such that $\gamma(u) = \overline{\gamma(t)}$ (complex conjugate). In fact, $u = -t$.

  $$\gamma(-t) = e^{-3it} + ae^{it} = \overline{e^{3it} + ae^{-it}} = \overline{\gamma(t)}$$

The curve therefore possesses these two symmetries, and hence the whole symmetry group D_4 of symmetries. □

The curves with this equation, for different values of the parameter a, can be seen to demonstrate a range of curve types, from a $(4, 3)$-foil to a 4-flower, as well as exhibiting three different connected components of the loop space, as in the example of the trefoil. For $a = 0.5$ and $a = 0.7$ it can clearly be seen in Figure 5.14 that the two particles lie inside or outside a crossing, and hence these two states give different connected components, since at some intermediate point there will necessarily be a value of a for which a collision occurs here.

The homotopy class of curves corresponding to the case $a = 1.4$ is seen in the following example.

This is an example of a flower type curve, with four petals. The presence of five particles on the curve means that to avoid collisions, the curve can be any size except that in which the time taken to pass along a petal and return to the crossing is $T/5$, in which case we would have a collision.

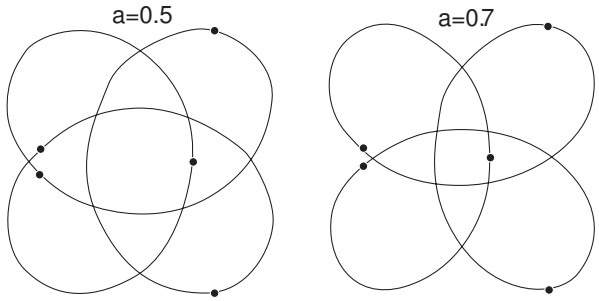

Figure 5.14: The curve $\gamma(t)$, showing the different components between $a = 0.5$ and $a = 0.7$

The four-petal flower curve has the symmetry group of a square, which is generated by the vertical reflection κ_1 and the diagonal reflection in the line of positive slope, denoted κ_3. The total symmetry group has eight elements, including two other reflections ($\kappa_3\kappa_1\kappa_3$, horizontally, which has elsewhere been denoted κ_2; and $\kappa_1\kappa_3\kappa_1$, in the other diagonal) as well as rotations $\kappa_1\kappa_3$, $(\kappa_1\kappa_3)^2$ and $\kappa_3\kappa_1$, by $\pi/2$, π and $3\pi/2$ clockwise, respectively.

The arrangements of particles possess symmetry at $t = kT/20$, with κ_1 symmetry at even values of k and $\kappa_3\kappa_1\kappa_3$ symmetry when k is odd. The rotational symmetries involve a time shift of some multiple of $T/20$. The choreography symmetry is present, as are two time-reversing symmetries, given by $\rho(g_0) = \kappa_1$ with $\sigma(g_0) = (12)(35)$, and $\rho(g_1) = \kappa_3$ with $\sigma(g_1) = (12)(35)$.

Fixed point space F_0:

$$\gamma(0) = g_0\gamma(0) = \kappa_1(12)(35)\gamma(0)$$

Therefore,

$$\begin{aligned}(z_1, z_2, z_3, z_4, z_5) &= \kappa_1(12)(35)(z_1, z_2, z_3, z_4, z_5) \\ &= (\bar{z}_2, \bar{z}_1, \bar{z}_5, \bar{z}_4, \bar{z}_3)\end{aligned}$$

Since $z_4 = \bar{z}_4$, this point must lie on the real line, and the other four points form two conjugate pairs either side of this line. Hence the fixed point space $F_0 = \mathrm{Fix}(g_0)$ is given by a point in $\mathbb{R}$, and the positions of z_1 and z_3, which will be distinct points in the upper or lower half-plane. We must also have that as well as $z_1 \neq z_3$, we have

Example 5.1.10 (Five particles on a four-flower)**.**

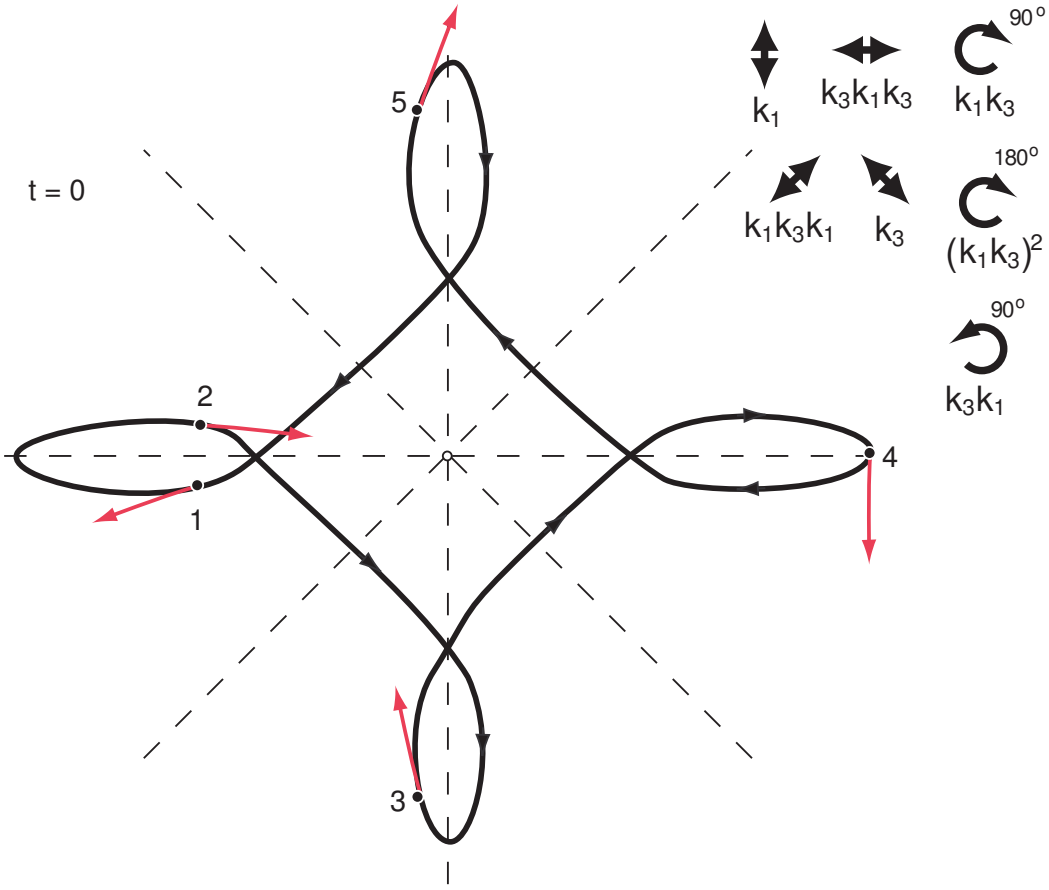

Figure 5.15: Five particles on a four-flower, at $t = 0$

$z_1 \neq \bar{z}_3$. This means we take the space $(\mathbb{C} \setminus \mathbb{R})^2$, and subtract two diagonal sets. The resulting space has four connected components, each of which is homotopic to $\mathbb{R}^4 \setminus \mathbb{R}^2 \simeq \mathbb{S}^1$. So $F_1 \simeq \mathbb{R} \times (\mathbb{S}^1 \sqcup \mathbb{S}^1 \sqcup \mathbb{S}^1 \sqcup \mathbb{S}^1) \simeq \mathbb{S}^1 \sqcup \mathbb{S}^1 \sqcup \mathbb{S}^1 \sqcup \mathbb{S}^1$.

Fixed point space F_1:

$$\hat{\gamma}(T/20) = g_1\hat{\gamma}(T/20) = \kappa_3(12)(35)\hat{\gamma}(T/20)$$

Therefore,

$$\begin{aligned}(z_1, z_2, z_3, z_4, z_5) &= \kappa_3(12)(35)(z_1, z_2, z_3, z_4, z_5) \\ &= (-i\bar{z}_2, -i\bar{z}_1, -i\bar{z}_5, -i\bar{z}_4, -i\bar{z}_3)\end{aligned}$$

This means that z_4 is a point on the diagonal axis of reflection, and the other points form two pairs under the reflection. This is just the same as the situation above up to a rotation, and so the fixed point space $F_1 = \mathrm{Fix}(g_1)$ is again homotopic to $\mathbb{S}^1 \sqcup \mathbb{S}^1 \sqcup \mathbb{S}^1 \sqcup \mathbb{S}^1$.

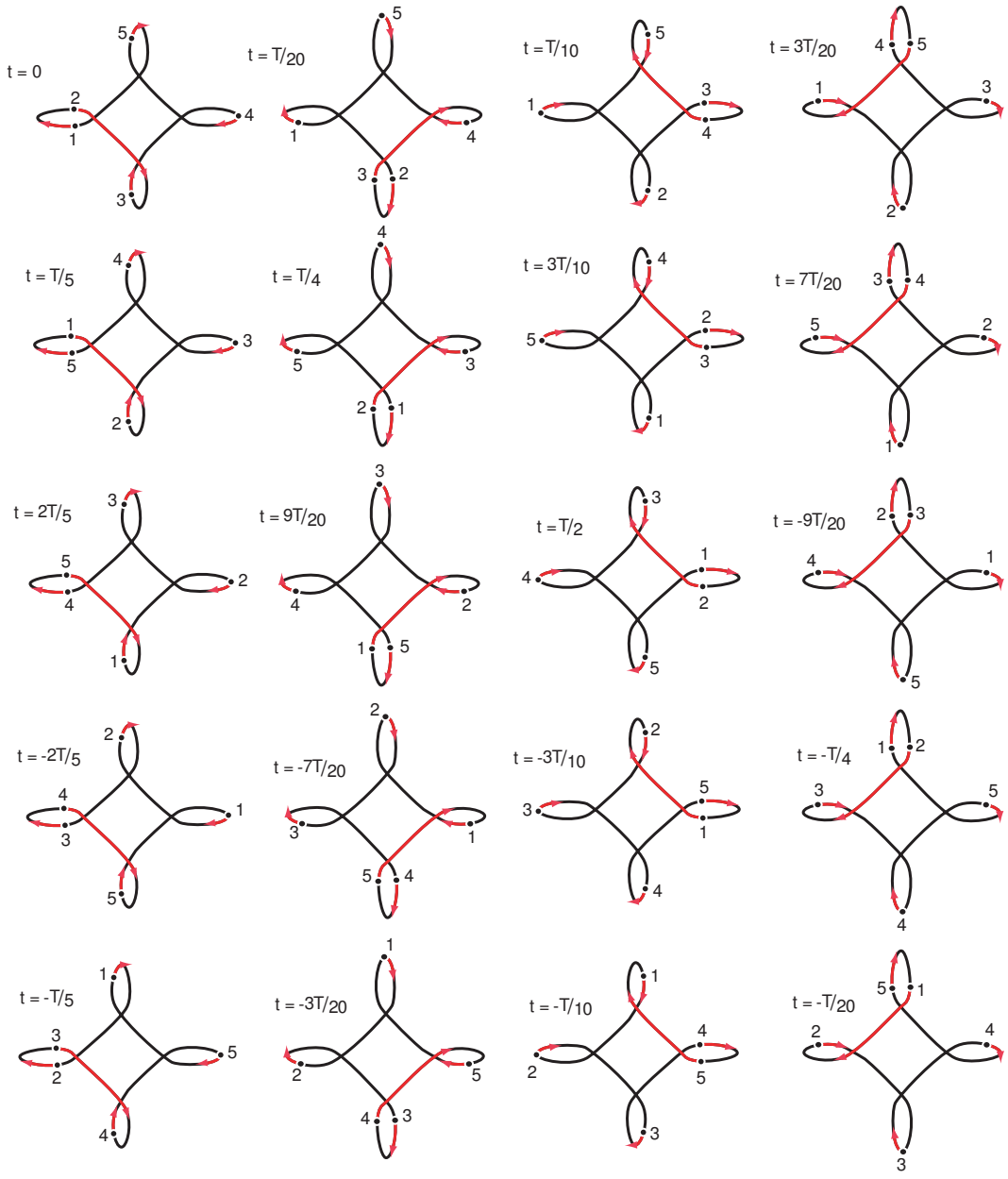

Figure 5.16: Five particles on a four-flower, at $t = {}^{kT}/_{20}$

This choreography has no symmetries which act trivially on the time circle - any which are not time reversing involve a time shift.

The full group of symmetries is given in Table 5.3 on page 120. It has order 40, and a dihedral structure generated by the starred elements, and hence is the dihedral group D_{20}. The maps ρ, σ and τ for this group can be seen in Figure 5.17.

Further examples of flower-type choreographies, including six particles on a three-flower, and eight particles on a four-flower, can be seen in the Appendix.

Table 5.3: Five particles on a four-flower

$\rho(g)$	$\tau(g)$	$\sigma(g)$	Order
I	0	e	1
I	$T/5$	(12345)	5
I	$2T/5$	(13524)	5
I	$-2T/5$	(14253)	5
I	$-T/5$	(15432)	5
$*\kappa_1$	$\overline{0}$	(12)(35)	2
κ_1	$\overline{T/5}$	(15)(24)	2
κ_1	$\overline{2T/5}$	(13)(45)	2
κ_1	$\overline{-2T/5}$	(25)(34)	2
κ_1	$\overline{-T/5}$	(14)(23)	2
κ_3	$\overline{T/20}$	(13)(45)	2
κ_3	$\overline{9T/20}$	(25)(34)	2
κ_3	$\overline{-3T/20}$	(14)(23)	2
κ_3	$\overline{T/4}$	(12)(35)	2
κ_3	$\overline{-7T/20}$	(15)(24)	2
$*\kappa_3\kappa_1$	$T/20$	(12345)	20
$\kappa_3\kappa_1$	$T/4$	e	4
$\kappa_3\kappa_1$	$9T/20$	(15432)	20
$\kappa_3\kappa_1$	$-7T/20$	(14253)	20
$\kappa_3\kappa_1$	$-3T/20$	(13524)	20
$\kappa_1\kappa_3$	$3T/20$	(14253)	20
$\kappa_1\kappa_3$	$7T/20$	(13524)	20
$\kappa_1\kappa_3$	$-9T/20$	(12345)	20
$\kappa_1\kappa_3$	$-T/4$	e	4
$\kappa_1\kappa_3$	$-T/20$	(15432)	20
$\kappa_3\kappa_1\kappa_3$	$\overline{T/10}$	(14)(23)	2
$\kappa_3\kappa_1\kappa_3$	$\overline{3T/10}$	(13)(45)	2
$\kappa_3\kappa_1\kappa_3$	$\overline{T/2}$	(12)(35)	2
$\kappa_3\kappa_1\kappa_3$	$\overline{-3T/10}$	(25)(34)	2
$\kappa_3\kappa_1\kappa_3$	$\overline{-T/10}$	(15)(24)	2
$\kappa_1\kappa_3\kappa_1$	$\overline{3T/20}$	(15)(24)	2
$\kappa_1\kappa_3\kappa_1$	$\overline{7T/20}$	(14)(23)	2
$\kappa_1\kappa_3\kappa_1$	$\overline{-9T/20}$	(13)(45)	2
$\kappa_1\kappa_3\kappa_1$	$\overline{-T/4}$	(12)(35)	2
$\kappa_1\kappa_3\kappa_1$	$\overline{-T/20}$	(25)(34)	2
$(\kappa_1\kappa_3)^2$	$T/10$	(13524)	10
$(\kappa_1\kappa_3)^2$	$3T/10$	(12345)	10
$(\kappa_1\kappa_3)^2$	$T/2$	e	2
$(\kappa_1\kappa_3)^2$	$-3T/10$	(15432)	10
$(\kappa_1\kappa_3)^2$	$-T/10$	(14253)	10

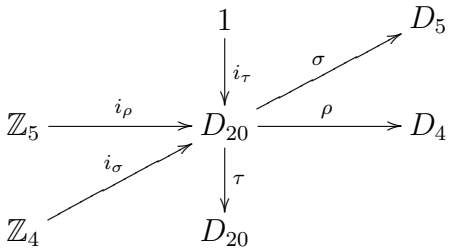

Figure 5.17: The maps ρ, σ and τ for five particles on a four-flower

5.2 Chains

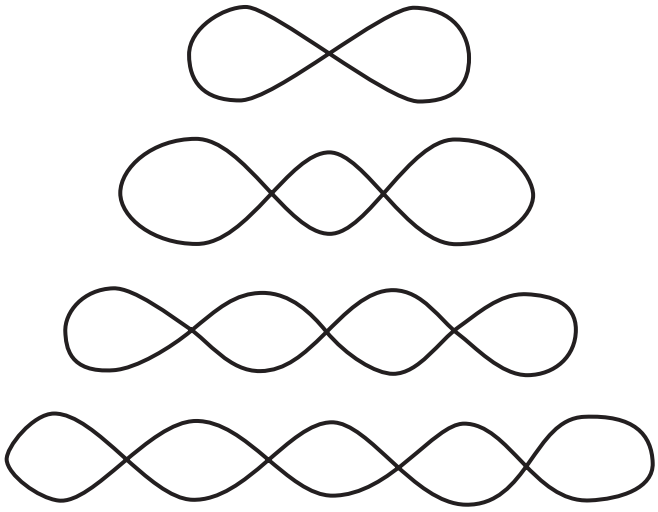

Figure 5.18: Linear chains, with one, two, three and four crossings

A curve which takes the form of an elongated circle which has been twisted at regular intervals along its length to form crossings is called an s-chain, where s is the number of segments formed. A figure eight shape is a simple example of a 2-chain, possessing merely one crossing and two segments. Such chains can be described numerically as **Lissajous-type** curves given by

$$x = A\cos(t) \quad y = B\sin(bt)$$

where b determines the number of crossings. The values of A and B determine the relative width and height of the curve.

Many choreographies have been found to exist numerically on chains - see Figure 4.2(a) in [11], or Figure 5 in [18]. The segments of the chain are not always all

the same size - the super-eight of Gerver is often found with the central segment being larger or smaller than the other two, depending on the number of particles. If the segments are either all the same size, or differ in a symmetrical way, the chain possesses the same spatial symmetries as a rectangle - those in D_2, consisting of a rotation by π and a pair of orthogonal reflections.

There exist examples of non-symmetrical chains, such as that shown in Figure 4.2(c) in [11], where 8 bodies move on a chain with six segments, where the second segment from the left is enlarged and the third reduced.

The examples of five particles on a figure eight, super-eight and four-chain, given below and shown in Figures 5.19, 5.22 and 5.25 respectively, all exhibit the same overall symmetry group, namely the dihedral group D_{10} of order twenty. In the case of the super-eight, the group is generated slightly differently, since the rotation symmetry is not time reversing and the reflection κ_2 is. The same group structure results. The three examples can be thought of as existing in the same loop space, of five particles in the plane with D_2 spatial symmetries, but being in different connected components of this loop space as we increase the number of segments.

There exist other types of chain which do not possess the same D_2 spatial symmetry group. In Example A.2.5 on page 171 we see a bifurcated chain for which one end splits into two, and while this still has one reflectional symmetry in the horizontal axis, no other symmetry is present.

Example 5.2.1 (Five particles on a figure eight)**.** The figure eight shape has previously been considered with three particles, and many choreographies have been discovered in which odd numbers of particles move on the figure eight curve. In the case of five particles, seen in Figure 5.19, it will become apparent that the symmetries of this choreography are similar to those of five particles on a four-chain and on a super-eight, and that these examples are closely related.

The figure eight curve has the symmetry group of a rectangle, which is generated by the reflection κ_1 and the reflection κ_2, and includes the rotation by π, $\kappa_1\kappa_2$.

The arrangements of particles possess symmetry at $t = kT/20$, as seen in Figure

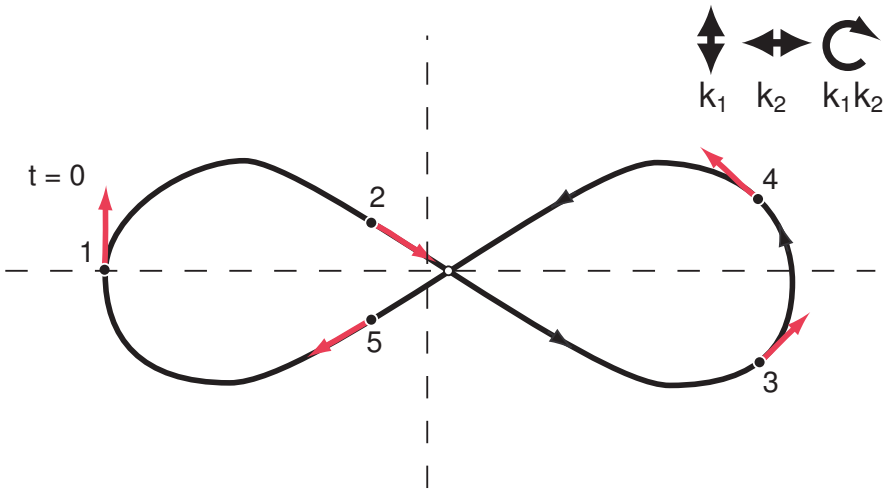

Figure 5.19: Five particles on a figure eight, at $t = 0$

5.20, with κ_1 symmetry at even values of k and $\kappa_1\kappa_2$ symmetry when k is odd. The symmetry of κ_2 involves a time shift of $T/10$. The choreography symmetry is present, as are two time-reversing symmetries, given by $\rho(g_0) = \kappa_1$ with $\sigma(g_0) = (25)(34)$, and $\rho(g_1) = \kappa_1\kappa_2$ with $\sigma(g_1) = (25)(34)$ and a time shift of $T/10$.

Fixed point space F_0:

$$\gamma(0) = g_0\gamma(0) = \kappa_1(25)(34)\gamma(0)$$

Therefore,

$$\begin{aligned}(z_1, z_2, z_3, z_4, z_5) &= \kappa_1(25)(34)(z_1, z_2, z_3, z_4, z_5)\\ &= (\bar{z}_1, \bar{z}_5, \bar{z}_4, \bar{z}_3, \bar{z}_2)\end{aligned}$$

Since $z_1 = \bar{z}_1$, this point must lie on the real line, and the other four points form two conjugate pairs either side of this line. Hence the fixed point space $F_0 = \mathrm{Fix}(g_0)$ is given by a point in $\mathbb{R}$, and the positions of z_2 and z_3, which will be distinct points in the upper or lower half-plane. We must also have that as well as $z_2 \neq z_3$, we have $z_2 \neq \bar{z}_3$. This means we take the space $(\mathbb{C} \setminus \mathbb{R})^2$, and subtract two diagonal sets. The resulting space has four connected components, each of which is homotopic to $\mathbb{R}^4 \setminus \mathbb{R}^2 \simeq \mathbb{S}^1$. So $F_1 \simeq \mathbb{R} \times (\mathbb{S}^1 \sqcup \mathbb{S}^1 \sqcup \mathbb{S}^1 \sqcup \mathbb{S}^1) \simeq \mathbb{S}^1 \sqcup \mathbb{S}^1 \sqcup \mathbb{S}^1 \sqcup \mathbb{S}^1$.

Fixed point space F_1:

$$\hat{\gamma}(T/4) = g_1\hat{\gamma}(T/4) = \kappa_1\kappa_2(13)(45)\hat{\gamma}(T/4)$$

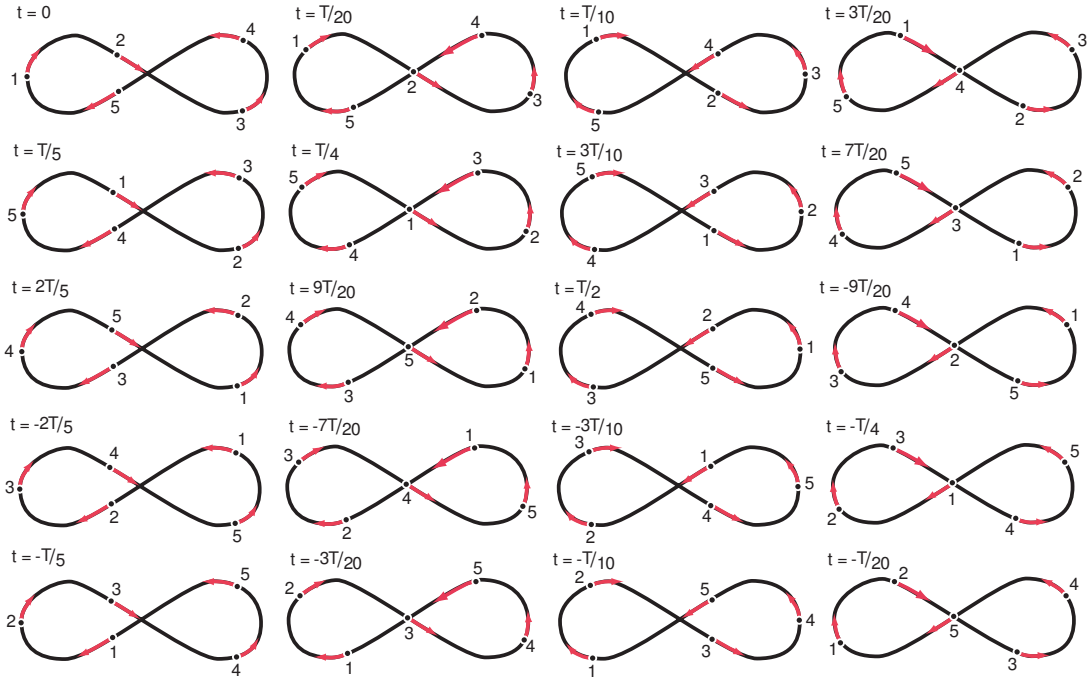

Figure 5.20: Five particles on a figure eight, at $t = kT/20$

Therefore,

$$\begin{aligned}(z_1, z_2, z_3, z_4, z_5) &= \kappa_1\kappa_2(13)(45)(z_1, z_2, z_3, z_4, z_5) \\ &= (-z_3, -z_2, -z_1, -z_5, -z_4)\end{aligned}$$

Since $z_2 = -z_2$, this forces $z_2 = 0$. The other four points form two pairs either side of 0, where $z_1 = -z_3$ and $z_4 = -z_5$. Hence the fixed point space $F_1 = \mathrm{Fix}(g_1)$ is given by two distinct points in the punctured plane, which also cannot be equal to each other's negatives.

$$F_1 = \{(z_1, z_4) \in \mathbb{C}^2 \mid z_1 \neq 0, z_4 \neq 0, z_1 \neq \pm z_4\}$$

This is the space $\mathbb{C}^2$ minus four complex planes. By Lemma A.1.1 on page 157 in the Appendix, this is $K(\mathbb{Z} \times \mathbb{F}_3, 1)$ where $\mathbb{F}_3$ is the free group on three generators.

This choreography has no symmetries which act trivially on the time circle - those which are not time reversing require a time shift.

The full group of symmetries is given in Table 5.4. It has order 20, and a dihedral structure generated by the starred elements, and hence is the dihedral group D_{10}.

The maps ρ, σ and τ for this group can be seen in Figure 5.21.

Table 5.4: Five particles on a figure eight

$\rho(g)$	$\tau(g)$	$\sigma(g)$	Order
I	0	e	1
I	$^{T}/_{5}$	(12345)	5
I	$^{2T}/_{5}$	(13524)	5
I	$^{-2T}/_{5}$	(14253)	5
I	$^{-T}/_{5}$	(15432)	5
$*\kappa_1$	$\overline{0}$	(25)(34)	2
κ_1	$\overline{^{T}/_{5}}$	(15)(24)	2
κ_1	$\overline{^{2T}/_{5}}$	(14)(23)	2
κ_1	$\overline{^{-2T}/_{5}}$	(13)(45)	2
κ_1	$\overline{^{-T}/_{5}}$	(12)(35)	2
$\kappa_1\kappa_2$	$\overline{^{T}/_{10}}$	(13)(45)	2
$\kappa_1\kappa_2$	$\overline{^{3T}/_{10}}$	(12)(35)	2
$\kappa_1\kappa_2$	$\overline{^{T}/_{2}}$	(25)(34)	2
$\kappa_1\kappa_2$	$\overline{^{-3T}/_{10}}$	(15)(24)	2
$\kappa_1\kappa_2$	$\overline{^{-T}/_{10}}$	(14)(23)	2
$*\kappa_2$	$^{T}/_{10}$	(14253)	10
κ_2	$^{3T}/_{10}$	(15432)	10
κ_2	$^{T}/_{2}$	e	2
κ_2	$^{-3T}/_{10}$	(12345)	10
κ_2	$^{-T}/_{10}$	(13524)	10

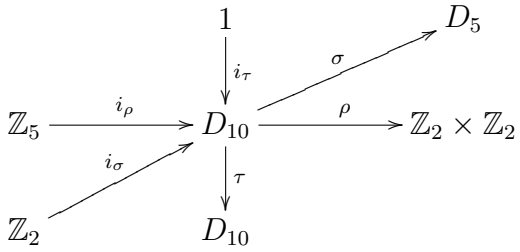

Figure 5.21: The maps ρ, σ and τ for five particles on a figure eight

The 'Super-Eight' of Gerver, commonly seen with four particles, also permits five, although in this case the central loop of the three is bigger, not smaller, than the other two.

The super-eight curve has the symmetry group of a rectangle, which is generated by the reflection κ_1 and the reflection κ_2, and includes the rotation by π, $\kappa_1\kappa_2$.

Example 5.2.2 (Five particles on a super-eight)**.**

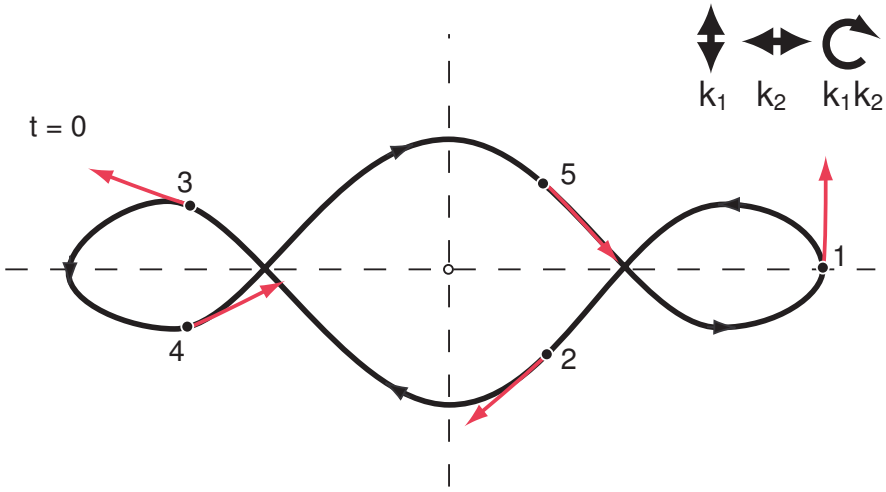

Figure 5.22: Five particles on a super-eight, at $t = 0$

The arrangements of particles possess symmetry at $t = kT/20$, with κ_1 symmetry at even values of k and κ_2 symmetry when k is odd. The symmetry of $\kappa_1\kappa_2$ involves a time shift of $T/10$ and a permutation of the particles.

The choreography symmetry is present, as are two time-reversing symmetries, given by $\rho(g_0) = \kappa_1$ with $\sigma(g_0) = (25)(34)$, and $\rho(g_1) = \kappa_2$ with $\sigma(g_1) = (13)(45)$ and a time shift of $T/10$.

Fixed point space F_0:

$$\gamma(0) = g_0\gamma(0) = \kappa_1(25)(34)\gamma(0)$$

Therefore,

$$\begin{aligned}(z_1, z_2, z_3, z_4, z_5) &= \kappa_1(25)(34)(z_1, z_2, z_3, z_4, z_5)\\ &= (\bar{z}_1, \bar{z}_5, \bar{z}_4, \bar{z}_3, \bar{z}_2)\end{aligned}$$

Since $z_1 = \bar{z}_1$, this point must lie on the real line, and the other four points form two conjugate pairs either side of this line. Hence the fixed point space $F_0 = \mathrm{Fix}(g_0)$ is given by a point in $\mathbb{R}$, and the positions of z_2 and z_3, which will be distinct points in the upper or lower half-plane. We must also have that as well as $z_2 \neq z_3$, we have $z_2 \neq \bar{z}_3$. This means we take the space $(\mathbb{C} \setminus \mathbb{R})^2$, and subtract two diagonal sets. The resulting space has four connected components, each of which is homotopic to $\mathbb{R}^4 \setminus \mathbb{R}^2 \simeq \mathbb{S}^1$. So $F_0 \simeq \mathbb{R} \times (\mathbb{S}^1 \sqcup \mathbb{S}^1 \sqcup \mathbb{S}^1 \sqcup \mathbb{S}^1) \simeq \mathbb{S}^1 \sqcup \mathbb{S}^1 \sqcup \mathbb{S}^1 \sqcup \mathbb{S}^1$.

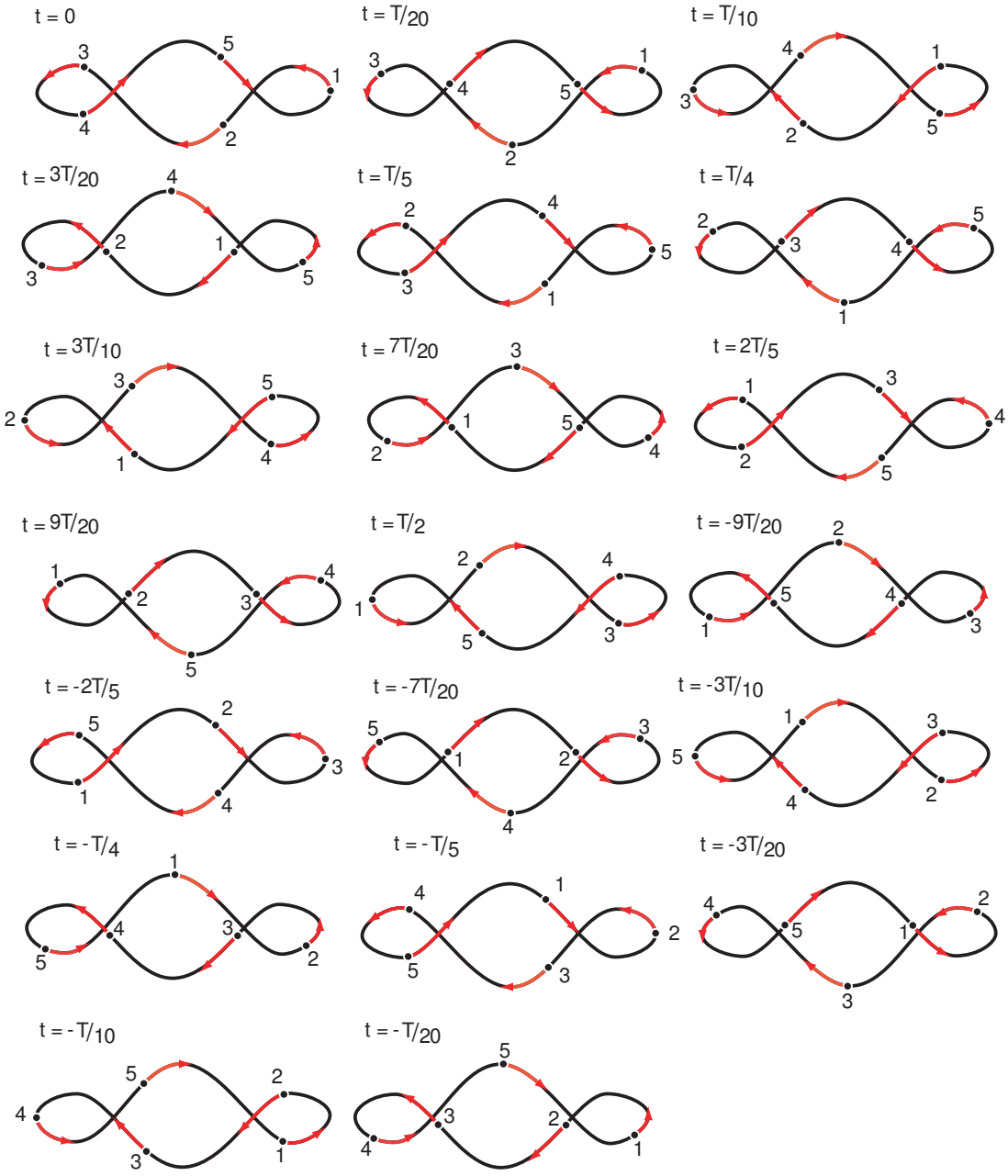

Figure 5.23: Five particles on a super-eight, at $t = kT/20$

Fixed point space F_1:

$$\hat{\gamma}(T/4) = g_1\hat{\gamma}(T/4) = \kappa_2(25)(34)\hat{\gamma}(T/4)$$

Therefore,

$$\begin{aligned}(z_1, z_2, z_3, z_4, z_5) &= \kappa_2(25)(34)(z_1, z_2, z_3, z_4, z_5)\\ &= (-\bar{z}_1, -\bar{z}_5, -\bar{z}_4, -\bar{z}_3, -\bar{z}_2)\end{aligned}$$

Since $z_1 = -\bar{z}_1$, this forces z_1 to lie in the vertical axis. The other four points form two pairs either side of the vertical axis, where $z_2 = -\bar{z}_5$ and $z_3 = -\bar{z}_4$. Hence the fixed point space F_1 is the same as the fixed point space F_0 up to a rotation, and hence is also $\mathbb{S}^1 \sqcup \mathbb{S}^1 \sqcup \mathbb{S}^1 \sqcup \mathbb{S}^1$.

This choreography has no symmetries which act trivially on the time circle - those which are not time reversing require a time shift.

The full group of symmetries is given in Table 5.5. It has order 20, and a dihedral structure generated by the starred elements, and hence is the dihedral group D_{10}. The maps ρ, σ and τ for this group can be seen in Figure 5.24.

Table 5.5: Five particles on a super-eight

$\rho(g)$	$\tau(g)$	$\sigma(g)$	Order
I	0	e	1
I	$^{T}/_{5}$	(12345)	5
I	$^{2T}/_{5}$	(13524)	5
I	$^{-2T}/_{5}$	(14253)	5
I	$^{-T}/_{5}$	(15432)	5
$^*\kappa_1$	$\overline{0}$	(25)(34)	2
κ_1	$\overline{^{T}/_{5}}$	(15)(24)	2
κ_1	$\overline{^{2T}/_{5}}$	(14)(23)	2
κ_1	$\overline{^{-2T}/_{5}}$	(13)(45)	2
κ_1	$\overline{^{-T}/_{5}}$	(12)(35)	2
κ_2	$\overline{^{T}/_{10}}$	(13)(45)	2
κ_2	$\overline{^{3T}/_{10}}$	(12)(35)	2
κ_2	$\overline{^{T}/_{2}}$	(25)(34)	2
κ_2	$\overline{^{-3T}/_{10}}$	(15)(24)	2
κ_2	$\overline{^{-T}/_{10}}$	(14)(23)	2
$^*\kappa_1\kappa_2$	$^{T}/_{10}$	(14253)	10
$\kappa_1\kappa_2$	$^{3T}/_{10}$	(15432)	10
$\kappa_1\kappa_2$	$^{T}/_{2}$	e	2
$\kappa_1\kappa_2$	$^{-3T}/_{10}$	(12345)	10
$\kappa_1\kappa_2$	$^{-T}/_{10}$	(13524)	10

The four-chain has similarities with the figure eight, in that it is a chain-type curve with an odd number of crossings - this means that it possesses a rotational symmetry which is time-reversing.

The four-chain curve has the same symmetry group as the figure eight. The

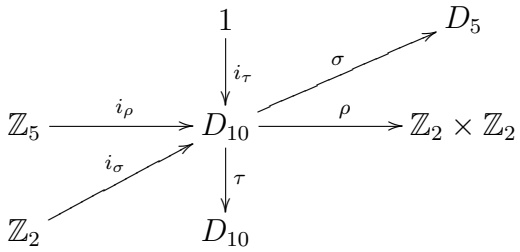

Figure 5.24: The maps ρ, σ and τ for five particles on a super-eight

Example 5.2.3 (Five particles on a four-chain)**.**

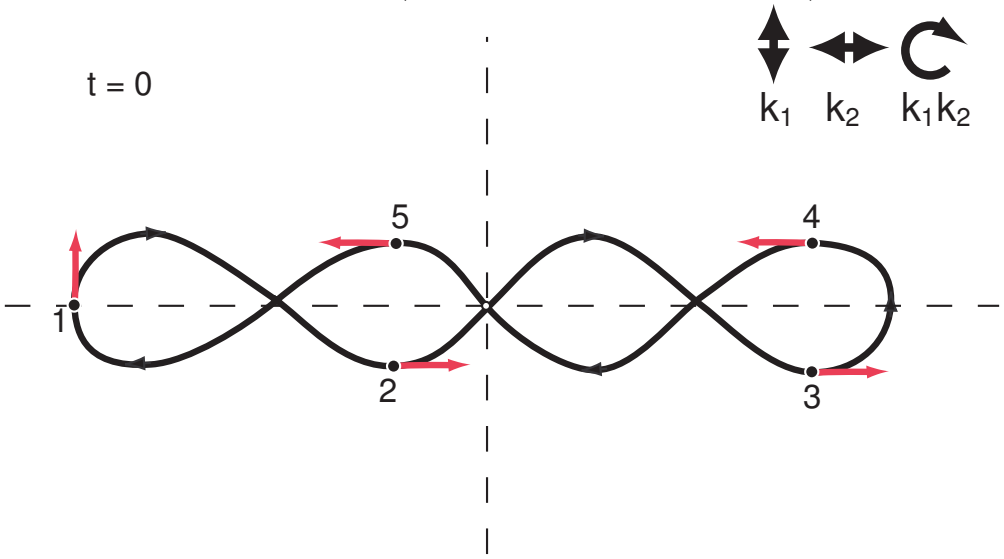

Figure 5.25: Five particles on a four-chain, at $t = 0$

arrangements of particles possess symmetry at the same times in the same way, and can be seen in Figure 5.26 on page 130.

The time-reversing symmetries and fixed point spaces are also the same. The group of symmetries is the same as that given in Table 5.4 on page 125.

5.3 Distorted figure eights

The figure eight curve, considered with three particles in Example 3.2.1, has the planar symmetry group D_2 consisting of two perpendicular reflections and a rotation by π.

$$D_2 = \{I, \kappa_1, \kappa_2, \kappa_1\kappa_2\}$$

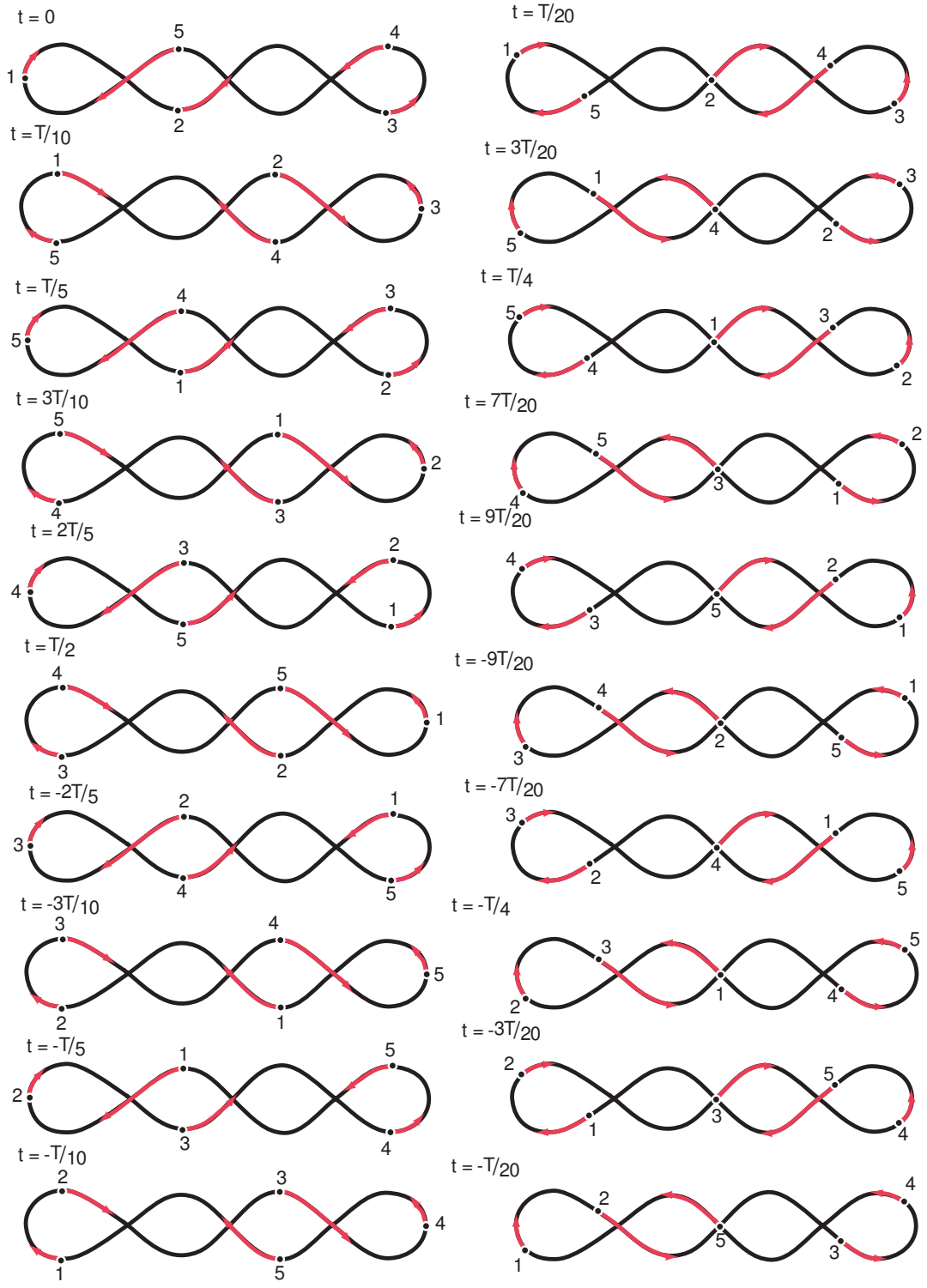

Figure 5.26: Five particles on a four-chain, at $t = kT/20$

We consider here distorted versions of the curve which possess a subgroup of these symmetries. The dihedral group D_2 has three different non-trivial subgroups, each

of order two, and we realise each as the planar symmetry group of a curve.

Example 5.3.1 (Three particles on a distorted figure eight)**.**

5.3.0.2 Vertical reflection only - $G = \{I, \kappa_1\}$

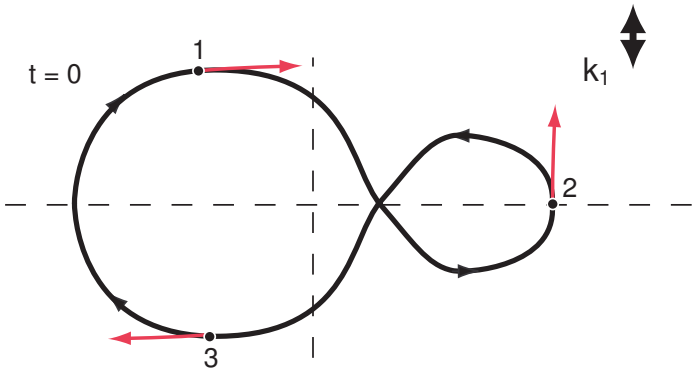

Figure 5.27: Three particles on a distorted figure eight with κ_1 symmetry, at $t = 0$

In this case, we have only the κ_1 reflection, which is time reversing and swaps a pair of particles each time. The choreography symmetry is also present. The resulting group of symmetries is the dihedral group D_3.

Choreographic motions with this shape of curve have been proven to exist with four and five particles, in [16]. Four particles are not permitted on an ordinary figure eight shape, since they would collide at the centre. Five particles can be found on an ordinary figure eight, as seen in Example 5.2.1 on page 122.

Table 5.6: Three particles on a distorted figure eight with κ_1 symmetry

$\rho(g)$	$\tau(g)$	$\sigma(g)$	Order
I	0	e	1
I	$T/3$	(123)	3
I	$-T/3$	(132)	3
κ_1	$\overline{0}$	(13)	2
κ_1	$\overline{T/3}$	(23)	2
κ_1	$\overline{-T/3}$	(12)	2

The maps ρ, σ and τ for this group can be seen in Figure 5.28.

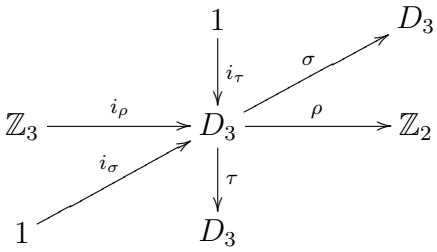

Figure 5.28: The maps ρ, σ and τ for three particles on a distorted figure eight with κ_1 symmetry

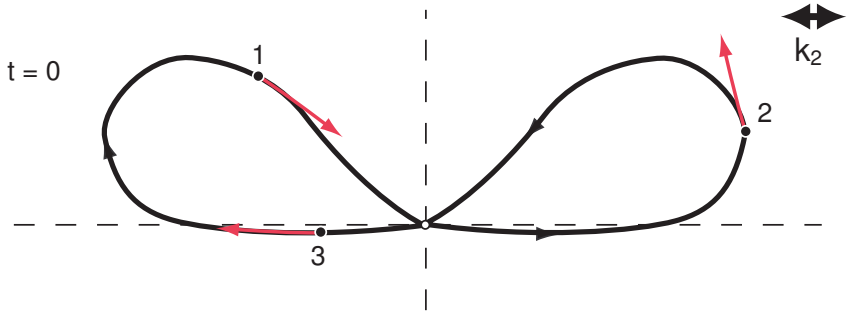

Figure 5.29: Three particles on a distorted figure eight with κ_2 symmetry, at $t = 0$

5.3.0.3 Horizontal reflection only - $G = \{I, \kappa_2\}$

In this case, there are no time-reversing symmetries, and we set the arrangement of points at $t = 0$ to possess the symmetry given by the reflection κ_2, which requires a time shift of $T/2$. The choreography symmetry is still present, and the group of symmetries is generated by this and the κ_2 reflection. The resulting group is $\mathbb{Z}_2 \times \mathbb{Z}_3 \simeq \mathbb{Z}_6$.

Table 5.7: Three particles on a distorted figure eight with κ_2 symmetry

$\rho(g)$	$\tau(g)$	$\sigma(g)$	Order
I	0	e	1
I	$T/3$	(123)	3
I	$-T/3$	(132)	3
κ_2	0	(132)	3
κ_2	$T/3$	e	3
κ_2	$-T/3$	(123)	3

The maps ρ, σ and τ for this group can be seen in Figure 5.30.

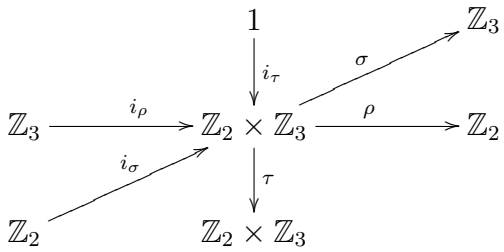

Figure 5.30: The maps ρ, σ and τ for three particles on a distorted figure eight with κ_2 symmetry

5.3.0.4 Order two rotation only - $G = \{I, \kappa_1\kappa_2\}$

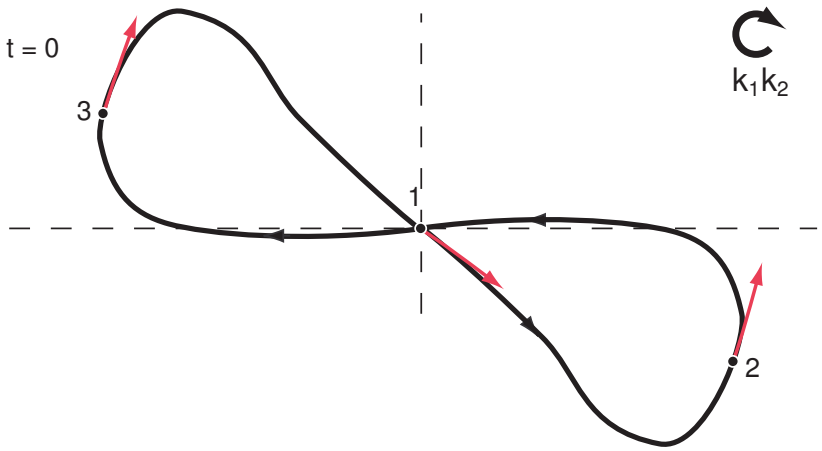

Figure 5.31: Three particles on a distorted figure eight with $\kappa_1\kappa_2$ symmetry, at $t = 0$

Here again the non-trivial symmetry is time-reversing, and so our group is again the dihedral group of order six, as in the first example, except the permutations corresponding to each of the reflections are in a different order.

Table 5.8: Three particles on a distorted figure eight with $\kappa_1\kappa_2$ symmetry

$\rho(g)$	$\tau(g)$	$\sigma(g)$	Order
I	0	e	1
I	$T/3$	(123)	3
I	$-T/3$	(132)	3
$\kappa_1\kappa_2$	$\overline{0}$	(23)	2
$\kappa_1\kappa_2$	$\overline{T/3}$	(12)	2
$\kappa_1\kappa_2$	$\overline{-T/3}$	(13)	2

The maps ρ, σ and τ for this group can be seen in Figure 5.32.

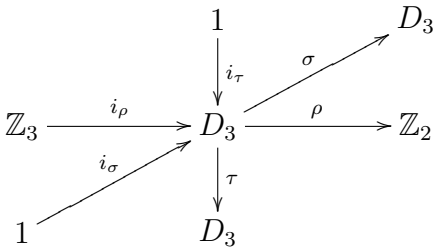

Figure 5.32: The maps ρ, σ and τ for three particles on a distorted figure eight with $\kappa_1\kappa_2$ symmetry

While only the usual figure eight has been proven to exist as a choreography with three particles, these curves all lie in the same homotopy class as that example. Since we have the condition that one solution must exist in each homotopy class of curves, as discussed in Chapter 6, it may be that not all of these other curves are realisable as motions of particles.

For a given homotopy class of curves, number of particles and group of symmetries, there will exist a maximal symmetry group for such a class of curves, found by deforming the shape until we have the largest possible planar symmetry group, whilst remaining homotopic to the original curve. Not all such choreographies will necessarily have this maximal symmetry - it may be that there are multiple connected components, only some of which have a larger symmetry group.

For example, four particles on a super-eight, as seen in Example 4.5.1 on page 88, has the symmetry group of a rectangle, but another connected component of this same setup is when the central segment of the super-eight does not overlap. This component has the maximal symmetry group of the circle, which is much larger, but the component containing the super-eight does not, since the two particles in the middle must pass around each other clockwise.

Example 5.2.1 on page 122 of five particles on a figure eight has been shown to exist numerically as a choreography, and so has a version of the figure eight possessing only κ_1 symmetry with five particles (see Figure 1 in [16]). The symmetry group of one is a subgroup of the other, and both are realised.

Chapter 6

Application to Variational Problems

Much of the progress made in finding examples of collision-free n-body solutions has been made using variational methods. In this chapter, we will discuss the various approaches which have been made to guarantee that solutions of certain types exist and are collisionless. In particular, we will consider the action functional of the system, and discuss its uses in finding solutions.

6.1 The action functional

Given a physical system, the **action functional** is given by the integral with respect to time of the Lagrangian of this system. Classical mechanics suggests that the path actually followed by a physical system is that for which the action is minimized, or stationary. The method used to find critical points of such a functional is called the 'direct method', and involves minimisation.

The Lagrangian may be defined using different types of potential - it is given by $L = T - V$, where T is the kinetic energy of the system, and V is the potential. A general formula for potential between two particles whose positions are denoted x_i,

x_j and masses m_i, m_j is given by

$$V = -G\frac{m_i m_j}{|x_i - x_j|^\alpha}$$

Here G is the gravitational constant. In the case where $\alpha = 1$ we have ordinary Newtonian (gravitational) potential energy, sometimes also called Keplerian potential. For values of $\alpha \geq 2$ we call this the **strong force**. For our closed path motions, the action functional may be written

$$\mathcal{A}(\gamma, \dot{\gamma}, t) = \int_0^T dt\ L(\gamma, \dot{\gamma}, t)$$

for γ a closed path mapping $\mathbb{T}$ into M.

In the case of strong force potential, many solutions of the n-body problem are much more easily proven to exist, since in this case any point at which collisions occur will have infinite action (since the denominator goes to zero very quickly) and will never be a minimum of the functional. In the case $\alpha = 1$ (Newtonian), this cannot be guaranteed and so other methods must be found to eliminate collisions.

In the following sections, we discuss certain relevant works which treat this problem, and describe their approaches.

Remark 6.1.1. In our consideration of choreographies, we assume all masses m_i are equal (and without loss of generality, equal to 1) and so in this case the potential only depends on the distance between the particles.

6.2 Ferrario and Terracini [14]

In [14], Ferrario and Terracini discuss the use of carefully chosen symmetry groups to restrict the space of loops. It had previously been established that considering a subspace of loops symmetric with respect to given symmetry conditions has led to finding new periodic orbits for the n-body problem, and Ferrario and Terracini built on this by establishing conditions under which the action functional will be **coercive**, and under which solutions found will be collision-free.

Coercivity is a condition which means the functional grows rapidly at the extremes of the space on which it is defined. More precisely, $f : \mathbb{R}^n \to \mathbb{R}^n$ is coercive if

$\frac{f(x)\cdot x}{\|x\|} \to +\infty$ as $\|x\| \to +\infty$. So, since our configuration space excludes collision points, this means the action will go to infinity as we approach a collision, and no minimum can correspond to collision points.

Coercivity also guarantees the existence of minima of the action functional, by classical arguments – and hence the existence of generalised solutions. Ferrario and Terracini give conditions on G which guarantee coercivity of the action functional when restricted to symmetric loops, i.e those equivariant with respect to G, as defined below. This means that choreographies in particular will definitely possess this property.

As well as introducing a system of notation, and considering the symmetry group via a set of three representations, as described in Chapter 3 in this thesis, they give general conditions on the group action, and define the *rotating circle property*, under which minimizers of the action functional will exist and be free from collisions. These results also hold for all degrees of homogeneous potential, not just the Newtonian potential. They also describe a method of generating suitable symmetry groups to find new families of collisionless orbits.

Remark 6.2.1. We must at this point note that the notation in [14] differs slightly from our own - they denote by $\mathcal{X}$ the space of centred configurations of particles (i.e. those whose centre of mass is at the origin). The space of collisionless configurations is denoted $\hat{\mathcal{X}}$, and given by $\hat{\mathcal{X}} = \mathcal{X} \setminus \Delta$.

The space of loops Λ is defined as a Sobolev space $\Lambda = H^1(\mathbb{T}, \mathcal{X})$ so that all maps are continuous and L^2, and have L^2 derivative. Collision-free loops are denoted $\hat{\Lambda}$. They then use the representations defined earlier to specify a subspace Λ^G of the space of loops Λ, given by

$$\forall g \in G, \forall t \in \mathbb{T}, \forall i = 1 \dots n : \rho(g) x_{\sigma(g^{-1})(i)}(t) = x_i(\tau(g)t)$$

That is, if we apply the space transformation and the permutation of particles to a set of particles, then the result will be the original positions of those particles at a modified time, and hence that the motion of particles will obey the symmetry group for all values of t.

Restricting the action functional $\mathcal{A}$ to this space of symmetric loops, which we denote $\mathcal{A}^G$, we find that certain conditions on the group action force this action functional to be coercive. Namely, in the case where the space $\mathcal{X}^G$, the set of points in $\mathcal{X}$ which are fixed by G, is empty, then the action functional $\mathcal{A}^G$ will be coercive.

By the Palais principle of symmetric criticality (see [26]), we have that a critical point of $\mathcal{A}^G$ is also a critical point of $\mathcal{A}$. Hence, we may work in this relative space under the action of G, and any critical point of the functional we find here will be a critical point of the full problem.

Proposition 6.2.2 (Proposition 4.1 from [14])**.** *The action functional $\mathcal{A}^G$ is coercive if and only if $\mathcal{X}^G = 0$.*

Proof. See [14]. □

In this paper, they also define the rotating circle property, which guarantees collisionless solutions by imposing a condition on the group action which ensures that at any point where a collision might occur, $n-1$ of the particles may be moved away by a rotation and hence the collision may be avoided.

In particular, any particle which is involved in a collision may be replaced by a circle which is invariant under the action of sufficiently many G-isotropy subgroups, and is acted on by G in such a way that it rotates the circle. This then allows the particle involved in a collision to be rotated away, while maintaining the trajectory.

If a group G has the rotating circle property, then all subgroups $H < G$ also have the property.

Proposition 6.2.3 (Proposition 4.12 from [14])**.** *If $\mathcal{X}^G = 0$, then there exists at least a minimum of the Lagrangian action $\mathcal{A}^G$, which yields a generalized solution of $m_i\ddot{x}_i = \frac{\delta U}{\delta x_i}$ in Λ^G, where U is the potential function.*

Proof. See [14]. □

In our examples, we have identified multiple connected components of the space of loops in which solutions may exist. We may deduce from the above the following result:

Theorem 6.2.4. *For a given symmetry group G of an n-body choreography, there exists a local minimum of the action functional in each connected component of the space Λ_G of G-loops. Hence, there exists at least one choreography solution of the n-body problem for each connected component of this space.*

Proof. Follows from Proposition 6.2.3 above. □

Remark 6.2.5. While the above gives us that there exists a solution in every connected component of this space, some of these solutions may be multiples of simpler ones - for example, in the Lagrange circular solution, a solution in another connected component could simply be the solution corresponding to travelling around the same circle twice as fast.

We may identify which of our examples may exploit the fact that $\mathcal{X}^G = 0$ implies solutions, since they will be those in which the action of G on the configuration space $\mathcal{X}$ has no fixed points. For example, on page 79 in Chapter 2 we considered the example of five particles on a super-eight, treated in more detail as Example 5.2.2 on page 125. We noted that if we restrict G to a subgroup of G containing only a non-time reversing rotation, by distorting the curve so it has only this symmetry, then there are no fixed points. In this case, we know the action functional on the space of relative loops is coercive, and hence that solutions exist.

Many examples are considered in [14], including Examples 3.2.1 and 5.2.1 of three and five particles on a figure eight, respectively.

The example of three particles on a figure eight is given with a group of symmetries generated by g_1, g_2 where (in our notation):

$$\rho(g_1) = \kappa_1\kappa_2, \tau(g_1) : t \mapsto -t, \sigma(g_1) = (23)$$

$$\rho(g_2) = \kappa_1\kappa_2, \tau(g_2) : t \mapsto -t + T/3, \sigma(g_2) = (12)$$

They take $t = 0$ to be the point we denote $t = {}^{T}/_{12}$, and the numbering of particles is also different.

6.3 Southall [32]

In his thesis, John Southall has considered various n-body and n-centre problems, and obtained results on which homotopy classes of loops contain periodic solutions of these problems. Among other things, he applies action-minimising methods to the planar two-centre problem under the Newtonian potential, and to planar 'central force problems', in which two bodies move under forces acting in the direction of the vector from one body to the other.

He makes use of relative periodic orbits, and looks at systems which are both integrable and non-integrable.

In his study of the two-centre problem, Southall uses a classification of the different types of orbits possible. As discussed in Section 2.6, two points in the plane may without loss of generality be considered to lie on the horizontal axis and equally spaced either side of the vertical axis. The shape of the motion of the free particle in the twice punctured plane (the plane minus the two fixed centres) is classified as:

- **P1**, if the orbit lies in an elliptic annulus encircling the two centres;
- **P2**, if the orbit lies within a simply connected region containing both centres (but is not of type P1);
- **P3**, if the orbit lies within one of two disconnected regions, each region containing only one of the two centres.

He restates these classifications in terms of which sections of the horizontal axis are crossed by particles during their motion. He also provides a description of all homotopy types of orbits in terms of 'words', made up of letters corresponding to crossing different parts of the axes in different directions.

Southall also studies the motion of bodies under other potentials - such as the Lennard-Jones Potential, which is given by

$$V_{LJ}(x) = \sum_{1\leq i\leq j\leq N} \left[\frac{1}{\|x_i - x_j\|^\beta} - \frac{1}{\|x_i - x_j\|^\alpha} \right], \qquad \beta > \alpha \geq 2$$

This potential is repulsive at short distances and attractive at large distances, and is used to model interactions between N identical atoms or neutral molecules. For this reason it is sometimes called the 'Molecular Potential', and Southall uses it to study the motion of N molecules, and proves the existence of periodic solutions using critical point theory. He goes on, using Morse theory, to prove the existence of at least two distinct critical orbits in every connected component of a space of loops satisfying certain conditions - and in particular, these conditions are satisfied for choreographies. This means that at least two choreographies exist under this potential, in each connected component. This work has been published in [28].

6.4 McCord, Montaldi, Roberts and Sbano [24]

This paper of 2003, titled "Relative periodic orbits of symmetric Lagrangian systems" uses topological properties of a Lagrangian system possessing a symmetry g to determine the number of relative periodic orbits present for each homotopy class of orbits.

The two major results of the paper, given below, are illustrated using examples including strong force n-centre problems, and systems on tori.

Remark 6.4.1. The map denoted Φ_ω in the paper is that which has been defined earlier in this thesis as $\widehat{\overline{\omega}}_*$, namely the map taking a path γ to the path $\overline{\omega} * \gamma$, and so I have denoted it by $\widehat{\overline{\omega}}_*$ in the following to make this work consistent and avoid confusion. The space $\Lambda^g(M)$ is as we have defined it, the space of all paths in M running from a point to its image under $g : M \to M$.

I have also replaced the notation $\overline{group}^{\,g}$ denoting the set of orbits of the g-twisted action, as defined below, with the notation $[group]^g$, to avoid confusion with my notation for inverses.

Theorem 6.4.2 (2.1 from [24])**.** *The map Φ_ω induces a bijection*

$$\pi_0(\Lambda^g(M)) \cong [\pi_1(M,m)]^g,$$

where $[\pi_1(M,m)]^g$ is the set of orbits of the g-twisted action of $\pi_1(M,m)$ on itself.

This theorem gives us that the number of connected components of the space of relative loops is equal to the number of orbits of the g-twisted action of $\pi_1(M)$ on itself. This is the same as our Theorem 2.5.3, where the orbits are called Reidemeister conjugacy classes.

Theorem 6.4.3 (2.2 from [24])**.** *Assume M is a $K(\pi,1)$. Then for any $\gamma \in \Lambda^g(M,m)$ the connected component of $\Lambda^g(M)$ containing γ, denoted $\Lambda^g_\gamma(M)$, is also a $K(\pi,1)$ with*

$$\pi_1(\Lambda^g_\gamma(M)) \cong Z^g_{\pi_1(M)}(\widehat{\omega}_*(\gamma))$$

where

$$Z^g_{\pi_1(M)}(\widehat{\omega}_*(\gamma)) \doteq \{\alpha \in \pi_1(M) : \alpha_g * \widehat{\omega}_*(\gamma) * \overline{\alpha} = \widehat{\omega}_*(\gamma)\}$$

i.e. the isotropy subgroup (or centraliser) at $\widehat{\omega}_*(\gamma)$ of the g-twisted action of $\pi_1(M,m)$ on itself, given by

$$\alpha \cdot \beta = \alpha_g * \beta * \overline{\alpha} \qquad \text{for } \alpha, \beta \in \pi_1(M,m)$$

where $\alpha_g = \overline{\omega} * g\alpha * \omega$.

Remark 6.4.4. In this paper, there is an automorphism of $\pi_1(M,m)$ defined by, for $\alpha \in \pi_1(M,m)$,

$$\alpha \mapsto \alpha_g = \overline{\omega} * g\alpha * \omega$$

for a path $\omega \in \Omega^g(M,m)$ - i.e, a path running from m to gm.

This is not the same as our map Φ^g_ω, defined earlier, which mapped $\alpha \in \pi^g_1(M,m)$ to $\Phi^g_\omega(\alpha) = \overline{\omega} * \alpha * g\omega \in \pi^g_1(M,m')$, for a path $\omega : m \rightsquigarrow m'$. The ω used in the paper's definition of α_g must have $m' = gm$, whereas this is a map between relative fundamental torsors with different basepoints.

This means that in the case where M is a $K(\pi,1)$ space, the homotopy type of each connected component of loops is known. The following simple example is given to illustrate how this works.

Example 6.4.5. Let $M = \mathbb{S}^1$, the circle, and first consider the case $g = id$, so we can study the usual loop space $\Lambda(\mathbb{S}^1)$. The g-twisted action of $\pi_1(\mathbb{S}^1)$ on itself is given by

conjugation, and since $\pi_1(\mathbb{S}^1) = \mathbb{Z}$ is abelian, this is trivial. So $\pi_0(\Lambda(\mathbb{S}^1)) \cong \mathbb{Z}$, where the homotopy classes of loops are specified by their winding number.

Since $\mathbb{S}^1$ is $K(\pi, 1)$, the theorem gives us that each component of the loop space is also a $K(\pi, 1)$ with $\pi = \mathbb{Z}$, and hence has the homotopy type of a circle.

Now let g be a reflection. Choose one of the fixed points of the reflection to be the base point m, and choose ω to be the trivial path based at m, $\omega : m \rightsquigarrow m$. Then for each $\alpha \in \pi_1(\mathbb{S}^1, m) \cong \mathbb{Z}$ we have $\alpha_g = \overline{\omega} * g\alpha * \omega = -\alpha$, and so the g-twisted action is given by the translation

$$\alpha \cdot \beta = \beta - 2\alpha$$

This has two orbits, so we write $[\pi_1(\mathbb{S}^1)]^g \cong \mathbb{Z}_2$, and the isotropy subgroups are trivial. Hence the space of loops $\Lambda^g(\mathbb{S}^1)$ in this case has two connected components, both of which are contractible.

These results may be used to find the number of connected components of the space of such loops, by examining the stabilisers of the g-twisted action.

The paper goes on to describe how, in the strong force case, a minimum of the action functional must exist in each connected component.

It gives the example of the two-centre problem, as stated on page 37 in Section 2.6, where the action of g is a reflection in the axis on which both centres lie. In this case, there are infinitely many connected components, each given by a word γ in the generators α_1 and α_2 of the form

$$\alpha_1^{r_1}\alpha_2^{s_1} \ldots \alpha_1^{r_j}\alpha_2^{s_j}$$

where all the r_i and s_i are non-zero.

The action functional will be coercive on the component of $\Lambda^g(M)$ containing γ if the action functional on the full loop space $\Lambda(M)$ is coercive on the component containing $g\gamma * \gamma$. It is shown that every component of $\Lambda^g(M)$ except those corresponding to the orbits of 1, α_1 and α_2 will contain at least one relative periodic orbit of the symmetric strong force two centre problem.

Chapter 7

Further work

7.1 Multiple choreographies

As discussed in Section 3.3, there exist choreographies for which the bodies do not all move on the same curve. The bodies may be split into two or more equally sized (or otherwise) groups, each of which has its own curve, and each group obeys the choreography condition of fixed time delay within the group. In Section 5.3, we discussed how in the case of the 'foil'-type choreography, each k-foil where k is even is not a single choreography, but consists of two or more overlapping curves. Some of these examples have been shown to exist as solutions to the n-body problem, and have been studied in [7], [14].

The same kind of representations may be applied to such choreographies as for the single curve case. The choreography symmetry will map under ρ to the trivial symmetry of the space, and τ will still give a non-reversing time shift of T/n, but the permutation given by σ will not be cyclic, but will have subcycles which partition $\{1, \ldots n\}$ into two or more groups, corresponding to the groups of particles on separate curves. The order of this element will now, instead of n, be the size of each group of particles, in the case where each group is the same size, and the least common multiple of their sizes if not. The total number of particles will be n, so for k equal groups (where $k|n$) each group is of size n/k and the order of the choreography symmetry is also n/k.

While groups of different sizes are not discussed in these examples, it might be possible to have unequal groups as part of a multiple choreography, possibly leading to more interesting and complex interactions between the groups of particles.

Example 7.1.1 (Six particles on a star of David shape)**.**

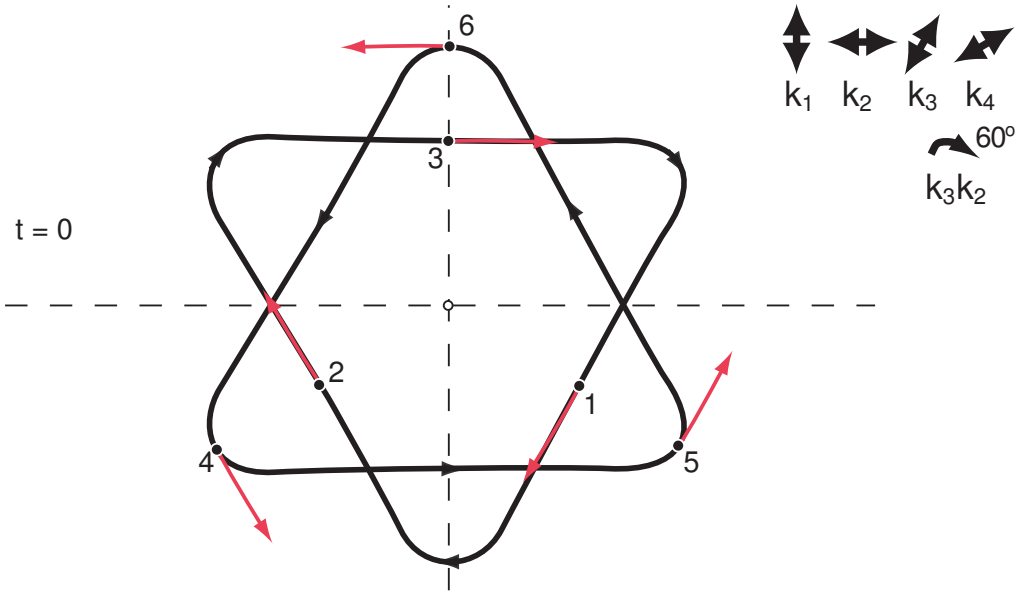

Figure 7.1: Six particles on a star of David, at $t = 0$

A good example of a double choreography is that of six particles on a Star of David, shown in Figure 7.1, studied in [14] (see Example 11.7), and considered in [7] (see Figure 2). It consists of six particles moving on two curves, each of which is a triangle with rounded corners, and which carry three particles each. In our notation from Section 5.1.2, it is a $(6, 2)$-foil and in this case we have contrary orientation.

The star of David shape has the symmetry group of a hexagon, which is generated by the rotation by $\pi/3$, and the reflection κ_1, and includes six reflections, three which have a line of symmetry passing through the points of the stars (which are time reversing), and three which pass through the points where the curves meet (which are not time reversing).

The arrangements of particles possess reflectional symmetry at $t = kT/12$, as seen in Figure 7.2. At even values of k, the particles lie at the corners of two concentric and similarly oriented triangles, one inside the other. Whether k is equal to 0 or 2 mod 4 decides the orientation of the triangles - pointing up, as at $k = 0 \mod 4$, or

pointing down, at $k = 2 \mod 4$. When k is odd, the particles lie at the points of the central hexagon shape. A rotational symmetry, either by $\pi/3$ or $2\pi/3$, is present at all values of t.

The double choreography symmetry is present, and it has $\sigma(g) = (123)(456)$ since the points move in two cycles. The choreography symmetry has order three. There are also two time-reversing symmetries, given by $\rho(g_0) = \kappa_2$ with $\sigma(g_0) = (12)(45)$, and $\rho(g_1) = \kappa_4\kappa_1$ with $\sigma(g_1) = (142536)$ with a time shift of $T/12$. There exist equivalent symmetries under different reflections. This choreography additionally

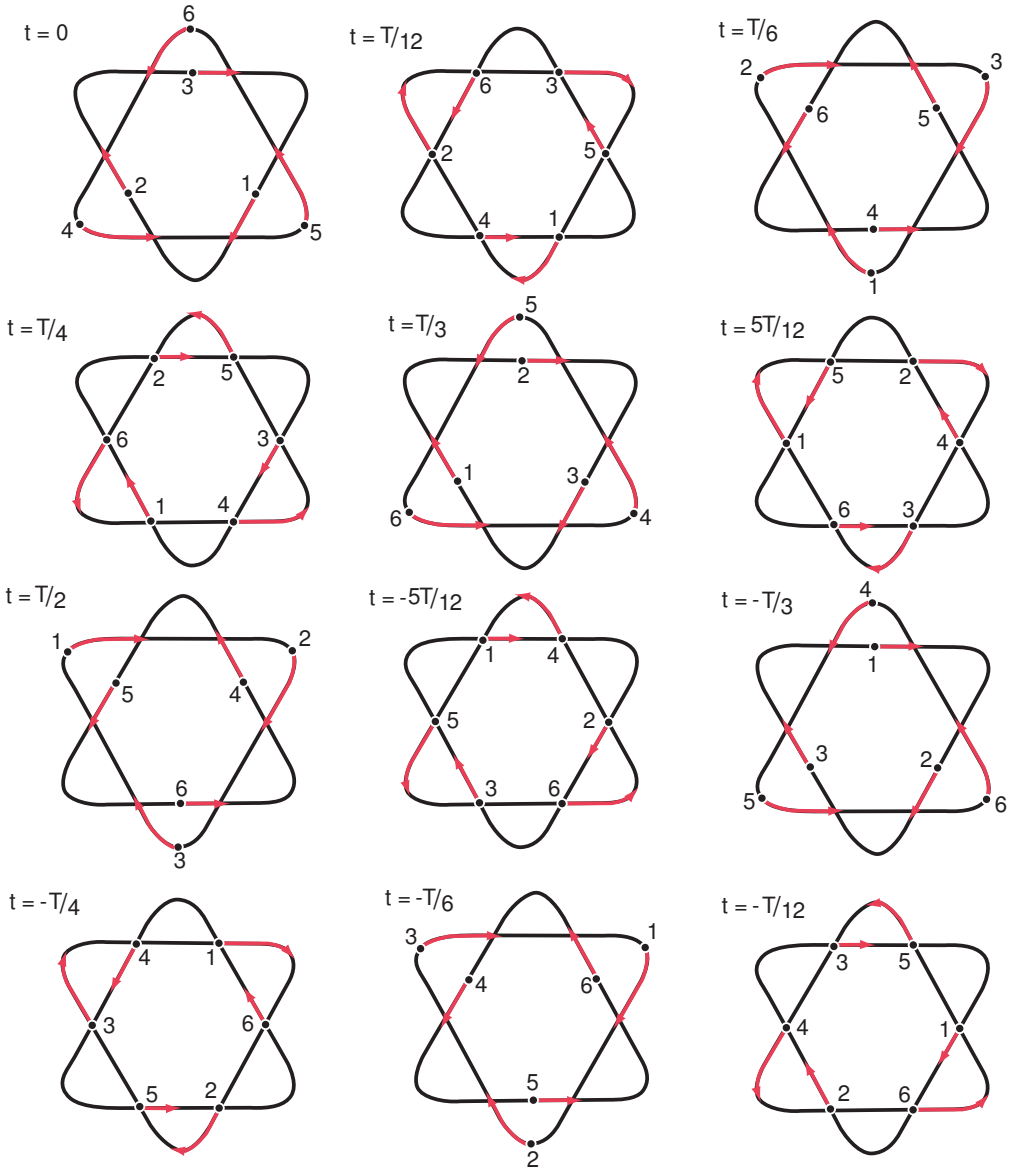

Figure 7.2: Six particles on a star of David, at $t = kT/12$

possesses a time preserving symmetry, denoted g_t — that is to say, at all values of t, $\rho(g_t) = \kappa_1\kappa_3$ and $\sigma(g_t) = (123)(465)$ with $\tau(g_t) : t \mapsto t$ is a symmetry of the choreography.

Fixed point space F_0:

$$\gamma(0) = g_0\gamma(0) = \kappa_2(12)(45)\gamma(0)$$

Therefore,

$$\begin{aligned}(z_1, z_2, z_3, z_4, z_5, z_6) &= \kappa_2(12)(46)(z_1, z_2, z_3, z_4, z_5, z_6) \\ &= (-\bar{z}_2, -\bar{z}_1, -\bar{z}_3, -\bar{z}_6, -\bar{z}_5, -\bar{z}_4)\end{aligned}$$

The fact that $z_3 = -\bar{z}_3$ and $z_5 = -\bar{z}_5$ means that z_3 and z_5 must sit on the imaginary axis. Then z_1 and z_2 form a κ_2-reflected pair either side of the imaginary axis, as do z_4 and z_6. Hence the fixed point space $F_0 = \mathrm{Fix}(g_0)$ is given by a copy of $\mathbb{R}^2 \setminus \Delta$, determining the positions of z_3 and z_5, and a space given by the positions of z_1 and z_4, which will be distinct points in the upper or lower half-plane. We must also have that as well as $z_1 \neq z_4$, we have $z_1 \neq \bar{z}_4$. This means we take the space $(\mathbb{C} \setminus \mathbb{R})^2$, and subtract two diagonal sets. The resulting space has four connected components, each of which is homotopic to $\mathbb{R}^4 \setminus \mathbb{R}^2 \simeq \mathbb{S}^1$. So F_0 will be homotopic to four copies of $\mathbb{S}^1$ crossed with two contractible sets, which gives a space with eight connected components, each of which is a copy of $\mathbb{S}^1$.

Fixed point space F_1:

$$\hat{\gamma}(T/12) = g_1\hat{\gamma}(T/12) = \kappa_4\kappa_1(142536)\hat{\gamma}(T/12)$$

Therefore,

$$\begin{aligned}(z_1, z_2, z_3, z_4, z_5, z_6) &= \kappa_4\kappa_1(142536)(z_1, z_2, z_3, z_4, z_5, z_6) \\ &= (e^{\frac{i\pi}{3}}z_4, e^{\frac{i\pi}{3}}z_5, e^{\frac{i\pi}{3}}z_6, e^{\frac{i\pi}{3}}z_2, e^{\frac{i\pi}{3}}z_3, e^{\frac{i\pi}{3}}z_1)\end{aligned}$$

These six points must sit at the corners of a hexagon, since each must be a rotation of $\frac{\pi}{3}$ from each other, and the order in which the points must proceed clockwise around the hexagon is 1,4,2,5,3,6. Hence the fixed point space $F_1 = \mathrm{Fix}(g_1)$ is given by the

position of one of these points in the punctured plane, and will therefore be $\mathbb{C}^*$, which is homotopic to $\mathbb{S}^1$.

The rotational symmetries $\kappa_1\kappa_3$ and $\kappa_1\kappa_6$ are present for all values of t, and hence may be used to restrict the manifold X to X', and the fixed point spaces F_0 and F_1 to F_0' and F_1', as in the example of the super-eight.

The time-preserving rotational symmetries are $\kappa_3\kappa_1$ with $(123)(465)$, and equivalently $\kappa_6\kappa_1$ with $(132)(456)$. The points with this symmetry satisfy

$$\begin{aligned}(z_1, z_2, z_3, z_4, z_5, z_6) &= \kappa_1\kappa_3(123)(465)(z_1, z_2, z_3, z_4, z_5, z_6) \\ &= (e^{\frac{2\pi i}{3}} z_2, e^{\frac{2\pi i}{3}} z_3, e^{\frac{2\pi i}{3}} z_1, e^{\frac{2\pi i}{3}} z_6, e^{\frac{2\pi i}{3}} z_4, e^{\frac{2\pi i}{3}} z_5)\end{aligned}$$

This means the points z_1, z_2 and z_3 all lie on an equilateral triangle, as do z_4, z_5 and z_6. This means the space X' is given by two points, which are distinct and lie in the punctured plane, without being equal to the images of each other under rotation.

This means

$$X' \simeq \{(z_1, z_4) \in (\mathbb{C}^*)^2 \mid z_1 \neq z_4,\ \omega z_4,\ \overline{\omega} z_4\}$$

where $\omega = e^{\frac{2\pi i}{3}}$.

We can then consider the restriction of the fixed point spaces to the manifold X'. F_0' is then given by:

$$F_0 \cap X' = \{z_3, z_5 \text{ on vertical axis (not 0)},$$

$$\text{positions of } z_1, z_2, z_4, z_6 \text{ given by rotation through } \frac{2\pi}{3}\}$$

Choosing two distinct values for z_3, z_5 defines the positions of the other points, and so $F_0' = (\mathbb{R}^*)^2 \setminus \Delta$.

$F_1' = F_1 \cap X'$ is the space of regular hexagons in the plane such that z_1 is two places away from z_2 and four from z_3 as we proceed clockwise, and z_4 is two places away from z_6 and four from z_5 in a clockwise direction. This is already given by the specified ordering on the particles in F_1, and hence $F_1' = F_1 = \mathbb{R}^2$. This space is contractible.

The full group of symmetries is given in Table 7.1. It has order 36 and an abelian normal subgroup of order 9. It has the structure $(\mathbb{Z}_3 \times \mathbb{Z}_3) \ltimes (\mathbb{Z}_2 \times \mathbb{Z}_2)$, where the first part is the abelian normal subgroup and the second part is the Klein four group.

Remark 7.1.2. This group does contain time reversing symmetries which are not of order two. Proposition 3.7.2 on page 64 states that this is impossible for a simple choreography - so since this example consists of multiple curves, and the symmetries of the whole shape map particles from one curve onto another, we have time reversing symmetries of order six. The fact that the two triangles are oppositely oriented is the reason for this time reversing rotation.

7.1.1 Chen [7]

In [7], Chen discusses the method of treating a systems of n particles as $\binom{n}{2}$ pairs of particles, each of which can be considered as a 'binary' in which a particle interacts with exactly one other. The total action will be the same as that of the whole system.

He applies his methods to the study of choreographies, and in particular multiple choreographies. He proves in particular the existence of infinitely many non-trivial double choreographic n-body solutions, using a proof that a restriction of the action functional to a space of G-invariant loops for a space of linear transformations G is coercive.

To generate the group of symmetries for a double choreography, Chen uses the group elements given in Example 7.1.1 of six particles on a Star of David by (for $n = 6$ particles):

$$\tau_3 : \tau(\tau_3) : t \mapsto -t \quad \sigma(\tau_3) = (123)(465) \quad \rho(\tau_3) = I$$

$$\sigma_3 : \tau(\sigma_3) : t \mapsto t + {}^{T}/_{3} \quad \sigma(\sigma_3) = (163524) \quad \rho(\sigma_3) = \kappa_5\kappa_1$$

up to a renaming of particles and shifted $t = 0$. He gives a general formula for such generators in $2k$ particles (under his numbering system) as

$$\sigma_k \cdot x(t) = e^{\frac{i\pi}{k}}(x_{2k}, x_1, x_2, \ldots, x_{2k-1})(-t)$$

Table 7.1: Six particles on a star of David

$\rho(g)$	$\tau(g)$	$\sigma(g)$	Order
I	0	e	1
I	$^{T}/_{3}$	(123)(465)	3
I	$^{-T}/_{3}$	(132)(456)	3
κ_1	$^{T}/_{6}$	(152436)	6
κ_1	$^{T}/_{2}$	(14)(26)(35)	2
κ_1	$^{-T}/_{6}$	(163425)	6
κ_2	$\overline{0}$	(12)(46)	2
κ_2	$\overline{^{T}/_{3}}$	(23)(56)	2
κ_2	$\overline{^{-T}/_{3}}$	(13)(45)	2
κ_3	$^{T}/_{6}$	(143526)	6
κ_3	$^{T}/_{2}$	(15)(24)(36)	2
κ_3	$^{-T}/_{6}$	(162534)	6
κ_4	$\overline{0}$	(23)(45)	2
κ_4	$\overline{^{T}/_{3}}$	(13)(46)	2
κ_4	$\overline{^{-T}/_{3}}$	(12)(56)	2
κ_5	$\overline{0}$	(13)(56)	2
κ_5	$\overline{^{T}/_{3}}$	(12)(45)	2
κ_5	$\overline{^{-T}/_{3}}$	(23)(46)	2
κ_6	$^{T}/_{6}$	(142635)	2
κ_6	$^{T}/_{2}$	(16)(25)(34)	2
κ_6	$^{-T}/_{6}$	(153624)	2
$\kappa_2\kappa_1$	$\overline{^{T}/_{6}}$	(15)(26)(34)	6
$\kappa_2\kappa_1$	$\overline{^{T}/_{2}}$	(16)(24)(35)	2
$\kappa_2\kappa_1$	$\overline{^{-T}/_{6}}$	(14)(25)(36)	6
$\kappa_3\kappa_1$	0	(123)(456)	3
$\kappa_3\kappa_1$	$^{T}/_{3}$	(132)(465)	3
$\kappa_3\kappa_1$	$^{-T}/_{3}$	e	3
$\kappa_4\kappa_1$	$\overline{^{T}/_{6}}$	(142536)	6
$\kappa_4\kappa_1$	$\overline{^{T}/_{2}}$	(152634)	6
$\kappa_4\kappa_1$	$\overline{^{-T}/_{6}}$	(162435)	6
$\kappa_5\kappa_1$	$\overline{^{T}/_{6}}$	(163524)	6
$\kappa_5\kappa_1$	$\overline{^{T}/_{2}}$	(143625)	6
$\kappa_5\kappa_1$	$\overline{^{-T}/_{6}}$	(153426)	6
$\kappa_6\kappa_1$	0	(132)(465)	3
$\kappa_6\kappa_1$	$^{T}/_{3}$	e	3
$\kappa_6\kappa_1$	$^{-T}/_{3}$	(123)(456)	3

$$\tau_k \cdot x(t) = (x_3, x_{2k}, x_5, x_2, \ldots, x_{2m-1}, x_{2(m-2)}, \ldots, x_{2(k-2)}, x_{2(k-1)})(t + {}^{T}/_{k})$$

He also discusses examples of $4n$ bodies on a $(4n, 2n)$-foil (as defined in Section 5.1.2) which consists of $2n$ overlapping ovals. He then covers some of the examples

treated by Ferrario and Terracini in [14], such as the figure eight, and also four particles on a Star of David shape, which is proven to exist.

7.2 Other considerations

In this section we suggest other directions in which our study of relative loops and minima of action may be taken.

7.2.1 Geodesics

The study of spaces of loops has many other applications, an example of which is the study of geodesics. Originally studied as a way to find the shortest path between two points on the Earth's surface, the study of geodesics may very usefully be applied to studying the motion of particles and other minimisation problems.

Definition 7.2.1. A **geodesic** is defined to be, for two points in a metric space, the (locally) shortest path between the two points.

Finding geodesics involves finding critical points of an energy functional on the path space. We may also define **closed geodesics**, which are geodesics which return to their starting point such that for any two points on the path, the section joining them is a geodesic. These are given by critical points on the energy functional on the space of closed loops.

We may also define a closed geodesic as the projection of a closed orbit under the **geodesic flow**.

While much work has been done in finding and studying geodesics, we will now attempt to apply the methods we have been using here to such paths, starting with the following definition which is an extension of our concept of relative loops.

Definition 7.2.2. We define a **relative closed geodesic** to be a path γ between two points in a space, where there exists a (finite order) g-action on the space, such that

- The path γ is a geodesic
- The path runs from a point to its image under g; that is, $\gamma(1) = g\gamma(0)$
- If we compose the section of path with its image under each successive action of g^n, the resulting closed loop is a closed geodesic.

The relative closed geodesics will be elements of Λ^g, as defined earlier. We have found the problem of finding n-body solutions is simplified by considering them up to a G-action, and in the same way we may use this to simplify the study of geodesics. Here we present some examples which illustrate the concept.

Example 7.2.3. Let $M = \mathbb{S}^2$, the 2-sphere, and let $G = \mathbb{Z}_3$ act by rotation of the sphere by $2\pi/3$ around the vertical axis.

On the sphere, geodesics are arcs of great circles, and closed geodesics are great circles. The relative closed geodesics will be those comprising great circles which are invariant under the $\mathbb{Z}_3$-action. The only such circle is that running around the equator, and so the only relative closed geodesic will be an arc which is a third of an equator.

Example 7.2.4. Let $M = \mathbb{S}^2$ and let $G = \mathbb{Z}_2$ act on M by the antipodal map. Again, great circles will be the closed geodesics, and relative closed geodesics will be those running from a point to its antipodal point, in such a way that the opposite section of path runs through antipodal points to those on the arc.

Since this is satisfied by any great circle which passes through a given point, there will be at each point relative closed geodesics which are arcs around to the antipodal point, and a copy of $\mathbb{S}^1/\mathbb{Z}_2$ at each point represents all the possible directions of arcs.

7.2.2 Different $K(\pi, 1)$ spaces

The construction of relative loop spaces and the existence of relative periodic orbits has mainly been considered here as taking place on the manifold $\mathbb{R}^{nd} \setminus \Delta$, a $K(\pi, 1)$ space, where in the case $d = 2$, $\pi = P_n$, the coloured braid group on n strands.

It is possible to replace this space with other, more well known $K(\pi, 1)$ spaces, such as the torus $\mathbb{T}^2 = \mathbb{S}^1 \times \mathbb{S}^1$, which is $K(\mathbb{Z} \times \mathbb{Z}, 1)$. The study of group actions on the torus is well established, and that of loop spaces, and the concept of relative loops may be considered here also.

Chapter 8

Conclusions

While much work has already been done in the study of the problems considered in this thesis, both on the classical n-body problem in particle mechanics and on the specific class of choreographical solutions, we have presented several new and interesting results on the subject, as well as exploring several illuminating worked examples.

Using the framework of representations defined by Ferrario and Terracini [14], we have made numerous useful statements on the nature of symmetry groups of simple choreographies in Chapters 3 and 4, both those which contain time-reversing symmetries and those with the more interesting constraint of time preserving symmetries. Notably:

- For any g, the symmetry $\rho(g)$ must be a symmetry of the curve (Proposition 3.5.3)
- If $\rho(g)$ acts trivially, then g must be a choreography symmetry (Proposition 3.5.5)
- The order of G is n times the order of the symmetry group of the curve (Proposition 3.5.6)
- A time reversing symmetry g must have $\rho(g)$ with order two (Proposition 3.7.2)

- If a symmetry group contains a time reversing rotation, it can contain no other rotations (Proposition 3.7.3)
- The image of σ must contain the cyclic group generated by the n-cycle $(123\ldots n)$ (Proposition 4.1.2)
- Either $\mathrm{im}\sigma \simeq D_n$, in which case the symmetry group is reversing, or $\mathrm{im}\sigma \simeq \mathbb{Z}_n$ in which case it is non-reversing (Proposition 4.1.3)
- The symmetry group of a choreography is reversing if and only if $\mathrm{im}\rho \simeq D_k$, where D_k is the symmetry group of the curve (Proposition 4.1.4)
- Time preserving symmetries must have $\rho(g)$ a rotation, not a reflection (Proposition 4.5.1)
- For a choreography to possess a time-preserving symmetry, n must be divisible by $|\ker(\tau)|$ (Proposition 4.5.2)

Following on from the classification of types of three-body choreographies given in [5], we use the techniques we have developed to classify strictly choreographical motions, in the case $n = 3$ (see Section 4.2).

Our main results are in Chapter 4: Theorem 4.4.6 defines how a relative loop may be extended to create a full choreography, and Theorem 4.6.1 allows us to study the topology of the space of such loops. While defining a choreography in terms of a relative loop has been done before, we give an explicit statement for the map from a relative loop to the full choreography, and show that it is a homeomorphism.

We make use of our definition of the fixed point space of a time reversing symmetry, and the results listed above on how such symmetries interact with the whole group. Since we prove that the space of relative loops for a given symmetry g is homeomorphic to a space of choreographies, our study of the path space $\mathcal{P}(X, F_0, F_1)$ in Example 4.6.1 is equivalent to an examination of the pace of choreographies. We use the fact that the spaces F_0 and F_1 are spaces with easily calculated homotopy groups, and may determine fully the homotopy type of the path space for given examples.

We also apply the work of Ferrario and Terracini in which they place conditions guaranteeing the existence and collisionlessness of solutions. In Theorem 6.2.4 we have shown that such a solution may exist in every connected component of the space of loops, and so there are infinitely many solutions in many cases. For examples, see Example 3.2.1 of three particles on a figure eight, and Example 4.5.1 of four particles on a Gerver super-eight. The calculation of the connected components can be found in Example 4.6.1 on page 96.

Appendix A

Appendix

A.1 Additional Results

Lemma A.1.1. *The space* $(\mathbb{C}^2 \setminus \{n \text{ complex planes}\})$ *is* $K(\mathbb{Z} \times \mathbb{F}_{n-1}, 1)$*, where* $\mathbb{F}_{n-1}$ *is the free group on* $n-1$ *generators.*

Proof. Let us denote by Y_n the space $(\mathbb{C}^2 \setminus \{n \text{ complex planes}\})$.

This space is homotopic to $(\mathbb{S}^3 \setminus n \text{ circles})$, which we will denote Y'_n. The circles we subtract from $\mathbb{S}^3$ will be great circles, and orbits of the action of $\mathbb{S}^1$ on $\mathbb{C}^2$ by $e^{i\theta}$.

This action is free on Y_n and Y'_n, since neither contain the origin.

We may note that $Y'_n/\mathbb{S}^1$ is equal to $(\mathbb{S}^2 \setminus n \text{ points})$, and also that

$$Y'_n/\mathbb{S}^1 \subset \mathbb{S}^3/\mathbb{S}^1 = \mathbb{S}^2 (= \mathbb{C}P^1)$$

We then have a fibration

$$\begin{array}{ccc} \mathbb{S}^1 & \hookrightarrow & \mathbb{S}^3 \setminus n \text{ circles} \\ & & \downarrow \\ & & \mathbb{S}^2 \setminus n \text{ points} \end{array}$$

Claim: this is the trivial bundle. Indeed, the set of $\mathbb{S}^1$-bundles over Y'_n is the same as the set of classes of maps from $(\mathbb{S}^2 \setminus n \text{ points})$ into $B\mathbb{S}^1$, the classifying space for $\mathbb{S}^1$ bundles. We have $B\mathbb{S}^1 = K(\mathbb{Z}, 2) = \mathbb{C}P^\infty$, and so this space of maps is in fact $H^2((\mathbb{S}^2 \setminus n \text{ points}), \mathbb{Z})$, the second cohomology group. However, since $\mathbb{S}^2 \setminus n$ points is a one-dimensional CW-complex, it has trivial H^2. So, the bundle must be trivial.

Then, we have that Y_n' is diffeomorphic to $\mathbb{S}^1 \times (\mathbb{S}^2 \setminus n \text{ points})$, and hence that

$$\begin{aligned} \pi_1(Y_n') = \pi_1(Y_n) &= \pi_1(\mathbb{S}^1) \times \pi_1(\mathbb{S}^2 \setminus n \text{ points}) \\ &= \mathbb{Z} \times \mathbb{F}_{n-1} \end{aligned}$$

In fact, since these spaces are both $K(\pi, 1)$, their product is $K(\mathbb{Z} \times \mathbb{F}_{n-1}, 1)$ as required.

□

A.2 Further Examples

In this section, we will give full descriptions of several illustrative examples of choreographies with different numbers of particles, describing the symmetries present and how they interact.

In each case, we give a description of the choreography, the symmetries present in time and space, and discuss the fixed point spaces resulting from any time reversing symmetries present. We also include a list of the elements of the symmetry group in each case.

In the following, we will consider $X^{(n)} = (\mathbb{R}^2)^n \setminus \Delta$, where n is the number of particles. To represent the positions of particles we will use notation as though $X = \mathbb{C}^n \setminus \Delta$, where points in X will be denoted $(z_1, z_2, \ldots, z_n), z_i \neq z_j$ for $i \neq j$.

Example A.2.1 (Six particles on a non-symmetrical figure)**.** Numerical methods have discovered many choreographies for which the curve on which the particles travel has no nontrivial symmetries. An example is shown in Figure A.1. In this case, as with any choreography possessing no non-trivial spatial symmetries, the only symmetry present is the choreography symmetry for which in this case $\rho(g) = I, \tau(g) : t \mapsto t + T/6$ and $\sigma(g) = (123456)$. The symmetry group in this case is simply the cyclic group of order 6, $\mathbb{Z}_6$.

So far, the example of four particles on a Gerver super-eight has been the only choreography to possess a time-preserving symmetry. The following two examples both possess this type of symmetry, and can be considered as part of a family of

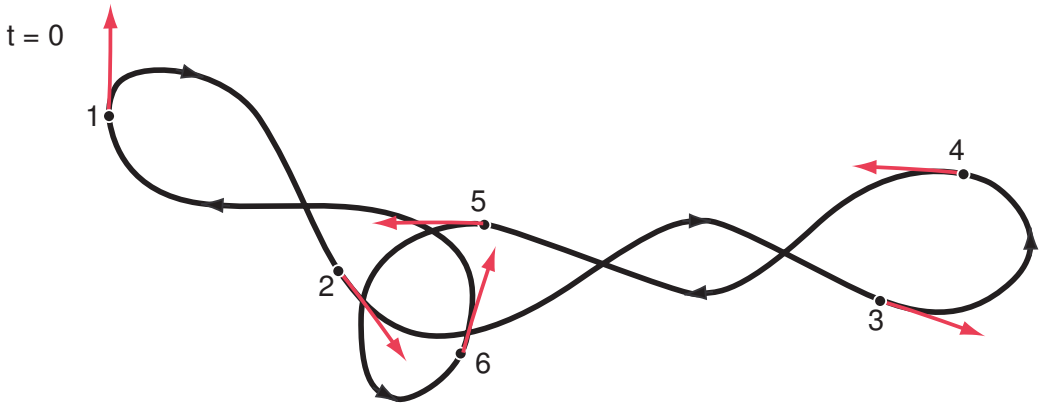

Figure A.1: Six particles on a non-symmetrical figure, at $t = 0$

Example A.2.2 (Six particles on a three-flower)**.**

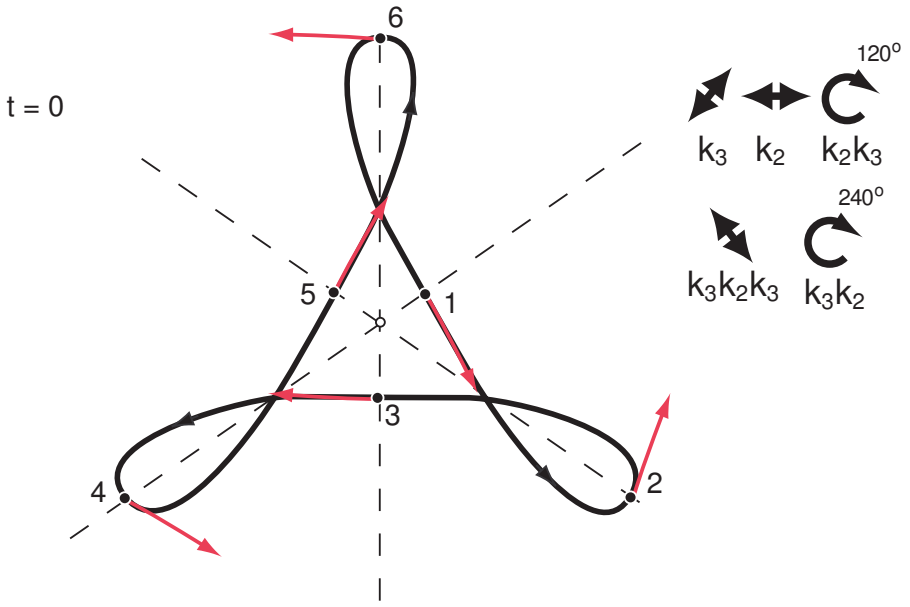

Figure A.2: Six particles on a three-flower, at $t = 0$

solutions. They are also both members of the family of rotationally symmetrical solutions, of flower type.

The three-flower curve has the symmetry group of a triangle, which is generated by the reflection in the horizontal axis κ_1 and the diagonal reflection κ_3, which is a reflection in the line of negative slope at an angle of $\pi/3$ below the horizontal. The group includes rotation by $2\pi/3$, given by $\kappa_3\kappa_1$, rotation by $4\pi/3$ given by $\kappa_1\kappa_3$, and the reflection in the other diagonal, $\kappa_1\kappa_3\kappa_1$.

The arrangements of particles possess reflectional symmetry at $t = kT/12$, with

the particles forming two triangles which sit one inside the other with opposite orientation at even values of k, and an irregular hexagon when k is odd. Rotational symmetries are present for all values of t.

The choreography symmetry is present, as are two time-reversing symmetries, given by $\rho(g_0) = \kappa_1$ with $\sigma(g_0) = (13)(46)$, and $\rho(g_1) = \kappa_1$ with $\sigma(g_1) = (12)(36)$ and a time delay of $T/8$.

Fixed point space F_0:

$$\gamma(0) = g_0\gamma(0) = \kappa_1(13)(46)\gamma(0)$$

$$\therefore (z_1, z_2, z_3, z_4, z_5, z_6) = \kappa_1(13)(46)(z_1, z_2, z_3, z_4, z_5, z_6)$$

$$= (\bar{z}_3, \bar{z}_2, \bar{z}_1, \bar{z}_6, \bar{z}_5, \bar{z}_4)$$

The particles z_2 and z_5 are equal to their own conjugate, and so must lie on the real line. We also have $z_1 = \bar{z}_3$ and $z_4 = \bar{z}_6$, which means they form distinct conjugate pairs either side of the real line. Hence the fixed point space $F_0 = \mathrm{Fix}(g_0)$ is given by two distinct points in $\mathbb{R}$, and two distinct points in the upper or lower half-plane. We must also have that as well as $z_1 \neq z_4$, we have $z_1 \neq \bar{z}_4$. This means we take the space $(\mathbb{C} \setminus \mathbb{R})^2$, and subtract two diagonal sets. The resulting space has four connected components, each of which is homotopic to $\mathbb{R}^4 \setminus \mathbb{R}^2 \simeq \mathbb{S}^1$. So F_0 will be four copies of $\mathbb{S}^1$ crossed with two contractible sets, which gives a space with eight connected components, each of which is a copy of $\mathbb{S}^1$.

Fixed point space F_1:

$$\hat{\gamma}(T/12) = g_1\hat{\gamma}(T/12) = \kappa_1(12)(36)(45)\hat{\gamma}(T/12)$$

$$\therefore (z_1, z_2, z_3, z_4, z_5, z_6) = \kappa_1(12)(36)(45)(z_1, z_2, z_3, z_4, z_5, z_6)$$

$$= (\bar{z}_2, \bar{z}_1, \bar{z}_6, \bar{z}_5, \bar{z}_4, \bar{z}_3)$$

The points form three conjugate pairs, either side of the real axis. Hence the fixed point space $F_1 = \mathrm{Fix}(g_1)$ is given by three distinct points in the upper or lower half-plane. We must also have that as well as $z_1 \neq z_3$, we have $z_1 \neq \bar{z}_3$, and similarly for each of the other pairs from $\{z_1, z_3, z_5\}$. This means we take the space $(\mathbb{C} \setminus \mathbb{R})^3$, and

subtract six diagonal sets. The resulting space has eight connected components, each of which is homotopic to $(\mathbb{R}^2)^3 \setminus \Delta$. This is a $K(\pi, 1)$ space with $\pi = P_3$. So F_1 will be eight copies of $(\mathbb{R}^2)^3 \setminus \Delta$.

The rotational symmetries are present for all values of t, and hence may be used to restrict the manifold X to X', and the fixed point spaces F_0 and F_1 to F_0' and F_1', as in the example of the super-eight. The time-preserving rotational symmetries are

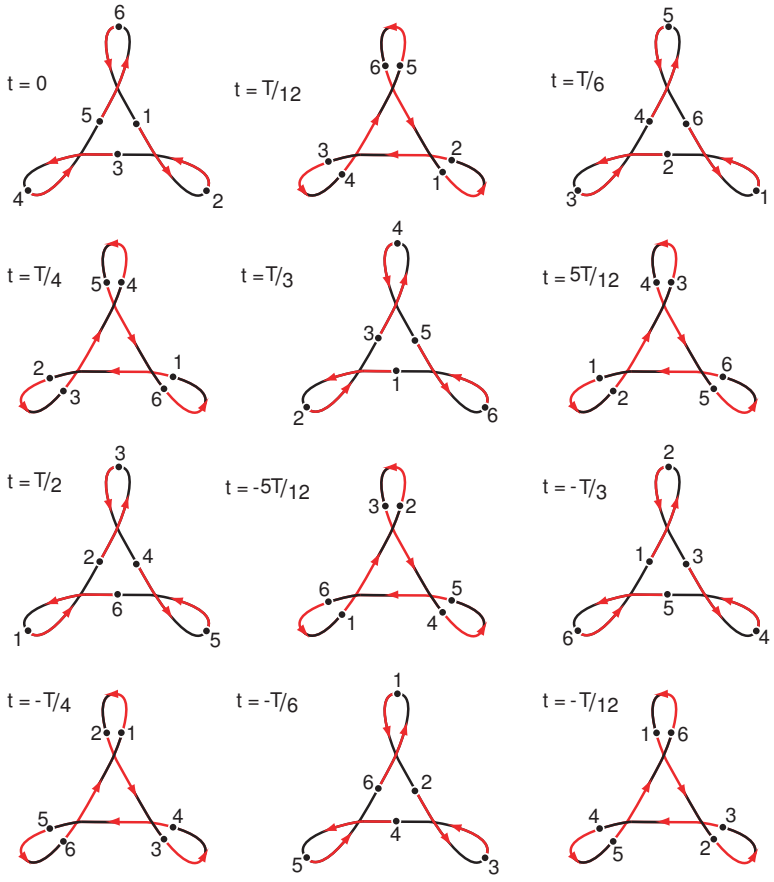

Figure A.3: Six particles on a three-flower, at $t = {}^{kT}/_{12}$

$\kappa_3\kappa_1$ with $(135)(246)$, and equivalently $\kappa_1\kappa_3$ with $(153)(264)$.

$$(z_1, z_2, z_3, z_4, z_5, z_6) = \kappa_3\kappa_1(135)(246)(z_1, z_2, z_3, z_4, z_5, z_6)$$

$$= (e^{\frac{2\pi i}{3}} z_3, e^{\frac{2\pi i}{3}} z_4, e^{\frac{2\pi i}{3}} z_5, e^{\frac{2\pi i}{3}} z_6, e^{\frac{2\pi i}{3}} z_1, e^{\frac{2\pi i}{3}} z_2)$$

This means the points z_1, z_3 and z_5 all lie on an equilateral triangle, as do z_2, z_4 and z_6. This means the space X' is given by two points, which are distinct and lie in the punctured plane, without being equal to the images of each other under rotation.

It may be noted that $(z_1)^3 = (z_3)^3 = (z_5)^3$, and $(z_2)^3 = (z_4)^3 = (z_6)^3$, so in fact we simply require that $(z_1)^3$ and $(z_2)^3$ are distinct points in the punctured plane. Hence $X' \simeq (\mathbb{C}^*)^2 \setminus \Delta$.

The restricted fixed point space $F_0' = F_0 \cap X'$ consists of $(z_1, z_2, z_3, z_4, z_5, z_6)$ such that $z_2, z_5 \in \mathbb{R}$, and $z_1 = \bar{z}_3$, $z_4 = \bar{z}_6$, with the additional restriction that $z_1 = e^{\frac{2\pi i}{3}} z_3 = e^{\frac{4\pi i}{3}} z_5$, and $z_2 = e^{\frac{2\pi i}{3}} z_4 = e^{\frac{4\pi i}{3}} z_6$. This means that this space must consist of two equilateral triangles, on each of which one point lies on the real line and the other two are a conjugate pair either side of it. Hence, the space is determined by the position of the two points in $\mathbb{R}$ minus the origin. Hence $F_0' \simeq (\mathbb{R}^*)^2 \setminus \Delta$.

The other restricted fixed point space, F_1', again has the restriction that $z_1 = e^{\frac{2\pi i}{3}} z_3 = e^{\frac{4\pi i}{3}} z_5$, and $z_2 = e^{\frac{2\pi i}{3}} z_4 = e^{\frac{4\pi i}{3}} z_6$, but this time the points lie in three sets of conjugate pairs. This means that the whole space is determined by the position of one particle, which without loss of generality may be considered to lie in the fundamental region given by a cone in the plane of angle $\pi/3$, taken upward from the positive half of the real line, and not including the origin or either boundary. This space is just a plane, and hence $F_1' \simeq 6[\mathbb{R}^2] \simeq 6[\text{pt}]$, since this point can be in any one of these six regions.

The full group of symmetries is given in Table A.1. It has order 36, but no elements of order 18. Its structure is that of $((\mathbb{Z}_3 \times \mathbb{Z}_3) \rtimes \mathbb{Z}_2) \rtimes \mathbb{Z}_2$. Its centre is generated by the element marked †. The maps ρ, σ and τ for this group can be seen in Figure A.4.

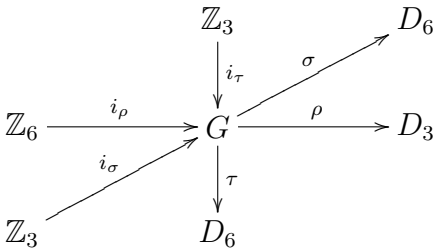

Figure A.4: The maps ρ, σ and τ for six particles on a three-flower

The four-flower has the symmetry group of a square, which is generated by the reflection in the horizontal axis κ_1 and the diagonal reflection κ_3, in the line of

Table A.1: Six particles on a three-flower

$\rho(g)$	$\tau(g)$	$\sigma(g)$	Order
I	0	e	1
I	$^{T}/_{6}$	(123456)	6
I	$^{T}/_{3}$	(135)(246)	3
† I	$^{T}/_{2}$	(14)(25)(36)	2
I	$^{-T}/_{3}$	(153)(264)	3
I	$^{-T}/_{6}$	(165432)	6
κ_1	$\overline{0}$	(13)(46)	2
κ_1	$\overline{^{T}/_{6}}$	(12)(36)(45)	2
κ_1	$\overline{^{T}/_{3}}$	(26)(35)	2
κ_1	$\overline{^{T}/_{2}}$	(16)(25)(34)	2
κ_1	$\overline{^{-T}/_{3}}$	(15)(24)	2
κ_1	$\overline{^{-T}/_{6}}$	(14)(23)(56)	2
κ_3	$\overline{0}$	(15)(24)	2
κ_3	$\overline{^{T}/_{6}}$	(14)(23)(56)	2
κ_3	$\overline{^{T}/_{3}}$	(13)(46)	2
κ_3	$\overline{^{T}/_{2}}$	(12)(36)(45)	2
κ_3	$\overline{^{-T}/_{3}}$	(26)(35)	2
κ_3	$\overline{^{-T}/_{6}}$	(16)(25)(34)	2
$\kappa_3\kappa_1$	0	(135)(246)	3
$\kappa_3\kappa_1$	$^{T}/_{6}$	(14)(25)(36)	6
$\kappa_3\kappa_1$	$^{T}/_{3}$	(153)(264)	3
$\kappa_3\kappa_1$	$^{T}/_{2}$	(165432)	6
$\kappa_3\kappa_1$	$^{-T}/_{3}$	e	3
$\kappa_3\kappa_1$	$^{-T}/_{6}$	(123456)	6
$\kappa_1\kappa_3$	0	(153)(264)	3
$\kappa_1\kappa_3$	$^{T}/_{6}$	(165432)	6
$\kappa_1\kappa_3$	$^{T}/_{3}$	e	3
$\kappa_1\kappa_3$	$^{T}/_{2}$	(123456)	6
$\kappa_1\kappa_3$	$^{-T}/_{3}$	(135)(246)	3
$\kappa_1\kappa_3$	$^{-T}/_{6}$	(14)(25)(36)	6
$\kappa_1\kappa_3\kappa_1$	$\overline{0}$	(26)(35)	2
$\kappa_1\kappa_3\kappa_1$	$\overline{^{T}/_{3}}$	(16)(25)(34)	2
$\kappa_1\kappa_3\kappa_1$	$\overline{^{T}/_{6}}$	(15)(24)	2
$\kappa_1\kappa_3\kappa_1$	$\overline{^{T}/_{2}}$	(14)(23)(56)	2
$\kappa_1\kappa_3\kappa_1$	$\overline{^{-T}/_{6}}$	(13)(46)	2
$\kappa_1\kappa_3\kappa_1$	$\overline{^{-T}/_{3}}$	(12)(36)(45)	2

Example A.2.3 (Eight particles on a four-flower)**.**

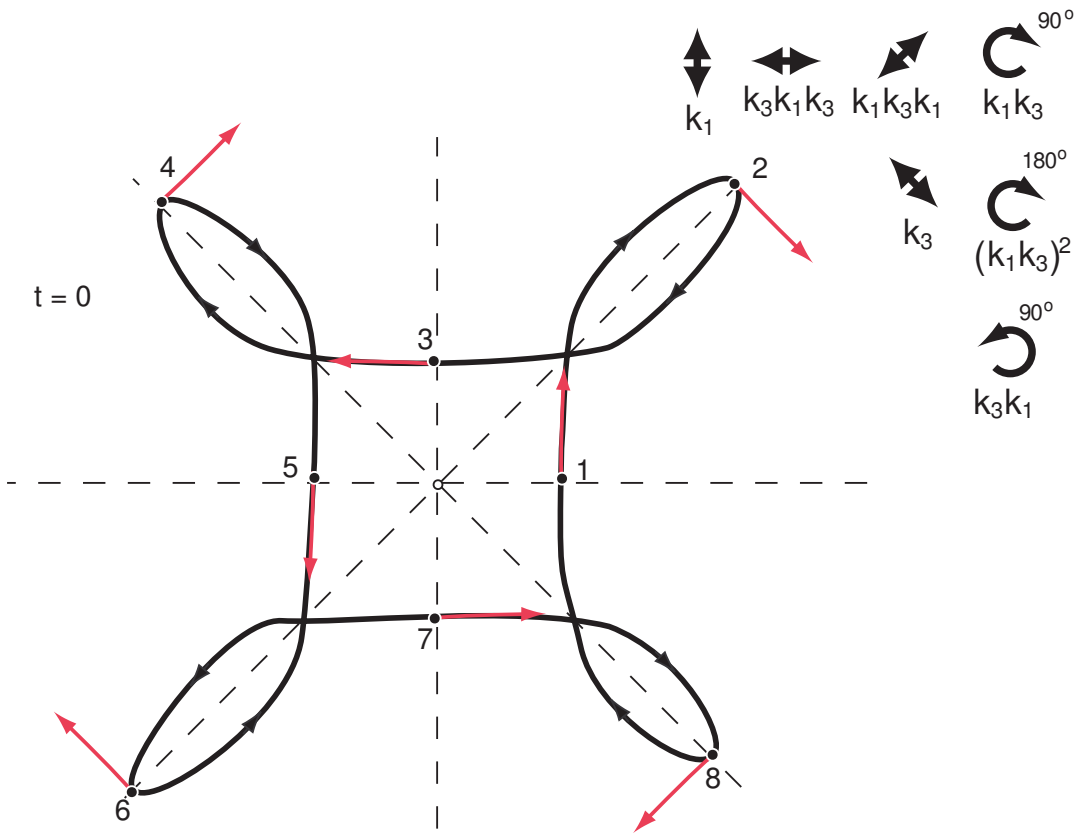

Figure A.5: Eight particles on a four-flower, at $t = 0$

negative slope at $\pi/4$ below the horizontal axis. The group incorporates the other two reflections, $\kappa_1\kappa_3\kappa_1$ and $\kappa_3\kappa_1\kappa_3$, as well as rotations $\kappa_1\kappa_3, (\kappa_1\kappa_3)^2$ and $\kappa_3\kappa_1$, by $\pi/2, \pi$ and $3\pi/2$ respectively.

The arrangements of particles possess reflectional symmetry at $t = kT/16$, with the particles forming two squares which sit one inside the other, differing in orientation by $\pi/4$, at even values of k, and an irregular octagon when k is odd. Rotational symmetries are present for all values of t. The choreography symmetry is present, as are two time-reversing symmetries, given by $\rho(g_0) = \kappa_1$ with $\sigma(g_0) = (28)(37)(46)$, and $\rho(g_1) = \kappa_1$ with $\sigma(g_1) = (18)(27)(36)(45)$ and a time delay of $T/8$.

Fixed point space F_0:

$$\gamma(0) = g_0\gamma(0) = \kappa_1(28)(37)(46)\gamma(0)$$

$$\therefore (z_1, z_2, z_3, z_4, z_5, z_6, z_7, z_8) = \kappa_1(28)(37)(46)(z_1, z_2, z_3, z_4, z_5, z_6, z_7, z_8)$$

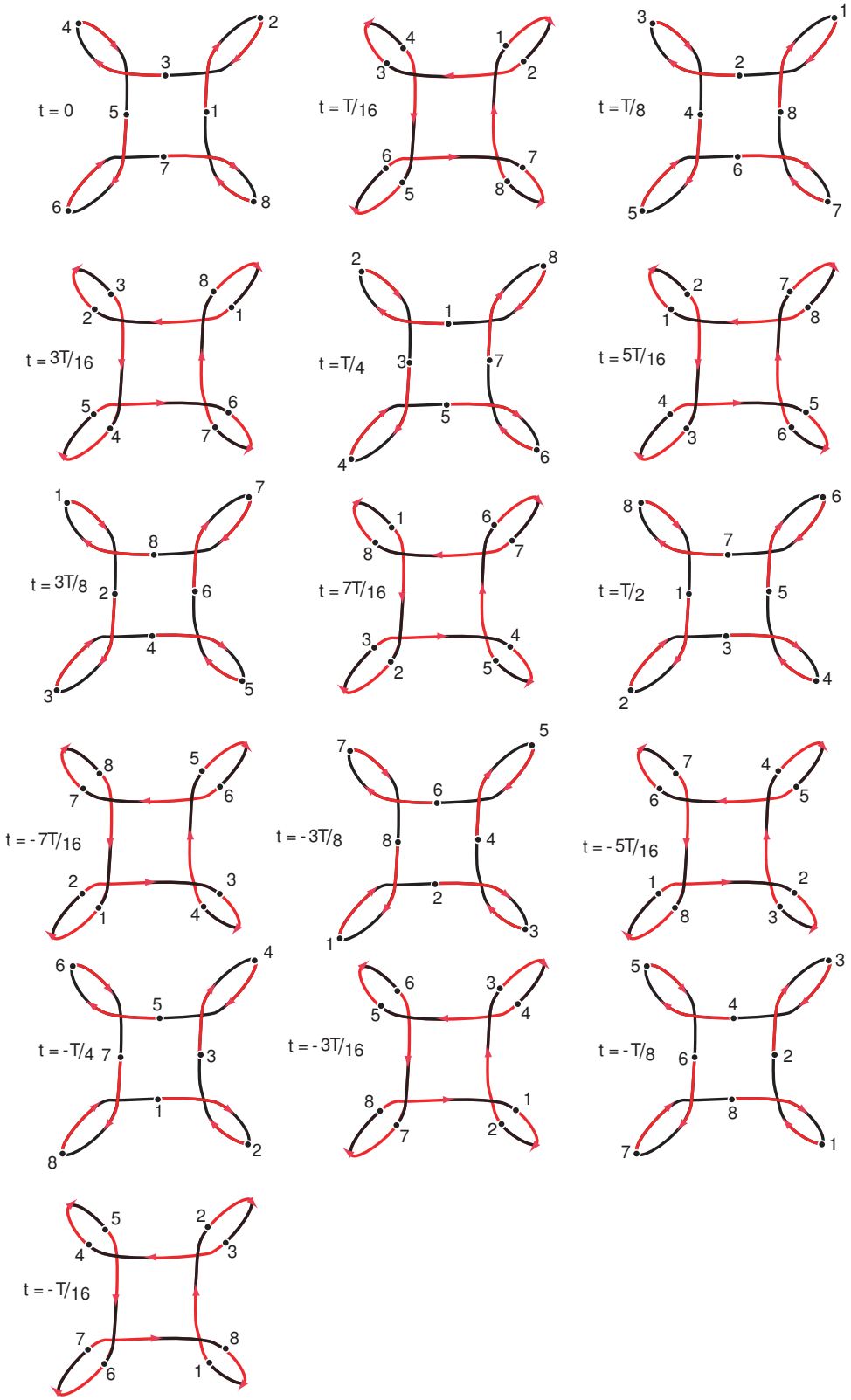

Figure A.6: Eight particles on a four-flower, at $t = {}^{kT}/_{16}$

$$= (\bar{z}_1, \bar{z}_8, \bar{z}_7, \bar{z}_6, \bar{z}_5, \bar{z}_4, \bar{z}_3, \bar{z}_2)$$

The particles z_1 and z_5 are equal to their own conjugate, and so must lie on the real line. We also have $z_2 = \bar{z}_8, z_3 = \bar{z}_7$ and $z_4 = \bar{z}_6$, which means they form distinct conjugate pairs either side of the real line. Hence the fixed point space $F_0 = \mathrm{Fix}(g_0)$ is given by two distinct points in $\mathbb{R}$, and three distinct points in the upper or lower half-plane. We must also have that as well as $z_2 \neq z_3$, we have $z_2 \neq \bar{z}_3$, and similarly for each of the other pairs from $\{z_2, z_3, z_4\}$. This means we take the space $(\mathbb{C} \setminus \mathbb{R})^3$, and subtract six diagonal sets. The resulting space has eight connected components, each of which is homotopic to $(\mathbb{R}^2)^3 \setminus \Delta$. This is a $K(\pi, 1)$ space with $\pi = P_3$. So F_0 will be eight copies of $(\mathbb{R}^2)^3 \setminus \Delta$, crossed with $\mathbb{R}^2 \setminus \Delta$ (which has two contractible components). Hence, F_0 will be homotopic to sixteen copies of $(\mathbb{R}^2)^3 \setminus \Delta$.

Fixed point space F_1:

$$\hat{\gamma}(T/16) = g_1\hat{\gamma}(T/16) = \kappa_1(18)(27)(36)(45)\hat{\gamma}(0)$$

$$\therefore (z_1, z_2, z_3, z_4, z_5, z_6, z_7, z_8) = \kappa_1(18)(27)(36)(45)(z_1, z_2, z_3, z_4, z_5, z_6, z_7, z_8)$$

$$= (\bar{z}_8, \bar{z}_7, \bar{z}_6, \bar{z}_5, \bar{z}_4, \bar{z}_3, \bar{z}_2, \bar{z}_1)$$

The points form four conjugate pairs, either side of the real axis. Hence the fixed point space $F_1 = \mathrm{Fix}(g_1)$ is given by four distinct points in the upper or lower half-plane. We must also have that as well as $z_1 \neq z_2$, we have $z_1 \neq \bar{z}_2$, and similarly for each of the other pairs from $\{z_1, z_2, z_3, z_4\}$. This means we take the space $(\mathbb{C} \setminus \mathbb{R})^4$, and subtract twelve diagonal sets. The resulting space has sixteen components, each of which is homotopic to $(\mathbb{R}^2)^4 \setminus \Delta$. This is a $K(\pi, 1)$ space with $\pi = P_4$. So F_1 will be sixteen copies of $(\mathbb{R}^2)^4 \setminus \Delta$.

The rotational symmetries are present for all values of t, and hence may be used to restrict the manifold X to X', and the fixed point spaces F_0 and F_1 to F_0' and F_1', as in the example of the super-eight.

The relevant rotational symmetries are $\kappa_1\kappa_3$ with $(1753)(2864)$, as well as $\kappa_3\kappa_1$ with $(1357)(2468)$ and $(\kappa_1\kappa_3)^2$ with $(15)(26)(37)(48)$.

$$(z_1, z_2, z_3, z_4, z_5, z_6, z_7, z_8) = (\kappa_1\kappa_3)(1753)(2864)(z_1, z_2, z_3, z_4, z_5, z_6, z_7, z_8)$$

$$= (-iz_7, -iz_8, -iz_1, -iz_2, -iz_3, -iz_4, -iz_5, -iz_6)$$

This means the points are in two groups of four, each group sitting at the four corners of a square centred at the origin, with $z_1 = -iz_7 = -z_5 = iz_3$ and $z_2 = -iz_8 = -z_6 = iz_4$. This means the space X' is given by two points, which are distinct and lie in the punctured plane, without being equal to each other's images under the rotation by multiples of ${}^{pi}/_{2}$.

It may be noted that $(z_1)^4 = (z_3)^4 = (z_5)^4 = (z_7)^4$, and $(z_2)^4 = (z_4)^4 = (z_6)^4 = (z_8)^4$, so in fact we simply require that $(z_1)^4$ and $(z_2)^4$ be distinct points in the punctured plane. Hence $X' \simeq (\mathbb{C}^*)^2 \setminus \Delta$.

The restricted fixed point space $F_0' = F_0 \cap X'$ consists of $(z_1, z_2, z_3, z_4, z_5, z_6, z_7, z_8)$ with the following restrictions:

- z_1 and z_5 both sit on the real line, and $z_1 = -z_5$
- $z_3 = \bar{z}_7$, and $z_3 = -z_7$, so both must sit on the imaginary axis, equal distances above and below the origin.
- Since $\bar{z}_8 = -iz_8$, we have z_8 lies on the positive diagonal line for which $re(z) = im(z)$, and $z_4 = -z_8$ so it lies on this line also but the other side of the origin
- Similarly, $\bar{z}_6 = iz_6$ so z_6, so z_6 must lie on the negative diagonal $re(z) = -im(z)$ and $z_2 = -z_6$
- We also have that $z_2 = \bar{z}_8$ and $z_4 = \bar{z}_6$, so these four points must form a square - so the positions of z_4, z_6 and z_8 are specified by z_2, which lies in a copy of the real line minus the origin.
- Similarly, $z_1 = iz_3$ and $z_5 = iz_7$ so the points z_1, z_3, z_5 and z_7 form a square with each corner lying on an axis, and their positions are specified by z_1 which must lie in a copy of the real line minus the origin.

Hence, the space is determined by the position of the two points in the horizontal and diagonal axes ($\mathbb{R}$ minus the origin in each case). Hence $F_0' \simeq (\mathbb{R}^*)^2$. This space has four contractible connected components.

The other restricted fixed point space, F_1', again has the restriction that $z_1 = -iz_7 = -z_5 = iz_3$ and $z_2 = -iz_8 = -z_6 = iz_4$, but this time the points lie in four sets of conjugate pairs. Given the position of z_1, the points z_7, z_5 and z_3 are its images under rotation by multiples of $\pi/2$, and the positions of the remaining four particles are the complex conjugates of these four. This means that the whole space is determined by the position of one particle which lies in a fundamental domain consisting of one eighth of the plane, from the horizontal axis up to the positive diagonal $re(z) = im(z)$. This region is homeomorphic to $\mathbb{R}^2$, and so $F_1' \simeq 8[\mathbb{R}^2] \simeq 8[\text{pt}]$, since this point can be in any one of these eight regions.

The full group of symmetries is given in Tables A.2 and A.3. It has order 64, and its centre is isomorphic to the Klein Four group. The quotient $G/Z(G)$ also has centre Klein Four, and the result of taking the quotient again is the Klein Four group.

The maps ρ, σ and τ for this group can be seen in Figure A.7.

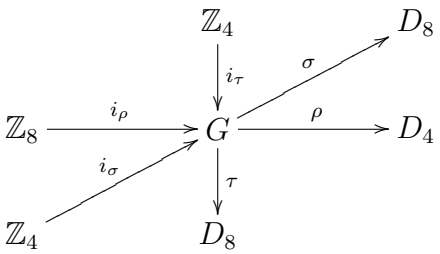

Figure A.7: The maps ρ, σ and τ for eight particles on a four-flower

Example A.2.4 (n particles on a circle)**.** Most commonly referred to as the Lagrange solution, and sometimes called the 'trivial' choreography, any number of particles will form an orbit as the points of a regular n-gon, rotating with constant speed about its centre. This motion has been well studied, being one of the earliest examples to be discovered.

The circle has symmetry group $O(2)$, including rotations R_θ by every angle $0 \leq \theta < 2\pi$, and reflections in lines at every angle also. Symmetries of the particles will be in the dihedral group D_n, generated by a rotation by $2\pi/n$ and any reflection which maps particles to other particles.

Table A.2: Eight particles on a four-flower

$\rho(g)$	$\tau(g)$	$\sigma(g)$	Order
I	0	e	1
I	$T/8$	(12345678)	8
I	$T/4$	(1357)(2468)	4
I	$3T/8$	(14725836)	8
I	$T/2$	(15)(26)(37)(48)	2
I	$-3T/8$	(16385274)	8
I	$-T/4$	(1753)(2864)	4
I	$-T/8$	(18765432)	8
κ_1	$\overline{0}$	(28)(37)(46)	2
κ_1	$\overline{T/8}$	(18)(27)(36)(45)	2
κ_1	$\overline{T/4}$	(17)(26)(35)	2
κ_1	$\overline{3T/8}$	(16)(25)(34)(78)	2
κ_1	$\overline{T/2}$	(15)(24)(68)	2
κ_1	$\overline{-3T/8}$	(14)(23)(58)(67)	2
κ_1	$\overline{-T/4}$	(13)(48)(57)	2
κ_1	$\overline{-T/8}$	(12)(38)(47)(56)	2
κ_3	$\overline{0}$	(13)(48)(57)	2
κ_3	$\overline{T/8}$	(12)(38)(47)(56)	2
κ_3	$\overline{T/4}$	(28)(37)(46)	2
κ_3	$\overline{3T/8}$	(18)(27)(36)(45)	2
κ_3	$\overline{T/2}$	(17)(26)(35)	2
κ_3	$\overline{-3T/8}$	(16)(25)(34)(78)	2
κ_3	$\overline{-T/4}$	(15)(24)(68)	2
κ_3	$\overline{-T/8}$	(14)(23)(58)(67)	2
$\kappa_3\kappa_1$	0	(1357)(2468)	4
$\kappa_3\kappa_1$	$T/8$	(14725836)	8
$\kappa_3\kappa_1$	$T/4$	(15)(26)(37)(48)	2
$\kappa_3\kappa_1$	$3T/8$	(16385274)	8
$\kappa_3\kappa_1$	$T/2$	(1753)(2864)	4
$\kappa_3\kappa_1$	$-3T/8$	(18765432)	8
$\kappa_3\kappa_1$	$-T/4$	e	4
$\kappa_3\kappa_1$	$-T/8$	(12345678)	8
$\kappa_1\kappa_3$	0	(1753)(2864)	4
$\kappa_1\kappa_3$	$T/8$	(18765432)	8
$\kappa_1\kappa_3$	$T/4$	e	4
$\kappa_1\kappa_3$	$3T/8$	(12345678)	8
$\kappa_1\kappa_3$	$T/2$	(1357)(2468)	4
$\kappa_1\kappa_3$	$-3T/8$	(14725836)	8
$\kappa_1\kappa_3$	$-T/4$	(15)(26)(37)(48)	4
$\kappa_1\kappa_3$	$-T/8$	(16385274)	8

Table A.3: Eight particles on a four-flower (contd.)

$\kappa_3\kappa_1\kappa_3$	$\overline{0}$	(15)(24)(58)	2
$\kappa_3\kappa_1\kappa_3$	$\overline{T/_8}$	(14)(23)(58)(67)	2
$\kappa_3\kappa_1\kappa_3$	$\overline{T/_4}$	(13)(48)(57)	2
$\kappa_3\kappa_1\kappa_3$	$\overline{3T/_8}$	(12)(38)(47)(56)	2
$\kappa_3\kappa_1\kappa_3$	$\overline{T/_2}$	(28)(37)(46)	2
$\kappa_3\kappa_1\kappa_3$	$\overline{-3T/_8}$	(18)(27)(36)(45)	2
$\kappa_3\kappa_1\kappa_3$	$\overline{-T/_4}$	(17)(26)(35)	2
$\kappa_3\kappa_1\kappa_3$	$\overline{-T/_8}$	(16)(25)(34)(78)	2
$\kappa_1\kappa_3\kappa_1$	$\overline{0}$	(17)(26)(35)	2
$\kappa_1\kappa_3\kappa_1$	$\overline{T/_8}$	(16)(25)(34)(78)	2
$\kappa_1\kappa_3\kappa_1$	$\overline{T/_4}$	(15)(24)(68)	2
$\kappa_1\kappa_3\kappa_1$	$\overline{3T/_8}$	(14)(23)(58)(67)	2
$\kappa_1\kappa_3\kappa_1$	$\overline{T/_2}$	(13)(48)(57)	2
$\kappa_1\kappa_3\kappa_1$	$\overline{-3T/_8}$	(12)(38)(47)(56)	2
$\kappa_1\kappa_3\kappa_1$	$\overline{-T/_4}$	(28)(37)(46)	2
$\kappa_1\kappa_3\kappa_1$	$\overline{-T/_8}$	(18)(27)(36)(45)	2
$(\kappa_1\kappa_3)^2$	0	(15)(26)(37)(58)	4
$(\kappa_1\kappa_3)^2$	$T/_8$	(16385274)	8
$(\kappa_1\kappa_3)^2$	$T/_4$	(1753)(2864)	4
$(\kappa_1\kappa_3)^2$	$3T/_8$	(18765432)	8
$(\kappa_1\kappa_3)^2$	$T/_2$	e	4
$(\kappa_1\kappa_3)^2$	$-3T/_8$	(12345678)	8
$(\kappa_1\kappa_3)^2$	$-T/_4$	(1357)(2468)	4
$(\kappa_1\kappa_3)^2$	$-T/_8$	(14725836)	8

The full group of symmetries of this choreography can be generated by the elements

$$(I, (12\ldots n), t \mapsto t + T/n)$$

$$(R_\theta, e, t \mapsto t + \theta)$$

$$(\kappa_1, \sigma, t \mapsto -t)$$

Where σ is the corresponding involution depending on how the points are initially arranged on the circle, and where κ_1 maps particles to particles - that is, in the initial arrangement at $t = 0$, exactly one or two particles lie on the axis of symmetry defined by κ_1.

There are no time-preserving symmetries. The time-reversing symmetries consist exactly of the reflections which may be denoted κ_1, assuming the arrangements of particles at $t = 0$ fit with the previous use of that notation, and they will be accompanied by some appropriate order two permutation.

There will be two cases, depending on whether n is odd or even:

- For odd values of n, all reflections will be conjugate. The fixed point spaces F_0 and F_1 will both then consist of one particle moving in $\mathbb{R}$, which is the one which was fixed by the reflection, and $\frac{n-1}{2}$ conjugate pairs of particles either side of the real line. Hence, $F_0, F_1 \simeq \mathbb{R} \times \mathbb{C}^{(\frac{n-1}{2})} \setminus \Delta$.

- For even values of n, there are two different conjugacy classes of reflections - one corresponding to a reflection which fixes two particles, and one corresponding to a reflection which fixes no particles. In this case, one of the fixed point spaces (without loss of generality, F_0) will consist of $\frac{n}{2}$ conjugate pairs, and the other will be $\frac{n}{2} - 1$ conjugate pairs, together with exactly two particles moving in $\mathbb{R}$. Hence, $F_0 \simeq \mathbb{C}^{\frac{n}{2}} \setminus \Delta$, and $F_1 \simeq (\mathbb{R}^2 \setminus \Delta) \times (\mathbb{C}^{(\frac{n}{2}-1)} \setminus \Delta)$.

The maps ρ, σ and τ for the symmetry group of this system can be seen in Figure A.8.

Example A.2.5 (Nine particles on a bifurcated 6-chain)**.** This example shows that not all chain-type curves have the symmetry group of the rectangle. It is presented

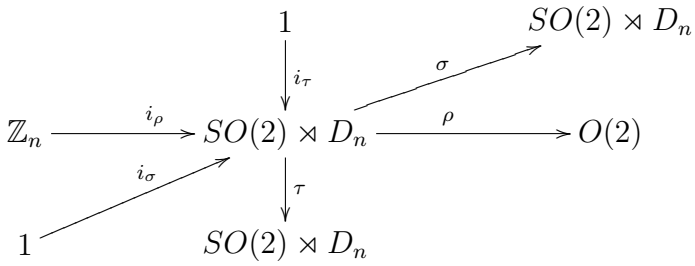

Figure A.8: The maps ρ, σ and τ for n particles on a circle

by Simó in [11] in Figure 4.2(d) as an example of an n-body choreography for the Newtonian potential, based on his calculations.

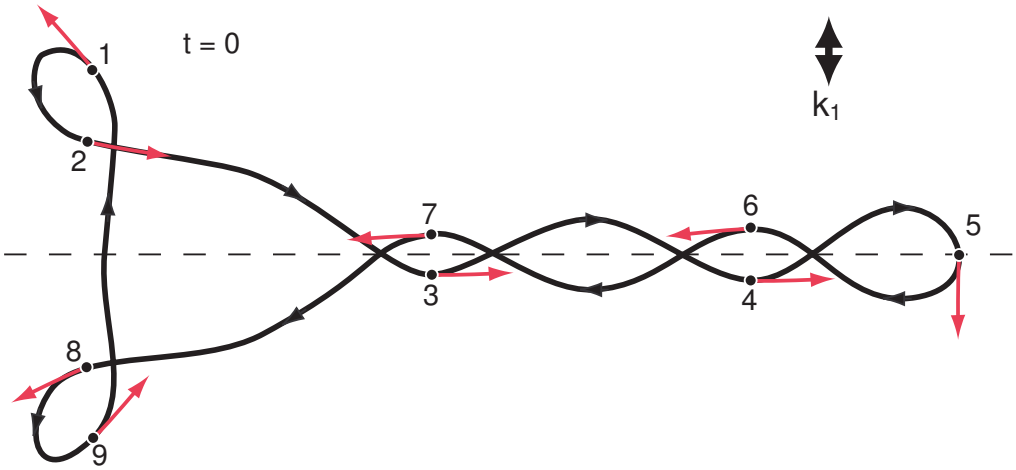

Figure A.9: Nine particles on a bifurcated 6-chain, at $t = 0$

The bifurcated chain has only one reflectional symmetry, κ_1, and no others and hence its symmetry group is $D_1 = \mathbb{Z}_2$.

The arrangements of particles possess reflectional symmetry at $t = kT/18$, with the nine particles forming four pairs and a single particle lying on the line of symmetry. For even values of k, this single particle is at the rightmost end, and when k is odd it is at the middle of the downward portion of the bifurcation on the left.

The choreography symmetry is present, as are the two time-reversing symmetries, given by $\rho(g_0) = \kappa_1$ with $\sigma(g_0) = (29)(38)(47)(56)$, and $\rho(g_1) = \kappa_1$ with $\sigma(g_0) = (19)(28)(37)(46)$ and a time delay of $T/9$.

Fixed point space F_0:

$$\gamma(0) = g_0\gamma(0) = \kappa_1(29)(38)(47)(56)\gamma(0)$$

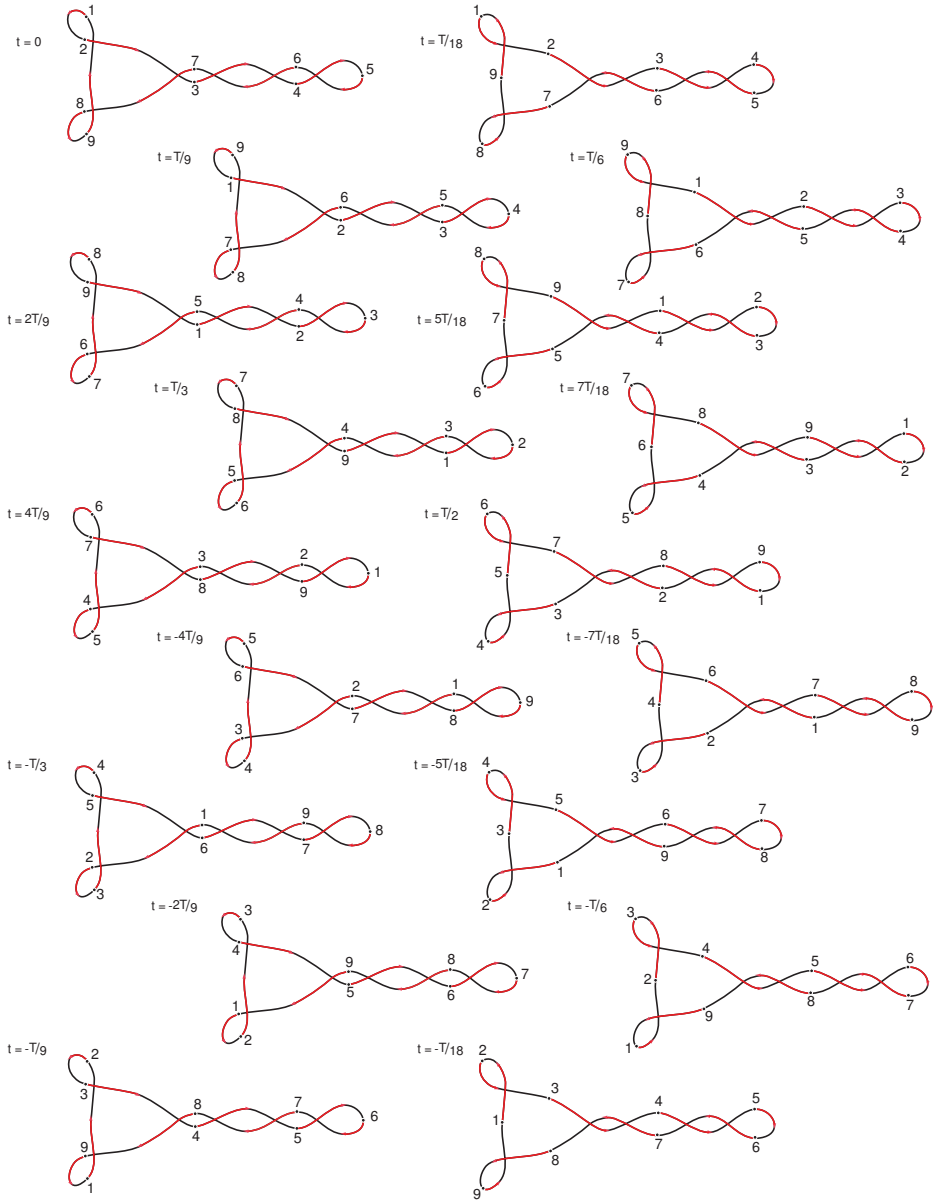

Figure A.10: Nine particles on a bifurcated 6-chain, at $t = {}^{kT}/_{18}$

$$\therefore (z_1, z_2, z_3, z_4, z_5, z_6, z_7, z_8, z_9) = \kappa_1(29)(38)(47)(56)(z_1, z_2, z_3, z_4, z_5, z_6, z_7, z_8, z_9)$$

$$= (\bar{z}_1, \bar{z}_9, \bar{z}_8, \bar{z}_7, \bar{z}_6, \bar{z}_5, \bar{z}_4, \bar{z}_3, \bar{z}_2)$$

The particle z_1 is equal to its own conjugate, and so must lie on the real line. We also have four pairs of conjugate particles, given by $z_2 = \bar{z}_9$, $z_3 = \bar{z}_8$, $z_4 = \bar{z}_7$ and $z_5 = \bar{z}_6$. These eight particles form distinct conjugate pairs either side of the real line. Hence the fixed point space $F_0 = \mathrm{Fix}(g_0)$ is given by one point in $\mathbb{R}$, and four distinct points in the upper or lower half-plane. We must also have that as well as $z_2 \neq z_3$, we have

$z_2 \neq \bar{z}_3$, and similarly for each of the other pairs from $\{z_2, z_3, z_4, z_5\}$. This means we take the space $(\mathbb{C} \setminus \mathbb{R})^4$, and subtract twelve diagonal sets. The resulting space has sixteen components, each of which is homotopic to $(\mathbb{R}^2)^4 \setminus \Delta$. This is a $K(\pi, 1)$ space with $\pi = P_4$. So F_0 will be sixteen copies of $(\mathbb{R}^2)^4 \setminus \Delta$, each crossed with a copy of $\mathbb{R}$ giving the position of z_1, which is homotopic to sixteen copies of $(\mathbb{R}^2)^4 \setminus \Delta$.

Fixed point space F_1:

$$\hat{\gamma}({}^{T}/_{18}) = g_1\hat{\gamma}({}^{T}/_{18}) = \kappa_1(19)(28)(37)(46)\gamma(0)$$

$$\therefore (z_1, z_2, z_3, z_4, z_5, z_6, z_7, z_8, z_9) = \kappa_1(19)(28)(37)(46)(z_1, z_2, z_3, z_4, z_5, z_6, z_7, z_8, z_9)$$

$$= (\bar{z}_9, \bar{z}_8, \bar{z}_7, \bar{z}_6, \bar{z}_5, \bar{z}_4, \bar{z}_3, \bar{z}_2, \bar{z}_1)$$

The particle z_5 is equal to its own conjugate, and so must lie on the real line. We also have four pairs of conjugate particles, given by $z_1 = \bar{z}_9$, $z_2 = \bar{z}_8$, $z_3 = \bar{z}_7$ and $z_4 = \bar{z}_6$. These eight particles form distinct conjugate pairs either side of the real line. Hence the fixed point space $F_1 = \mathrm{Fix}(g_1)$ is given by one point in $\mathbb{R}$, and four distinct points in the upper or lower half-plane. We must also have that as well as $z_1 \neq z_2$, we have $z_1 \neq \bar{z}_2$, and similarly for each of the other pairs from $\{z_1, z_2, z_3, z_4\}$. This means we take the space $(\mathbb{C} \setminus \mathbb{R})^4$, and subtract twelve diagonal sets. The resulting space has sixteen components, each of which is homotopic to $(\mathbb{R}^2)^4 \setminus \Delta$. This is a $K(\pi, 1)$ space with $\pi = P_4$. So F_1 will be sixteen copies of $(\mathbb{R}^2)^4 \setminus \Delta$.

The full group of symmetries is given in Table A.4. It has order 18, and is in fact the dihedral group D_9. It can be generated by the elements marked $*$. The maps ρ, σ and τ for this group can be seen in Figure A.11.

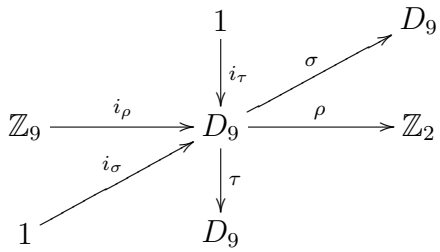

Figure A.11: The maps ρ, τ and σ, for nine particles on a bifurcated 6-chain

Table A.4: Nine particles on a bifurcated 6-chain

$\rho(g)$	$\tau(g)$	$\sigma(g)$	Order
I	0	e	1
$*$ I	$^{T}/_{9}$	(123456789)	9
I	$^{2T}/_{9}$	(135792468)	9
I	$^{T}/_{3}$	(147)(258)(369)	3
I	$^{4T}/_{9}$	(159483726)	9
I	$^{-4T}/_{9}$	(162738495)	9
I	$^{-T}/_{3}$	(174)(285)(396)	3
I	$^{-2T}/_{9}$	(186429753)	9
I	$^{-T}/_{9}$	(198765432)	9
$*$ κ_1	$\overline{0}$	(29)(38)(47)(56)	2
κ_1	$\overline{^{T}/_{9}}$	(19)(28)(37)(46)	2
κ_1	$\overline{^{2T}/_{9}}$	(18)(27)(36)(45)	2
κ_1	$\overline{^{T}/_{3}}$	(17)(26)(35)(89)	2
κ_1	$\overline{^{4T}/_{9}}$	(16)(25)(34)(79)	2
κ_1	$\overline{^{-4T}/_{9}}$	(15)(24)(69)(78)	2
κ_1	$\overline{^{-T}/_{3}}$	(14)(23)(59)(68)	2
κ_1	$\overline{^{-2T}/_{9}}$	(13)(49)(58)(67)	2
κ_1	$\overline{^{-T}/_{9}}$	(12)(39)(48)(57)	2

Example A.2.6 (Three particles on a curve with square symmetry)**.** This example was discovered in the exploration of higher order symmetry groups for three particles, as discussed in Section 4.2 and in particular in Remark 4.2.1. Having chosen order four symmetry, and picked two reflections (which are time-reversing in the case of the Lagrange circular symmetry), we use the same spaces F_0 and F_1 as in the circular case, but choose a non-homotopic path connecting them, to find solutions in a different connected component - as in Example 4.6.4 on page 99, where the same process was undertaken for the figure eight curve. This alternative path was approximated using Fourier series of order up to 29, extended to a full choreographical motion, and iterated towards a local minimum of the action functional with strong force potential. The resulting curve is given below in Figure A.12.

It may be noted that while this curve uses the strong force potential, a similar curve with this symmetry for three particles is also found under the Newtonian potential. While this is not a proof of this solution's existence, the numerical data strongly suggests such a solution exists.

The curve has the symmetry group of a square, which is generated by the vertical reflection κ_1 and the diagonal reflection in the line of positive slope, denoted κ_3. The total symmetry group has eight elements, including two other reflections ($\kappa_3\kappa_1\kappa_3$, horizontally, which has elsewhere been denoted κ_2; and $\kappa_1\kappa_3\kappa_1$, in the other diagonal) as well as rotations $\kappa_1\kappa_3$, $(\kappa_1\kappa_3)^2$ and $\kappa_3\kappa_1$, by $\pi/2$, π and $3\pi/2$ clockwise, respectively.

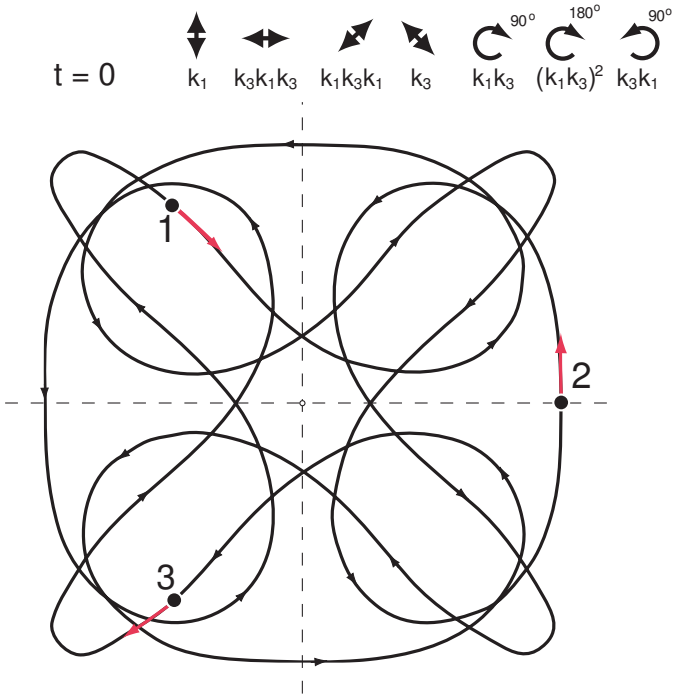

Figure A.12: Three particles on a curve with square symmetry, at $t = 0$

The arrangements of particles possess reflectional symmetry at $t = kT/24$, with reflections in the vertical and horizontal axes at even values of k, and diagonal reflections when k is odd. This can be seen in Figure A.13.

The full group of symmetries is given in Table A.5. It has order 24. Its structure is that of D_{12}, the dihedral group with 24 elements. The maps ρ, σ and τ for this group can be seen in Figure A.14.

Table A.5: Three particles on a curve with square symmetry

$\rho(g)$	$\tau(g)$	$\sigma(g)$	Order
I	0	e	1
I	$T/3$	(123)	3
I	$2T/3$	(132)	3
κ_1	$\overline{0}$	(13)	2
κ_1	$\overline{T/3}$	(12)	2
κ_1	$\overline{-T/3}$	(23)	2
κ_3	$\overline{T/12}$	(12)	2
κ_3	$\overline{5T/12}$	(23)	2
κ_3	$\overline{-T/4}$	(13)	2
$\kappa_3\kappa_1\kappa_3$	$\overline{T/6}$	(23)	2
$\kappa_3\kappa_1\kappa_3$	$\overline{T/2}$	(13)	2
$\kappa_3\kappa_1\kappa_3$	$\overline{-T/6}$	(12)	2
$\kappa_1\kappa_3\kappa_1$	$\overline{T/4}$	(13)	2
$\kappa_1\kappa_3\kappa_1$	$\overline{-5T/12}$	(12)	2
$\kappa_1\kappa_3\kappa_1$	$\overline{-T/12}$	(23)	2
$\kappa_3\kappa_1$	$T/12$	(123)	12
$\kappa_3\kappa_1$	$5T/12$	(132)	12
$\kappa_3\kappa_1$	$-T/4$	e	4
$\kappa_1\kappa_3$	$T/4$	e	4
$\kappa_1\kappa_3$	$-5T/12$	(123)	12
$\kappa_1\kappa_3$	$-T/12$	(132)	12
$(\kappa_1\kappa_3)^2$	$T/6$	(132)	6
$(\kappa_1\kappa_3)^2$	$T/2$	e	2
$(\kappa_1\kappa_3)^2$	$-T/6$	(123)	6

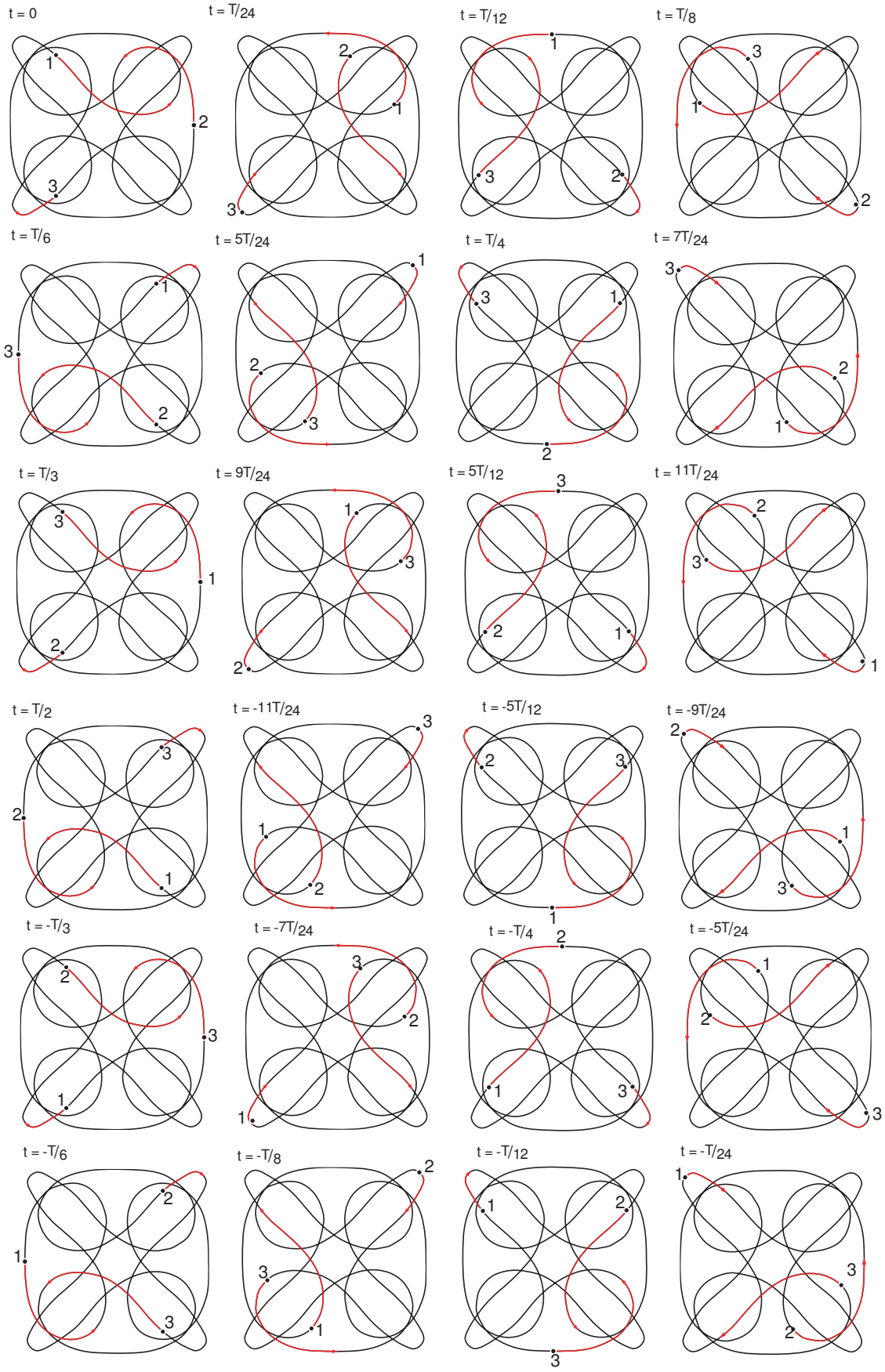

Figure A.13: Three particles on a curve with square symmetry, at $t = {}^{kT}/_{24}$

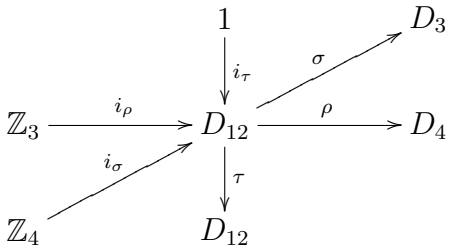

Figure A.14: The maps ρ, σ and τ for three particles on a curve with square symmetry

Bibliography

[1] The American Mathematical Society - Variational Methods in Celestical Mechanics Conference 2003: List of Open Problems. `http://www.aimath.org/WWN/varcelest/varcelest.pdf`.

[2] E. Barrabés, J. M. Cors, C. Pinyol, and J. Soler. Hip-hop solutions of the $2n$-body problem. *Celestial Mechanics and Dynamical Astronomy 95 (55-66)*, 2006.

[3] V. Barutello and S. Terracini. Action minimizing orbits in the n-body problem with simple choreography constraint. *Nonlinearity 17 No. 6 (20152039)*, 2004.

[4] V. Barutello and S. Terracini. Double choreographical solutions for n-body type problems. *Celestial Mechanics and Dynamical Astronomy*, 2006.

[5] V. Barutello, S. Terracini, and D. Ferrario. Symmetry groups of the planar 3-body problem and action-mimizing trajectories. *Archive for Rational Mechanics and Analysis 190 (189226)*, 2008.

[6] A. V. Borisov, I. S. Mamaev, and A. A. Kilin. Absolute and relative choreographies in the problem of point vortices moving on a plane. *Regular and Chaotic Dynamics Volume 9, No. 2*, 2004.

[7] K. Chen. Binary decompositions for planar n-body problems and symmetric periodic solutions. *Arch. Rational Mech. Anal. 170 (247-276)*, 2003.

[8] A. Chenciner. Symmetries and "simple" solutions of the classical n-body problem. *XIVth International Congress on Mathematical Physics (4-20)*, 2003.

[9] A. Chenciner. Are there perverse choreographies? *New advances in celestial mechanics and Hamiltonian systems (63-76)*, 2004.

[10] A. Chenciner, R. Cushman, C. Robinson, and J. Xia. Action minimising periodic orbits in the Newtonian n-body problem, in Celestial Mechanics, dedicated to Don Saari for his 60th birthday. *Contemporary Mathematics 292, American Mathematical Society (71-90)*, 2002.

[11] A. Chenciner, J. Gerver, R. Montgomery, and C. Simó. Simple choreographic motions of N bodies: A preliminary study. *Geometry, mechanics, and dynamics (287-308)*, 2002.

[12] A. Chenciner and R. Montgomery. A remarkable periodic solution of the three-body problem in the case of equal masses. *Annals of Mathematics 152 (881-901)*, 2000.

[13] A. Chenciner and A. Venturelli. Minima de l'intégrale d'action du problème Newtonien de 4 corps de masses égales dans $\mathbb{R}^3$: orbites Hip-Hop. *Celestial Mechanics and Dynamical Astronomy 77 (139-152)*, 2000.

[14] D. Ferrario and S. Terracini. On the existence of collisionless equivariant minimizers for the classical n-body problem. *Inventiones Mathematicae 155 (305-362)*, 2003.

[15] A. Hatcher. *Algebraic Topology*. Cambridge University Press, 2002.

[16] T. Kapela. N-body choreographies with a reflectional symmetry - Computer assisted existence proofs. *EQUADIFF*, 2003.

[17] T. Kapela and C. Simó. Computer assisted proofs for nonsymmetric planar choreographies and stability of the Eight. *Nonlinearity 20 (1241-1255)*, 2007.

[18] T. Kapela and P. Zgliczyński. The existence of simple choreographies for the N-body problem - a computer-assisted proof. *Nonlinearity 16*, 2003.

[19] R. Krawczyk. Newton-algorithmen zur bestimmung von nullstellen mit fehlerschranten. *Computing 4 (187-201)*, 1969.

[20] S. Mac Lane. *Homology*. Springer-Verlag, 1967.

[21] R. S. MacKay and J. D. Meiss. *Hamiltonian Dynamical Systems: A Reprint Selection*. CRC Press, 1987.

[22] D. Margalit and J. McCammond. Geometric presentations for the pure braid group. *Journal of Knot Theory and Its Ramifications 18(1) pp1-20*, 2009.

[23] Y. Matsumoto. *Translations of Mathematical Monographs, Volume 208: Introduction to Morse Theory*. American Mathematical Society, 2002.

[24] C. McCord, J. Montaldi, M. Roberts, and L. Sbano. Relative periodic orbits of symmetric Lagrangian systems. *EQUADIFF*, 2003.

[25] D. McDuff and D. Salamon. *Introduction to Symplectic Topology*. Oxford Science Publications, 1995.

[26] Richard S. Palais. The principle of symmetric criticality. *Communications in Mathematical Physics 69 pp.19-30*, 1979.

[27] L. M. Perko and E. L. Walter. Regular polygon solutions of the n-body problem. *Proceedings of the American Mathematical Society Volume 94, Number 2*, 1985.

[28] L. Sbano and J. Southall. Periodic solutions of the N-body problem with Lennard-Jones-type potentials. *Dynamical Systems*, October 2009.

[29] C. Simó. n-body Choreographies. `http://www.maia.ub.es/dsg/nbody.html`.

[30] C. Simó. Dynamical properties of the figure eight solution of the three-body problem. *Celestial Mechanics (Evanston, IL, 1999) Contemp. Math. 292 (209-28)*, 2002.

[31] A. T. Skjeltorp, S. Clausen, and G. Helgesen. Application of braid statistics to particle dynamics. *Physics A (267-280)*, 1999.

[32] J. Southall. Variational Methods and Periodic Solutions of n-body and n-centre problems. *PhD Thesis, University of Surrey*, 2006.

[33] E. Spanier. *Algebraic Topology.* McGraw-Hill, 1966.

[34] S. Terracini. On the variational approach to the periodic n-body problem. *Celestial Mechanics and Dynamical Astronomy*, 2006.

[35] Z. Xie and S. Zhang. A simpler proof of regular polygon solutions of the N-body problem. *Physics Letters A 227*, 2000.